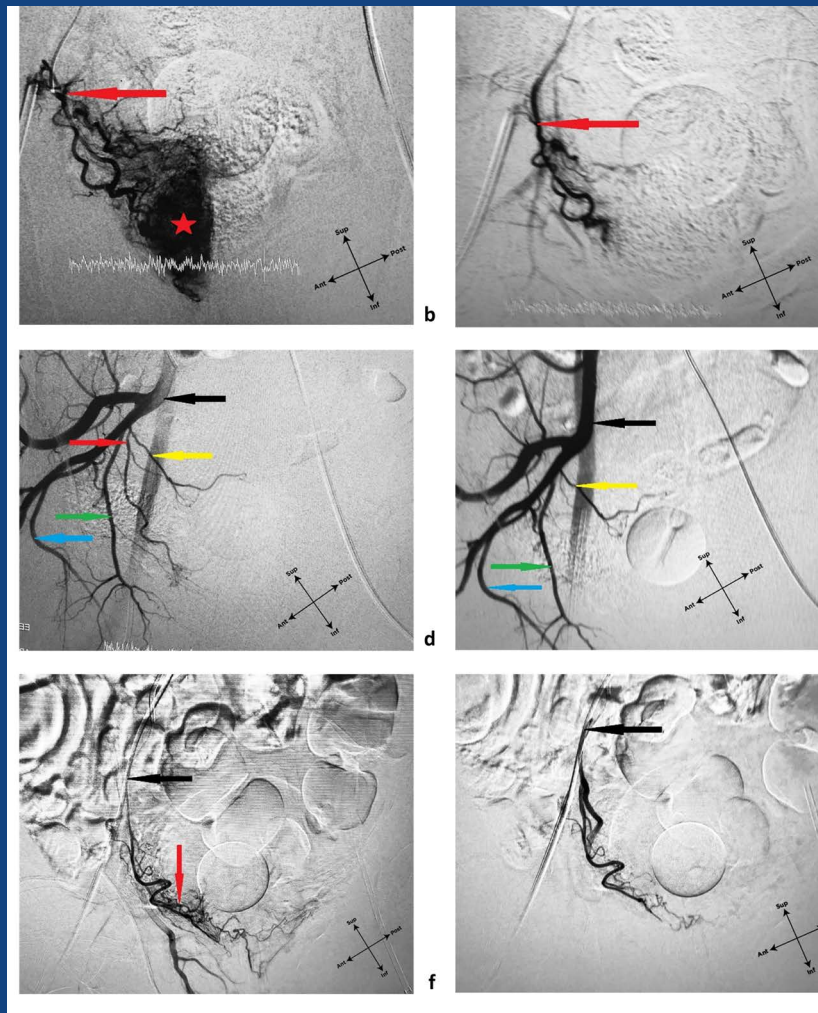


EJA

European Journal of Anatomy

Volume 30- Number 3

May 2026



Indexed in:

CLARIVATE

- JCR:2020
- Q4 (21/23)
- I.F. J.C.I.: 0.19

DIALNET

EMBASE / Excerpta Medica

SCOPUS

- SJCR: 2020
- Q4 (31/39)
- I.F.: 0.162

Emerging Sources Citation Index

LATINDEX. Catálogo v1.0 (2002-2017)

Official Journal
of the Spanish
Society of Anatomy

Published by: **LOKI & DIMAS**

www.eurjanat.com



Original Articles

Implications of medial circumflex femoral artery positioning for surgical risk: a retrospective MRI study 303

Nuriye Oz, Suat Morkuzu, Ege Alkan, Kamil Karaali, Cihan Yazar, Lutfiye B. Suzen

Prevalence and anatomical variations of the palmaris longus muscle in the Jordanian population: a new classification proposal..... 309

Mohammad Al-Shalalfeh, Ahmad Alaudat, Saqer Ayyash, Ahmed Salman

Age-related morphological transformations of cephalometric parameters in artificially deformed and non-deformed skulls: a comparative craniometric analysis across successive life stages 319

Sardar Abdullayev Anar

Efficacy and wider perspectives on the Rigo-Chêneau Brace in adolescent idiopathic scoliosis: a retrospective perspective 327

José M. Morales-de-Pando, Juan Sánchez-Palacios, Gloria González-Medina, José A. Prada-Oliveira

Adverse effects of zinc oxide nanoparticles on the prostate gland of adult albino rat and the possible protective role of rutin C: histological, immunohistochemical and biochemical study 333

Mohamed Z. Kotb, Afaf A. Mohamed, Amany E. Hamoud, Fayza A.R.A. Gawad, Reda I. Amer

Anatomical variation of the prostatic artery and the impact of its embolization on IPSS in benign prostatic hyperplasia..... 345

Ahmed F. AlDomairy, Gamal-eldine M. Niazi, Radwa M. Elsabban

Relationship between dorsal digit ratio and hand grip strength in young adult Nigerian population..... 357

Smart I. Mbagwu, Chidiebere A. Nnajeze, Kelechi E. Ichie

Correlation of p53 expression with morphological features in complete and partial hydatidiform moles 367

Melisa Lelić, Emin Grbić, Daniel Petrović, Suada Ramić, Jasminka Mustedanagić-Mujanović, Adna Mujkić

Variations of the anterior belly of the digastric muscle: a cadaveric and meta-analysis study 375

Marcelo Prado, José Neto, Carolina Basto, Iapunira Aragão, Felipe Aragão, Francisco Reis, José Aragã

Medical Education

Innovative museum techniques in enhancing Medical Education: a study on interactive and experiential learning for medical students 387

Priya G, Mahima Sophia M

Anatomy Museums in Medical Education: utilization patterns and perceived learning benefits among Indian medical graduates 395

Manikanta Reddy V, Rajesh S, Maruti R. Annamraju, Teresa Rani S, Krishna Manasa A

Teaching In Anatomy

Role of spatial cognition ability in teaching and learning

human embryology: traditional versus 3D atlas..... 401

Rakhshinda Iram, Zilli Huma, Najma Baseer, Shah Khalid

Implications of medial circumflex femoral artery positioning for surgical risk: a retrospective MRI study

Nuriye Oz¹, Suat Morkuzu¹, Ege Alkan¹, Kamil Karaali², Cihan Yazar³, Lutfiye B. Suzen^{1,4}

¹ Department of Anatomy, Faculty of Medicine, Akdeniz University, Antalya, Turkey

² Department of Radiology, Faculty of Medicine, Akdeniz University, Antalya, Turkey

³ Department of Orthopedics and Traumatology, Faculty of Medicine, Dicle University, Diyarbakir, Turkey

⁴ Department of Anatomy, Faculty of Dentistry, Antalya Bilim University, Antalya, Turkey

SUMMARY

Hip pain, including Ischiofemoral impingement, often requires surgery. This study aimed to evaluate the shortest distance between the lesser trochanter and the medial circumflex femoral artery (MCFA). A total of 40 patients (18 males and 22 females) were included. MR images were retrospectively examined. Measurements of the shortest distance between the lesser trochanter and the MCFA before its branches were taken. The average age of the 40 patients was 49.65 ± 13.89 years, ranging from 29 to 78 years old. Of the 40 patients, 18 (45%) were men and 22 (55%) were women. The shortest distance between the left-side MCFA and the lesser trochanter was found to be 25.10 ± 6.80 mm in men and 24.84 ± 8.73 mm in women. The shortest distance between the right-side MCFA and the lesser trochanter was found to be 28.62 ± 8.91 mm in men and 26.26 ± 6.41 mm in women. In all patients, the shortest distance between the MCFA and the lesser trochanter was 24.98 ± 7.63 mm on the left side and 27.31 ± 7.61

mm on the right side. No significant sex differences were found for either the right ($p=0.349$) or left ($p=0.916$) sides. However, there was a significant difference between the right and left sides ($p=0.005$).

This study identified a significant asymmetry in the positioning of the MCFA relative to the lesser trochanter, with no notable differences between sexes. These findings enhance our understanding of the course and morphology of the MCFA, which may be beneficial for comprehending and improving surgical interventions for Ischiofemoral impingement.

Key words: Medial circumflex femoral artery – Lesser trochanter – Ischiofemoral impingement – MCFA – Lesser trochanter osteoplasty

INTRODUCTION

Hip pain, a common condition associated with notable functional impairment, impacts approximately 30 to 40 percent of individuals engaged in

Corresponding author:

Nuriye Oz, PhD. Department of Anatomy, Faculty of Medicine, Akdeniz University, Pinarbasi, Akdeniz Universitesi Tip Fakultesi Anatomi Ana-bilim Dali, Kampus Antalya, Turkey, 07070. Phone: +902422276950; Fax: +902422274485. E-mail: nuriyeoz@akdeniz.edu.tr - ORCID: 0000-0003-4452-3615

Submitted: December 19, 2024. Accepted: March 24, 2025.

<https://doi.org/10.52083/DROT9097>

sporting activities and 12 to 15 percent of adults aged over 60 (Thorborg et al., 2017; Christmas et al., 2002). While both extraarticular and intraarticular hip issues can contribute to pain (Ahuja et al., 2020), its manifestation is typically observed in anterior, lateral, or posterior regions. However, diagnosing posterior hip pain poses a challenge due to its diverse underlying causes, with musculoskeletal conditions like Ischiofemoral impingement being among the differential diagnoses (Chamberlain, 2021).

The etiology of Ischiofemoral impingement is complex, involving anatomical variations in the proximal femur or pelvis, and other pathological conditions (Hernando et al., 2016). Ischiofemoral impingement occurs due to aberrant interaction between the lesser trochanter of the femur and the ischium, manifesting as atypical discomfort in the groin and/or posterior buttock region (Stafford and Villar, 2011). Surgical intervention, notably lesser trochanter osteoplasty, is often necessary to alleviate symptoms and restore hip function but can increase the risk of complications, particularly concerning the medial circumflex femoral artery (MCFA) (Nakano et al., 2020; Goodwin et al., 2017; Siebenrock et al., 2019).

The MCFA, a vital vessel supplying blood to the femoral head and surrounding tissues, is in close proximity to the lesser trochanter, making it vulnerable to injury during surgical procedures (Siebenrock et al., 2019). In the majority of cases (78.3%), the MCFA had its origin in the deep femoral artery. In a smaller number of cases (11.7%), the MCFA had its origin in the common femoral artery, and in a still smaller number of cases (5%), the MCFA had its origin in the superficial femoral artery. One case showed a common trunk with the deep femoral artery (Vuksanović-Božarić et al., 2018). It runs between the pectineus and iliopsoas tendon, then posteriorly between the quadratus femoris and inferior gemellus muscles. Branches include those to the trochanteric area and inferior retinacular vessels, providing terminal branches to the femoral head by piercing the hip capsule near the superior gemellus tendon. Anastomoses are centrally located anterior to the lesser trochanter and peripherally situated laterally or posteriorly (Siebenrock et al., 2019; Zlotowicz et al.,

2018; Tzouma et al., 2020).

While existing studies have described the general anatomy of the MCFA (Siebenrock et al., 2019), they have not provided detailed measurements of the artery's proximity to the lesser trochanter, particularly using MRI. This lack of detailed anatomical data creates a gap in surgical risk assessment and planning. This study aims to fill this gap by offering precise measurements of the shortest distance between the MCFA and the lesser trochanter, based on MRI scans from a diverse patient cohort. By identifying potential "safe" and "danger" zones, the research seeks to enhance preoperative planning and minimize the risk of MCFA injury during lesser trochanter osteoplasty, contributing to a more precise and safer surgical strategy.

MATERIALS AND METHODS

This study was approved by the Clinical Research Ethics Committee of Akdeniz University, per the Declaration of Helsinki (KA EK-581).

Our study included 40 patients (18 males and 22 females) aged between 29 and 78 years, (mean age: 49.65 ± 13.89 years). We retrospectively scanned the MR images of patients in the Hospital Management Information System. In this study, inclusion criteria were: (1) 18 years and older; (2) Available MRI of lower extremity. Exclusion criteria were: (1) Patients who had undergone hip surgery or trauma; (2) Patients diagnosed with vascular diseases affecting the lower extremity. Patients meeting the inclusion criteria were included in the study for evaluation.

MR images of the lower extremity were examined retrospectively using the PACS (Picture Archiving and Communication System) system. The measurements were performed jointly by an experienced anatomist and radiologist. The measurements were later repeated by the same anatomist. The two measurements were averaged and then statistically analyzed. We evaluated the origin of MCFA and found that it originated from the deep femoral artery in all subjects. After that, we measured the shortest distance between the lesser trochanter and the MCFA before its branching point (Fig. 1). The tools included in the PACS

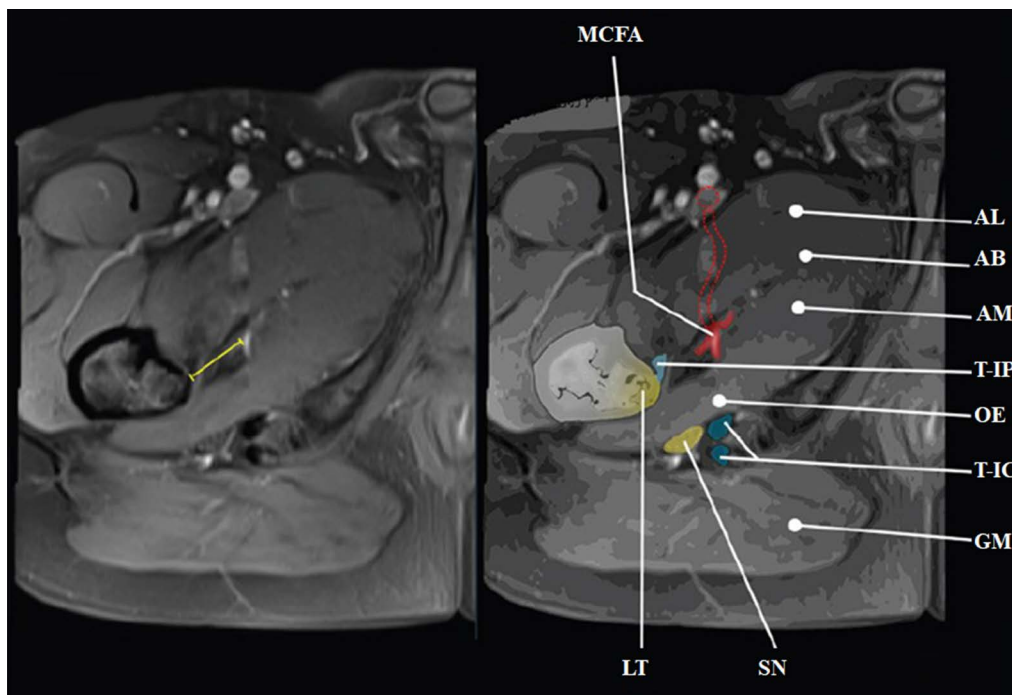


Fig. 1.- Shortest distance between MFCFA and lesser trochanter (yellow line). LT: Lesser trochanter. MFCFA: Medial femoral circumflex artery and its course (red dashed line). AL: Adductor longus muscle. AB: Adductor brevis muscle. AM: Adductor magnus muscle. t-IP: Tendon of iliopsoas muscle. OE: Obturatorius externus muscle. t-IC: Tendons of ischio-crural muscles. GM: Gluteus maximus muscle.

system were used for measurements.

Statistical analysis

In this context, the IBM SPSS 23.0 (IBM Corp., Armonk, NY) package program was used in order to evaluate the data of the study group. The Shapiro-Wilk test was used in order to check whether the data conformed to normal distribution. Student-t test was used in order to evaluate the sex differences. A value of $p < 0.05$ was considered statistically significant. The paired-t test was used in order to detect a difference between the right and left sides.

RESULTS

The mean, standard deviation, minimum and

maximum distances are presented in Table 1. Forty patients were included in this study. Of the 40 patients, 18 (45%) were men and 22 (55%) were women. The shortest distance between the left-side MFCFA and the lesser trochanter was found to be 25.10 ± 6.80 mm in men and 24.84 ± 8.73 mm in women. The shortest distance between the right side MFCFA and the lesser trochanter was found to be 26.26 ± 6.41 mm in women and 28.62 ± 8.91 mm in men. In all patients, the shortest distance between the MFCFA and the lesser trochanter was 24.98 ± 7.63 mm on the left side and 27.31 ± 7.61 mm on the right side. No sex differences were found for either the right ($p=0.349$) or left ($p=0.916$) sides. There was a significant difference between the right and left sides for all subjects ($p=0.005$) and males ($p=0.014$). No statistically significant difference was found between the right and left sides for the female group ($p=0.169$).

Table 1. Comparison of right and left side mean distances (mm) of the MFCFA to the lesser trochanter

		Mean	Sd	Median	Minimum	Maximum	p
All Subjects (N=40)	Right	27.31	7.61	26.99	15.94	42.19	0.005
	Left	24.98	7.63	24.49	13.28	40.64	
Male (N=18)	Right	28.62	8.91	27.82	15.95	42.19	0.014
	Left	24.84	8.74	23.11	13.40	40.64	
Female (N=22)	Right	26.26	6.42	26.03	16.80	40.24	0.169
	Left	25.10	6.81	25.24	13.28	38.89	

DISCUSSION

The precise measurement of the shortest distance between the MCFA and the lesser trochanter using MRI scans revealed the asymmetry in the positioning of the MCFA relative to the lesser trochanter, with a statistically significant difference between the right and left sides. This study found no significant sex differences in the shortest distance between the MCFA and the lesser trochanter on either side.

The absence of significant sex differences in the shortest distance between the MCFA and the lesser trochanter on both the right and left sides suggests that the observed asymmetry is not influenced by sex, which may indicate that these measurements are broadly applicable across different patient populations. This finding is crucial for surgeons, as it indicates that surgical risk related to MCFA injury is comparable between male and female patients, allowing for standardized surgical approaches without sex-specific adjustments.

Several anatomical studies have investigated the course of the MCFA in relation to the hip joint and surrounding structures (Zlotorowicz et al., 2018; Tzouma et al., 2020; Sussmann et al., 2007). In our study, the shortest distance between the MCFA and the lesser trochanter was 24.98 ± 7.63 mm on the left side and 27.31 ± 7.61 mm on the right side. The MCFA's proximity to the lesser trochanter has been documented in previous anatomical studies, through direct measurements and their clinical implications. For example, studies by Hapa et al. (2018) reported the mean distance of the lesser trochanter to the MCFA was 22 mm. Lazaro et al. (2015) have reported that at the inferomedial aspect a consistent branch originates from the transverse MFCA 4.1 cm (3.0 to 5.8 cm) from the lesser trochanter. The transition from the transverse to the ascending MFCA on the quadratus femoris's anterior surface is 2.2 cm (2.0 to 2.3 cm) proximal and 1.2 cm (0.5 to 1.9 cm) medial to the lesser trochanter. These studies emphasized the importance of recognizing anatomical variations in order to avoid vascular injury during surgical procedures involving the hip.

The significant difference in the distances be-

tween the right and left sides has important clinical implications. The shorter distance on the left side may suggest a higher risk of MCFA injury during surgical procedures targeting the lesser trochanter. Surgeons should be particularly cautious when operating on the left hip, ensuring meticulous planning and precise surgical techniques to avoid accidental damage to the MCFA. The identification of "safe" and "dangerous" zones around the lesser trochanter can aid surgeons in planning their approach. Based on the measurements obtained in this study, the left side appears to be more critical due to the closer proximity of the MCFA. These findings align with the literature, which also noted the importance of side-specific considerations in hip surgeries (Deak and Varacallo, 2024). The average distances serve as a reference point for preoperative planning, allowing surgeons to anticipate areas where the MCFA is in close proximity to the lesser trochanter.

Given the variability in distances among patients, surgeons should consider preoperative imaging to assess the specific anatomical relationship in each case. Personalized surgical strategies based on detailed anatomical assessments can improve patient outcomes by reducing the risk of MCFA injury (Guttler et al., 2007).

This study has limitations, variability in MRI slice thickness and arterial filling phases may impact the accuracy of distance measurements.

In conclusion, this study enhances our understanding of the anatomical relationship between the MCFA and the lesser trochanter, providing critical data for improving the safety and efficacy of lesser trochanter surgery. The significant asymmetry observed between the right and left sides, along with the lack of sex differences, underscore the need for careful pre- and intraoperative surgical planning and individualized approaches.

AUTHOR CONTRIBUTIONS

NO: Data Collection and/or Processing, Literature Review, Analysis, Writing, SM: Literature Review, Writing, EA: Conception, Analysis, Data Collection and/or Processing, KK: Data Collection and/or Processing, CY: Critical Review, LBS: Conception, Supervision, Critical Review. All authors read and approved the final manuscript.

ETHICS COMMITTEE APPROVAL

This study was approved by the Clinical Research Ethics Committee of Akdeniz University (Ethics committee approval: KAEK-581).

Data availability: The data are not publicly available due to privacy or ethical restrictions.

REFERENCES

AHUJA V, THAPA D, PATIAL S, CHANDER A, AHUJA A (2020) Chronic hip pain in adults: Current knowledge and future prospective. *J Anaesthesiol Clin Pharmacol*, 36(4): 450-457.

CHAMBERLAIN R (2021) Hip pain in adults: evaluation and differential diagnosis. *Am Fam Physician*, 103(2): 81-89.

CHRISTMAS C, CRESPO CJ, FRANCKOWIAK SC, BATHON JM, BARTLETT SJ, ANDERSEN RE (2002) How common is hip pain among older adults? Results from the Third National Health and Nutrition Examination Survey. *J Fam Pract*, 51(4): 345-348.

DEAK N, VARACALLO M (2024) Hip precautions. In: StatPearls. Treasure Island (FL) ineligible companies. Disclosure: Matthew Varacallo declares no relevant financial relationships with ineligible companies.

GOODWIN JA, CHHABRA A, PATEL KA, HARTIGAN DE (2017) Lesser trochanter osteoplasty for ischiofemoral impingement. *Arthrosc Tech*, 6(5): e1755-e1760.

GUTTLE K, POKORNY D, SOSNA A (2007) The role of understanding the media femoral circumflex artery course in total hip replacement. *Acta Chir Orthop Traumatol Cech*, 74(6): 377-381.

HAPA O, DEMIRKIRAN ND, HUSEMOGLU B, EDIZER M, HAVITCIOGLU H (2018) Anatomic implications of lesser trochanterplasty. *Acta Orthop Traumatol Turc*, 52(1): 54-57.

HERNANDO MF, CEREZAL L, PEREZ-CARRO L, CANGA A, GONZALEZ RP (2016) Evaluation and management of ischiofemoral impingement: a pathophysiologic, radiologic, and therapeutic approach to a complex diagnosis. *Skeletal Radiol*, 45(6): 771-787.

LAZARO LE, KLINGER CE, SCULCO PK, HELFET DL, LORICH DG (2015) The terminal branches of the medial femoral circumflex artery: the arterial supply of the femoral head. *Bone Joint J*, 97-B(9): 1204-1213.

NAKANO N, SHOMAN H, KHANDUJA V (2020) Treatment strategies for ischiofemoral impingement: a systematic review. *Knee Surg Sports Traumatol Arthrosc*, 28(9): 2772-2787.

SIEBENROCK KA, KEEL MJB, TANNAST M, BASTIAN JD (2019) Surgical hip dislocation for exposure of the posterior column. *JBJS Essent Surg Tech*, 9(1): e2.

STAFFORD GH, VILLAR RN (2011) Ischiofemoral impingement. *J Bone Joint Surg Br*, 93(10): 1300-1302.

SUSSMANN PS, ZUMSTEIN M, HAHN F, DORA C (2007) The risk of vascular injury to the femoral head when using the posterolateral arthroscopy portal: cadaveric investigation. *Arthroscopy*, 23(10): 1112-1115.

THORBORG K, RATHLEFF MS, PETERSEN P, BRANCI S, HOLMICH P (2017) Prevalence and severity of hip and groin pain in sub-elite male football: a cross-sectional cohort study of 695 players. *Scand J Med Sci Sports*, 27(1): 107-114.

TZOUMA G, KOPANAKIS NA, TSAKOTOS G, SKANDALAKIS PN, FILIPPOU D (2020) Anatomic variations of the deep femoral artery and its branches: clinical implications on anterolateral thigh harvesting. *Cureus*, 12(4): e7867.

VUKSANOVIĆ-BOŽARIĆ A, ABRAMOVIĆ M, VUČKOVIĆ L, GOLUBOVIĆ M, VUKČEVIĆ B, RADUNOVIĆ M (2018) Clinical significance of understanding lateral and medial circumflex femoral artery origin variability. *Anat Sci Int*, 93: 449-455.

ZLOTOROWICZ M, CZUBAK-WRZOSEK M, WRZOSEK P, CZUBAK J

(2018) The origin of the medial femoral circumflex artery, lateral femoral circumflex artery and obturator artery. *Surg Radiol Anat*, 40(5): 515-520.

Prevalence and anatomical variations of the palmaris longus muscle in the Jordanian population: a new classification proposal

Mohammad Al-Shalalfeh¹, Ahmad Alaudat², Saqer Ayyash³, Ahmed Salman^{4,5}

¹ School of Medicine, The University of Jordan, Amman 11942, Jordan

² School of Medicine, The Hashemite University, P.O. Box 330127, Zarqa 13133, Jordan

³ Department of General Surgery and Neurosurgery, Islamic Hospital

⁴ Department of Anatomy and Histology, Faculty of Medicine, The University of Jordan, Amman 11942, Jordan

⁵ Department of Anatomy, Faculty of Medicine, Menoufia University, Egypt

SUMMARY

The palmaris longus (PL) muscle is a superficial flexor muscle that exhibits a notable anatomical variability and is frequently used in reconstructive surgery. Its absence or morphological differences may influence surgical planning. This study aims to determine the prevalence and morphological variation of PL in the Jordanian population, and assess its relationship with sex, hand dominance and parental origin. A cross-sectional study of 403 University of Jordan students was conducted. PL presence was assessed bilaterally using multiple tests (Schaeffer's, Thompson's, Mishra's test I and II, and Pushpakumar's tests). Photographs of the forearm were taken and independently reviewed to classify the PL morphology into normal, bifurcated, radial deviation, ulnar deviation, reversed, or absent.

PL was present bilaterally in 228 participants (56.5%), absent bilaterally in 92 (22.8%), and unilaterally absent in 83 (20.6%). Unilateral absence was more frequent in the left (12.9%) than the

right (7.7%). Sex was significantly associated with PL presence, while parental origin (mother's origin), (father's origin) and hand dominance were not. Most Jordanians in this study had bilaterally present PL, with notable morphological diversity. Females were more likely to have an absent PL than males, whereas hand dominance and parental origin did not influence its presence. The novel classification of PL variations proposed here may assist surgeons in preoperative evaluation for tendon grafting.

Key words: Palmaris longus types – Forearm anatomy – Graft surgery – Muscle tendon – Palmaris longus classification – Jordanian

INTRODUCTION

Palmaris longus (PL) is one of the superficial flexor muscles in the anterior forearm (Ioannis et al., 2015). It originates from the medial epicondyle of the humerus and inserts into the palmar aponeurosis and flexor retinaculum (Qa'oud et al., 2019). It is innervated by the median nerve (C7,

Corresponding author:

Dr Ahmed Salman, Department of Anatomy and Histology, Faculty of Medicine, The University of Jordan, Amman 11942, Jordan. E-mail: Ahmed.salman@ju.edu.jo

Submitted: December 4, 2025 **Accepted:** December 19, 2025

<https://doi.org/10.52083/IHDX9655>

C8) and supplied by the anterior ulnar recurrent artery and median artery (Anderson and Bordoni, 2025). Anatomically, PL shows a wide range of variations, including reversed, duplicated, bifid, or hypertrophied PL muscles (Park et al., 2010). PL can be absent in parts of the population, either in one or both forearms. For instance, it can be unilaterally absent in 16% of the Caucasian population, while bilaterally absent in 9% (Soltani et al., 2012).

Although the absence of this muscle does not impair wrist or hand function significantly (Sater et al., 2010; Thejodhar et al., 2008), some sources suggest that the presence of the PL tendon increases the risk of carpal tunnel syndrome (Boltuch et al., 2020); others praise its benefits for being a landmark for the median nerve in surgical procedures (Hou et al., 2023).

Palmaris longus is commonly used as a tendon graft in reconstructive surgeries for multiple tendon ruptures (Chu et al., 2008) and provides a reliable option for soft-tissue upper-lip augmentation (Trussler et al., 2008). The palmaris longus tendon (PLT) sling appears to be a safe and effective treatment for children with congenital ptosis requiring frontalis sling operation due to its expendable nature in order to achieve a good functional and structural outcome (Wong et al., 2005).

Palmaris longus is also found in vertebrates, more specifically in mammals only, and is best developed in those that use their forelimbs for ambulation. For example, palmaris longus is always present in orangutans; however, its presence varies in other higher ape species such as chimpanzees and gorillas (Capdarest-Arest et al., 2014; Iqbal et al., 2015).

It is also theorized that palmaris longus absence is associated with a type of hereditary trait. A study showed that the inheritance mode of palmaris longus is aligned with an autosomal dominant transmissional model (Vučinić et al., 2025). Based on these findings, this study hypothesizes that people whose ancestors depend on heavy manual labor (referred in this study as parental origin) have more possibilities to express palmaris longus; consequently, other factors such as hand dominance and sex may influence its ex-

pression.

While the presence of the palmaris longus (PL) in Jordanians has been briefly noted, existing studies are few and lack detailed morphological analysis. Crucially, there is an absence of data applying a modern, nuanced classification system to this population. This gap prevents meaningful comparison of PL variant prevalence with other global populations, and limits the muscle's clinical applicability.

This study, therefore, intends to establish the prevalence and variability of the PL muscle among Jordanians in order to provide information to clinical practitioners useful in gross examination of the forearm, and to add to the PL inheritance.

MATERIALS AND METHODS

Study design, place, and participants

An analytical cross-sectional study was conducted at the University of Jordan in Amman to determine the prevalence of the palmaris longus muscle among students and the relationship of its presence to other factors.

Ethical considerations

The ethical approval for this study was obtained from the institutional review boards (IRB) of the University of Jordan on the 1st of July 2024 (Decision No. 240/2024). Participants were fully informed of the purpose of this study, and verbal informed consent was obtained before participation, which was documented through a required confirmation checkbox at the beginning of the online questionnaire. As no identifiable data were collected, responses were confidentially recorded and securely stored to maintain data integrity.

Data collection procedure

Data for this study were collected through face-to-face interviews with random students at the University of Jordan from July 2024 to October 2024. Participants were excluded based on whether they had a history of surgery involving the palmaris longus tendon or whether they were not Jordanians. After obtaining their consent, interviewers asked participants questions about

their age, nationality, home province (north region [Irbid, Ajloun, Jerash and Mafraq], middle region [Amman, Madaba, Al-Balqa and Zarqa], and south region [Ma'an, Karak, Tafleh and Aqaba]), parental origin (categorized as Bedouin, farmer, or urban), and dominant hand.

Interviewers checked the presence of the palmaris longus muscle by performing a series of tests in the following order to determine on which hand the palmaris longus muscle was prominent: Schaeffer's test, Thompson's test, Mishra's test I, Pushpakumar's test, and Mishra's test II (Fig. 1). The tests used in this research were validated by Mishra (2001) and Sebastin and Lim (2006).

If none of the tests revealed the muscle in the forearm, it was considered absent. After concluding the interview, a photograph of the participants' forearms was taken for further confirmation and reliability checking.

After completion of the data collection, two trained investigators independently used the photo dataset to identify and exclude duplicate entries and participants who met the exclusion criteria; any conflict was resolved by discussion. The photographs were also reviewed to classify the palmaris longus muscle according to its insertion into one of six categories: normal, bifurcated, radial deviation, ulnar deviation, reversed, or absent. We used the Palmaris Longus (PL) tendon as the anatomical guide for classification. Insertion on the ulnar side of the hand was classified as ulnar deviation; insertion on the radial side as radial deviation; and central insertion into the mid-palm as normal. Other variants included a bifurcated tendon (split prior to insertion) and a reversed muscle (distal muscle belly) (Fig. 2).

In cases of disagreement, the photographs were reexamined jointly, and consensus was reached through discussion. If consensus was not reached a senior anatomist was consulted to provide the final judgment. To ensure standardization, all photographs were taken by the same team of two trained investigators using a single camera. Each participants' arm was positioned in a standardized posture designed to clearly demonstrate the PL tendon during each specific test.

Description of the tests used

In Schaeffer's test, each participant is asked to oppose their thumb to their little finger and flex their wrist slightly, which will show a tendon that is medial to the flexor carpi radialis; this is a positive sign of palmaris longus presence (Fig. 1A).

In Thompson's test, each participant is asked to make a fist, flex the wrist against resistance, and the thumb is flexed over the fingers, which will show a tendon that is between the flexor carpi radialis and flexor carpi ulnaris; this is a positive sign of palmaris longus presence (Fig. 1B).

In Pushpakumar's "Two-Finger Sign" test, each participant is asked to fully extend the index and middle fingers while the wrist and other fingers remain flexed, which shows a tendon between the flexor tendons; this is a positive sign of palmaris longus presence (Fig. 1C).

In Mishra's Test I, the examiner hyperextends the metacarpophalangeal joints of all fingers while the participant flexes the wrist; the appearance of a tendon in the wrist region indicates the presence of a PL muscle (Fig. 1D).

In Mishra's Test II, each participant is asked to

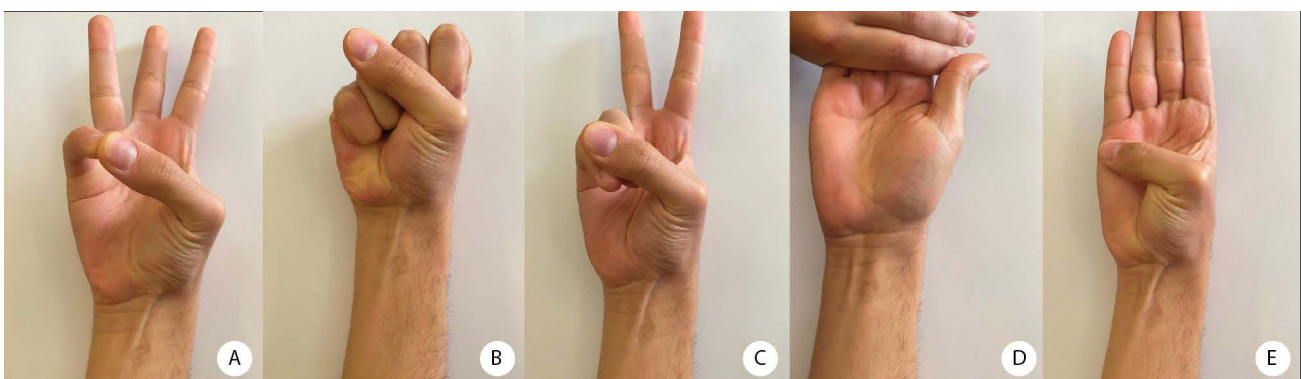


Fig. 1.- Pictures of various clinical tests for testing the presence of the palmaris longus. (A) Schaeffer's test. (B) Thompson's test. (C) Pushpakumar's "two-finger sign". (D) Mishra's test I. (E) Mishra's test II.

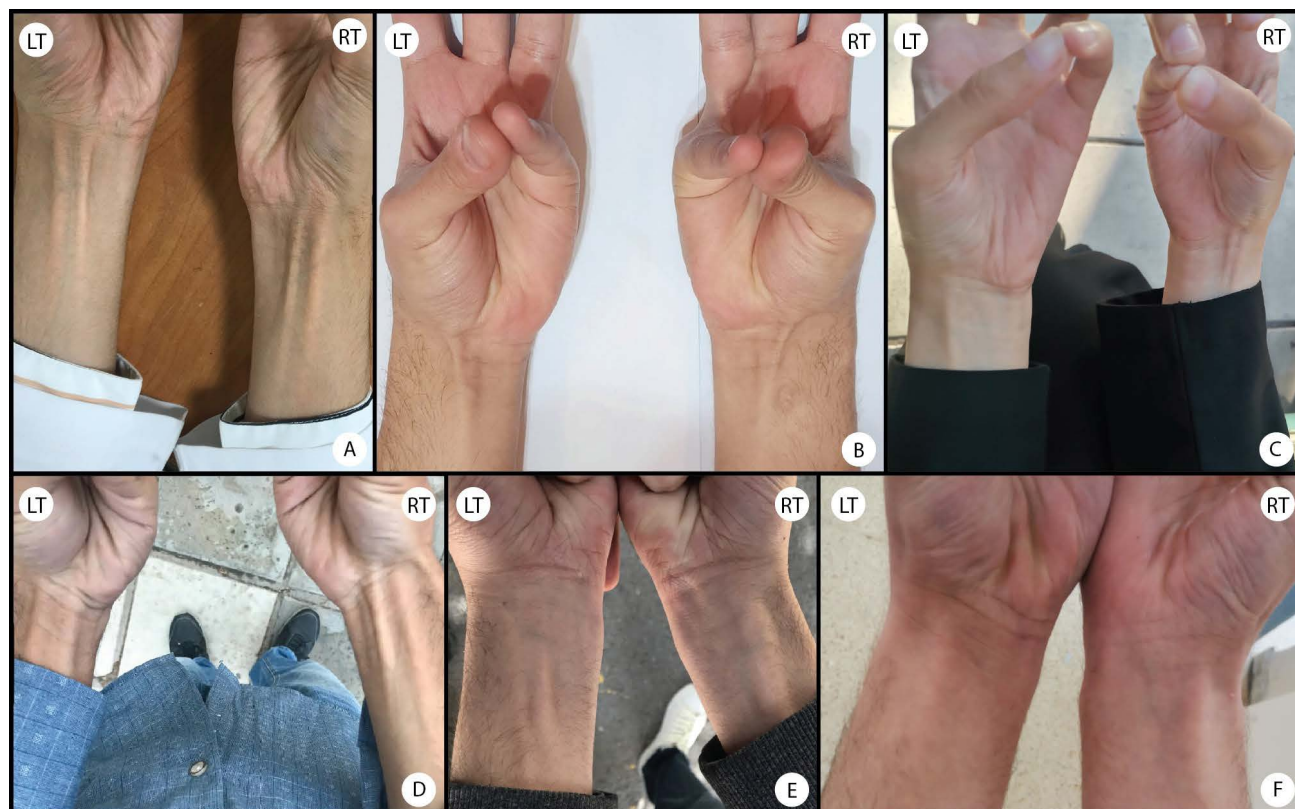


Fig. 2.- These pictures demonstrate types of PL found during the interviews, with (A) representing normal insertion (both forearms), (B) bifurcated insertion (both forearms), (C) radial deviation of insertion (right forearm), (D) ulnar deviation of insertion (left forearm), (E) reversed muscle (right forearm), and (F) bilateral absence. RT: right, LT: left

abduct the thumb against resistance while the wrist is partially flexed, which will show the tendon in the medial wrist during this movement (Fig. 1E).

Data analysis

The statistical software JASP (version 0.19.0.0) was used for data processing and analysis. Descriptive statistics, including frequency and percentage, were calculated for categorical variables, while mean and standard deviation were reported for continuous variables. The chi-square (χ^2) test was used in order to assess the significance of associations between two or more categorical variables. A p-value of less than 0.05 was considered statistically significant.

RESULTS

Participants characteristics

This study included 403 students from the University of Jordan aged between 18 and 56 years old. The mean age of the participants was 21.5 years with a standard deviation of 3.68. The sample was composed of 220 males (54.6%), 183

females (45.4%). Table 1 shows the sociodemographic characteristics of the participants.

Prevalence of Palmaris longus and its types

228 participants showed the presence of the PL muscle in both forearms (56.6%), while 92 did not show any presence of the muscle (22.8%). 83 participants showed unilateral presence of PL, 52 of them having the PL present on the right forearm (12.9%) and 31 on the left forearm (7.7%) (Fig. 3). Regarding the type of the PL muscle, among the 311 participants with a PL muscle (either unilaterally or bilaterally), 110 had a normal PL insertion in both forearms. Additionally, 45 participants had a normal PL insertion in the left forearm only, while 83 participants had it only in the right forearm.

Regarding bifurcation, 11 had both PL muscles bifurcated, 34 had a right bifurcated PL, and 27 had a left bifurcated PL. Twenty-five were found to have radially deviated PL in both forearms, 49 in the right forearm, and 72 in the left forearm.

On ulnar deviation, only one case had an ulnar deviation in both PLs, two had the deviation on the

Table 1. Sociodemographics

Demographics	Frequency	Percentage
Age	21.54 ± 1.99	
Sex		
Male	220	54.6
Female	183	45.4
Home province		
North Region	32	7.9
Middle region	353	87.6
South Region	18	4.5
Fathers' origin		
Farmer	159	39.5
Urban	148	36.7
Bedouin	96	23.8
Mothers' origin		
Farmer	165	40.9
Urban	158	39.2
Bedouin	80	19.9
Hand dominance		
Right-handed	370	91.8
Left-handed	33	8.2

Mean ± SD, frequency (%)

left forearm, and three on the right forearm. Although none of the participants showed reversed PL in both hands, one student had a reversed PL

on the right forearm, and two students had their left PL reversed. Among the 228 participants with bilateral palmaris longus (PL) muscles, only 81

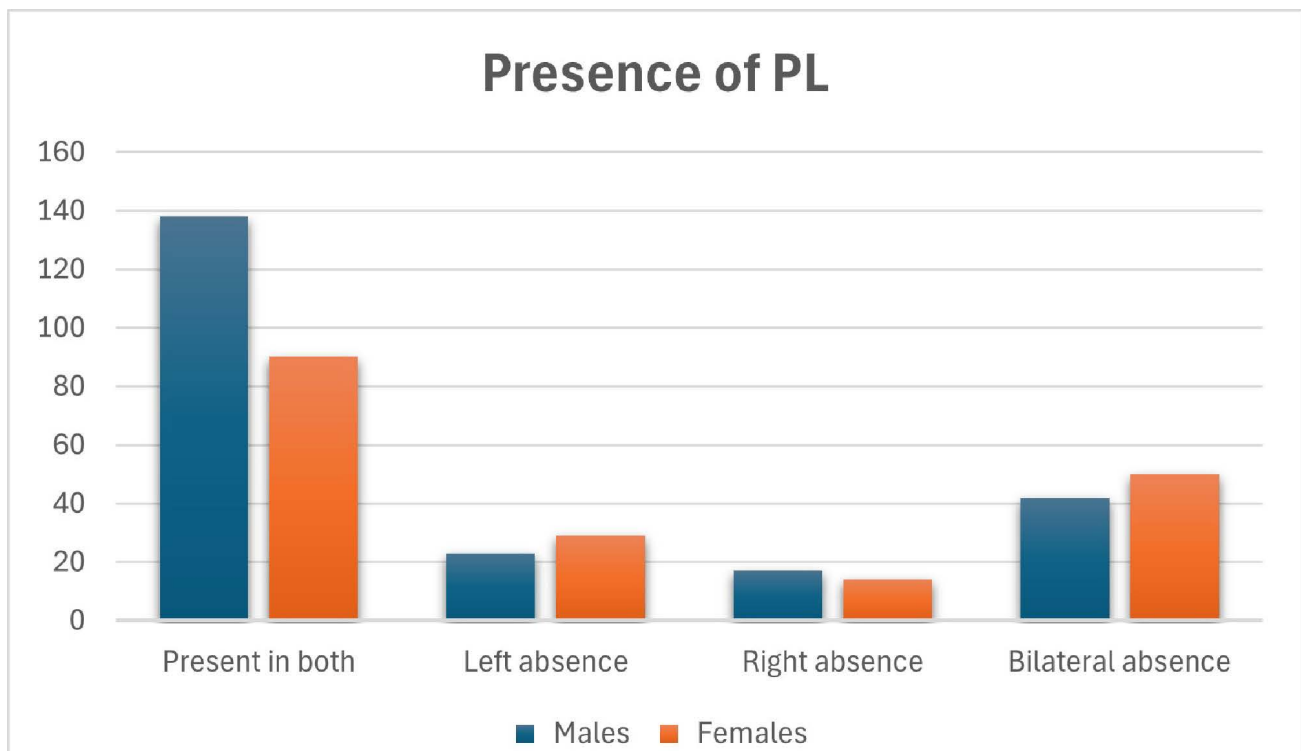


Fig. 3.- The following bar chart presents the distribution of PL muscle presence patterns on forearms, with regard to sex.

Table 2. Prevalence of PL

Palmaris longus presence	Frequency	Percentage
Palmaris longus presence		
Present in both	228	56.6
Left absence	52	12.9
Right absence	31	7.7
Bilateral absence	92	22.8
Types of Palmaris Longus in both forearm		
Both are Normal	110	27.3
Both are bifurcated	11	2.7
Both have a radial deviation	25	6.2
Both have an ulnar deviation	1	0.3
Asymmetric	81	20.1
Unilateral absence	83	20.6
Bilateral absence	92	22.8
Type of Palmaris Longus in the right forearm		
Normal	193	47.9
Bifurcated	34	8.4
Radial deviation	49	12.2
Ulnar deviation	3	0.7
Reversed	1	0.3
Absent	123	30.5
Type of Palmaris Longus in the left forearm		
Normal	156	38.7
Bifurcated	27	6.7
Radial deviation	72	17.9
Ulnar deviation	2	0.5
Reversed	2	0.5
Absent	144	35.7

* The total sample size of the types of PL in both forearms is 228 due to the exclusion of unilateral and bilateral absence.

(20.1%) exhibited morphologically distinct PL insertion types between their left and right forearms. The prevalence and variations of PL insertions across all participants are detailed in Table 2.

Bivariate analysis

The study found a statistically significant association between the presence of PL and sex, in which males were more likely to have PL present in both forearm than females ($p = 0.037$), and no significant association was found regarding mothers' origin, $p = 0.719$, fathers' origin ($p = 0.656$) nor hand dominance ($p = 0.372$). Table 3 shows the results of the analysis.

DISCUSSION

This study found that the majority of the participants had a PL muscle, mostly bilaterally, with considerable anatomical variation regarding insertion, bifurcation, and deviation, while the muscle was completely absent in almost one quarter of them. Unilateral PL presented right-sided predominance, and asymmetrical morphology between forearms was demonstrated in one-fifth of the individuals with bilateral PL. PL presence was highly associated with sex, as males were more likely to present bilateral PL, whereas no association was found regarding parental origin and hand dominance.

Table 3. Bivariate analysis

Variable	Present in both	Left absence	Right absence	Bilateral absence	p-value
Sex					0.037*
Males	138	23	17	42	
Females	90	29	14	50	
Fathers' origin					0.656
Urban	85	17	15	31	
Farmer	89	21	8	41	
Bedouin	54	14	8	20	
Mothers' origin					0.719
Urban	93	20	14	31	
Farmer	94	21	9	41	
Bedouin	41	11	8	20	
Hand dominance					0.372
Right	211	45	30	84	
Left	17	7	1	8	

The study was conducted at the University of Jordan as a way to represent the Jordanian population. The sample contained students from different governorates. Since PL presence is determined genetically (Morais, 2013; Thompson et al., 1921; Vučinić et al., 2018) and not influenced by age, the student population at the University of Jordan serves as a suitable representation of the broader Jordanian population.

In this study, 56.6% of participants had PL present in both hands. Comparing these results with other studies that tried to investigate the prevalence of the absence of the palmaris longus (PL) muscle in various populations yielded interesting results. The highest prevalence of PL in both forearms was seen in the Yoruba ethnic population of Nigeria (93.3%) (Mbaka and Ejiwunmi, 2009), and the lowest was seen in Turkey (36.1%) (Ceyhan and Mavt, 1997). The Egyptian population showed a prevalence of 65.7% (Qa'oud et al., 2019), which is close to the Bahraini (63.2%) (Sater et al., 2010) and Jordanian population (61.4%) (Freih and Samir, 2008). The Palestinian population exhibited a prevalence of 58% (Sabouba et al., 2021), whereas the Malaysian population (Malay ethnic group) had a significantly higher prevalence of 88.3% (Yong et al., 2017) (Table 4).

In this sample, bifurcated PL insertion was observed in 15.1% of participants unilaterally (8.4%

on the right and 6.7% on the left), while bilateral bifurcated PL was present in 2.7% of participants. In comparison, the Bahraini study (Sater et al. 2010) reported a bilateral bifurcation rate of 2.1% and a unilateral rate of 5%, which are lower than this study's unilateral and bilateral rates.

This study's findings corroborate the established relationship between sex and PL muscle presence observed in previous literature. The majority of studies—including those conducted in Bahrain (Sater et al., 2010), Malaysia (Yong et al., 2017), and Palestine (Sabouba et al., 2021)—reported higher PL absence rates in females. However, Erić et al. (2011) documented an opposing trend, with males showing greater bilateral absence. Meanwhile, several studies found no statistically significant sex-based differences (Kapoor et al., 2008; Mbaka and Ejiwunmi, 2009; Qa'oud et al., 2019). These inconsistent findings across populations suggest potential geographic or ethnic variations in PL morphology (Table 4).

As demonstrated by previous studies, PL follows an autosomal dominant inheritance pattern with variable expression (Vučinić et al., 2025). Incomplete penetrance is affected by multiple factors, including modifier genes, environmental factors, epigenetic regulation, age-related penetrance, and sex. Among these, sex influences best explain the study's findings (Yong et al., 2017).

Table 4. Comparison between different studies that investigated the prevalence of the palmaris longus

Study	Population	Overall absence	Unilateral absence	Bilateral absence	Sex differences	Side differences
This study's findings	Jordan	43.4	20.6	22.8	Higher bilateral absence in females	Left-sided absence higher
Eric et al. (2010)	Vojvodina, Serbia	37.5	21.6	15.9	Bilateral absence is higher in males (18.5% vs 13.3% in females)	Left-sided absence is higher in females (17.3% vs 8.8% in males); right-sided absence is higher in males (12.3% vs 5% in females)
Qa'oud et al. (2019)	Egypt	34.3	19.1	15.2	No significant sex relationship	Right-sided absence is higher
Sater et al. (2010)	Bahrain	36.8	Not specified	Not specified	Higher absence in females	Left-sided absence higher
Sabouba et al. (2021)	Palestine	32	Not specified	Not specified	Higher absence in females	Left-sided absence higher
Yong et al. (2017)	Malay population	11.7	8.0	3.7	Higher absence in females	Left-sided absence higher
Ceyhan and Mavt (1997)	Gaziantep, Turkey	63.9	Not specified	Not specified	Not specified	Not specified
Freih and Samir (2008)	Jordan	38.6	Not specified	Not specified	Not specified	Not specified
Thompson et al. (2001)	Northern Ireland	Not specified	Not specified	Not specified	Higher absence in males	Not specified
Kapoor et al. (2008)	India	Not specified	Not specified	Not specified	Higher absence in males, but not significant	Not specified
Mbaka et al. (2008)	Nigeria	Not specified	Not specified	Not specified	Higher bilateral absence in males	Not specified
Mbaka and Ejiwunmi (2009)	Yoruba, Nigeria	6.7	5.4 (males) / 6.0 (females)	Not specified	No significant sex association	Not specified

The numbers above are written as percentages

While some studies suggest that the palmaris longus (PL) muscle is better developed in mammals relying on forelimbs for locomotion (Capdarest-Arest et al., 2014; Iqbal et al., 2015), the study found no association between participants' ancestral origins (including lineages with historically strenuous occupations like farming) and PL presence. These results challenge the study's initial hypothesis that genetic selection related to occupational demands influenced PL expression. Furthermore, the study observed no correlation between PL absence (unilateral or bilateral) and hand dominance, a finding consistent with several previous studies (Eric et al., 2011; Qa'oud et al., 2019; Yong et al., 2017).

Overall, PL presence appears to be affected by ethnicity, sex, and body side, with a higher prevalence in Africa and Southeast Asia compared to

the Middle East region.

This study highlights useful information about anatomical variations of the palmaris longus, mainly for clinical practitioners during their physical examination and surgical planning. These findings enhance the understanding of PL multiple patterns and contribute to the understanding of the theory behind its inheritance and existence by other factors. This study lays the ground for future research that aims to understand the variants' morphology for the palmaris longus. The findings of this study have direct implications for clinical practice, potentially in surgical planning for tendon grafting procedures. Knowledge of the PL presence and its morphological variation allow surgeons to anticipate potential anatomical challenges and to select suitable tendons, minimizing intraoperative complications. The classification

proposed here offers enhanced granularity compared to previous systems by including radial and ulnar deviations, bifurcation, reversed muscles, and asymmetry between left and right forearms, providing a more comprehensive framework for identifying PL variants.

Limitations

This work is based on a visual evaluation of the palmaris longus tendon by clinical tests and photographs only, without dissection or imaging confirmation. Whilst the sensitivity and reproducibility of clinical assays are well established, small differences may remain un-noticed. The study population are University of Jordan students and may not serve as an accurate representation of the general Jordanian population. Prospective imaging or cadaveric dissection studies are required to confirm the classification and evaluate its generalizability.

While the classification is based on validated clinical tests and photographic assessment, future studies should incorporate ultrasound, MRI, or cadaveric dissection to confirm these observations and further validate the classification's reproducibility. Additionally, expanding the study population beyond university students to include a broader age range and diverse geographical regions in Jordan could improve generalizability. Clinicians are encouraged to apply this classification in preoperative evaluations and anatomical education, and researchers should consider integrating imaging or dissection studies to refine the understanding of PL morphology and its clinical relevance.

CONCLUSION

In conclusion, this study investigated the prevalence of PL in Jordan and found that sex was associated with its presence, whereas hand dominance and parental origin were not. This finding does not support the initial hypothesis of the potential influence of occupational type on PL gene expression. Moreover, this study provided new data on anatomical variation of PL that are observable during routine clinical examination, along with the relative frequency of each type. These findings may assist the surgeons in preop-

erative evaluation when considering the PL tendon for grafting procedures. Further research is warranted to explore the underlying cause of the observed sex differences and to expand further knowledge on PL morphology.

AUTHORS' CONTRIBUTIONS

Mohammad Al-Shalalfeh: Data collection and management, Investigation, Methodology, Formal analysis, Software, Prepared figures 1-3, Writing – original draft, Writing – review and editing. Ahmad Alaudat: Data collection and management, Investigation, Methodology, Writing – original draft, Writing – review and editing. Saqer Ayyash: Conceptualization, Writing – original draft, Writing – review and editing. Ahmed Salman: Supervision, Conceptualization, Methodology, Writing – review and editing, Project administration.

REFERENCES

- ANDERSON TB, BORDONI B (2025) Anatomy, Shoulder and Upper Limb, Forearm Nerves. In *StatPearls*. Treasure Island (FL): StatPearls Publishing.
- BOLTUCH AD, MARCOTTE MA, TREAT CM, MARCOTTE AL (2020) The palmaris longus and its association with carpal tunnel syndrome. *J Wrist Surg*, 9(6): 493-497.
- CAPDAREST-AREST N, GONZALEZ JP, TÜRKER T (2014) Hypotheses for ongoing evolution of muscles of the upper extremity. *Medical Hypotheses*, 82(4): 452-456.
- CEYHAN O, MAVT A (1997) Distribution of agenesis of palmaris longus muscle in 12 to 18 years old age groups. *Indian J Med Sci*, 51(5): 156-160.
- CHU P-J, LEE H-M, HOU Y-T, HUNG S-T, CHEN J-K, SHIH J-T (2008) Extensor-tendons reconstruction using autogenous palmaris longus tendon grafting for rheumatoid arthritis patients. *J Orthop Surg Res*, 3: 16.
- ERIC M, KRIVOKUĆA D, SAVOVIĆ S, LEKSAN I, VUCINIĆ N (2010) Prevalence of the palmaris longus through clinical evaluation. *Surg Radiol Anat*, 32(4): 357-361.
- ERIC M, KOPRIVČIĆ I, VUČINIĆ N, RADIĆ R, KRIVOKUĆA D, LEKŠAN I, SELTHOFER R (2011) Prevalence of the palmaris longus in relation to the hand dominance. *Surg Radiol Anat*, 33(6): 481-484.
- FREIH AH, SAMIR J (2008) Absence of the palmaris longus tendon in Mid-Eastern population. *J Bahrain Med Soc*, 20: 70-73.
- HOU P, YU W, WANG C, QIU S, SUN L, ZHANG W (2023) The position of the median nerve in relation to the palmaris longus tendon at the wrist: a study of 784 MR images. *J Hand Surg*, 48(7): 630-634.
- IOANNIS D, ANASTASIOS K, KONSTANTINOS N, LAZAROS K, GEORGIOS N (2015) Palmaris longus muscle's prevalence in different nations and interesting anatomical variations: -review of the literature. *J Clin Med Res*, 7(11): 825-830.
- IQBAL S, IQBAL R, IQBAL F (2015) A bitendinous palmaris longus: aberrant insertions and its clinical impact - a case report. *J Clin Diagn Res*, 9(5): AD03-AD05.
- KAPOOR SK, TIWARI A, KUMAR A, BHATIA R, TANTUWAY V, KAPOOR S (2008) Clinical relevance of palmaris longus agenesis: common anatomical aberration. *Anat Sci Int*, 83(1): 45-48.
- MBAKA GO, AKINLOLU AA, AYANUGA AO, SHALLIE PD, ADEFULE AK, AKPAN HB, EJIWUNMI AB (2008) The incidence of agenesis of palmaris longus among the Yoruba Tribe in Nigeria. *Nigerian J Med Rehab*, 11-14.
- MBAKA GO, EJIWUNMI AB (2009) Prevalence of palmaris longus absence--a

study in the Yoruba population. *Ulster Med J*, 78(2): 90-93.

MISHRA S (2001) Alternative tests in demonstrating the presence of palmaris longus. *Indian J Plastic Surg*, 34(01): 012-014.

MORAIS MA, SANTOS WG, MALYSZ T (2013) Agenesis of palmaris longus muscle: is this a phenotype of variable expressivity?" *J Morphol Sci*, 30(4): 249-253.

PARK MJ, NAMDARI S, YAO J (2010) Anatomic variations of the palmaris longus muscle. *Am J Orthop (Belle Mead, N.J.)*, 39(2): 89-94.

QA'OD M, AL-ZOUBI A, JARADAT M (2019) Palmaris longus tendon absence prevalence in an Egyptian population. *World Family Med J / Middle East J Family Med*, 17: 14-19.

SABOUBAM, AB-ALWAFAR, MHESIN D, ZIDAN E, ZORBAF, QADDUMI J (2021) Prevalence of absence of the palmaris longus muscle among medical students of An-Najah National University: a cross-sectional study from Palestine. *Palest Med Pharmac J*, 7(1).

SATER MS, DHARAP AS, ABU-HIJLEH MF (2010) The prevalence of absence of the palmaris longus muscle in the Bahraini population. *Clin Anat*, 23(8): 956-961.

SEBASTIN SJ, LIM AYT (2006) Clinical assessment of absence of the palmaris longus and its association with other anatomical anomalies-- a Chinese population study. *Ann Acad Med Singapore*, 35(4): 249-253.

SOLTANI AM, PERIC M, FRANCIS CS, NGUYEN TJ, CHAN LS, GHIASSI A, STEVANOVIC MV, WONG AK (2012) The variation in the absence of the palmaris longus in a multiethnic population of the United States: an epidemiological study. *Plastic Surg Int*, 2012(1): 282959.

THEJODHAR P, POTU BK, VASAVI RG (2008) Unusual palmaris longus muscle. *Indian J Plastic Surg*, 41(1): 95-96.

THOMPSON JW, MCBATTS J, DANFORTH CH (1921) Hereditary and racial variation in the musculus palmaris longus. *Am J Physical Anthropol*, 4(2): 205-218.

THOMPSON NW, MOCKFORD BJ, CRAN GW (2001) Absence of the palmaris longus muscle: a population study. *Ulster Med J*, 70(1): 22-24.

TRUSSLER AP, KAWAMOTO HK, WASSON KL, DICKINSON BP, JACKSON E, KEAGLE JN, JARRAHY R, BRADLEY JP (2008) Upper lip augmentation: palmaris longus tendon as an autologous filler. *Plastic Reconst Surg*, 121(3): 1024-1032.

VUČINIĆ N, ERIĆ M, GRGUREVIĆ L, DUMIĆ-ČULE I, TIČINOVIĆ N (2018) Palmaris longus absent in one identical twin: a case report. *Acta Clin Croatica*, 57(4): 772-775.

VUČINIĆ N, NOVAKOVIĆ AD, ERIĆ M, PUPOVAC N (2025) Testing the inheritance pattern of palmaris longus muscle absence." *Surg Radiol Anat*, 47(1): 131.

WONG CY, FAN DSP, NG JSK, GOH TYH, LAM DSC (2005) Long-term results of autogenous palmaris longus frontalis sling in children with congenital ptosis. *Eye (London)*, 19(5): 546-548.

YONG MW, YUSOF N, RAMPAL L, ARUMUGAM M (2017) Prevalence of absence of palmaris longus and its association with gender, hand dominance and absence of FDS tendon to little finger among Malay population. *J Hand Surg Asian-Pacific*, 22(4): 484-489.

Age-related morphological transformations of cephalometric parameters in artificially deformed and non-deformed skulls: a comparative craniometric analysis across successive life stages

Anar Abdullayev

Department of Human Anatomy and Medical Terminology, Azerbaijan Medical University, Baku, Azerbaijan

SUMMARY

The human skull is a biologically dynamic structure that undergoes continuous morphological modification throughout the lifespan. These changes reflect intrinsic developmental processes, as well as extrinsic influences, including culturally mediated practices such as artificial cranial deformation. Comparative craniometric research provides an effective framework for assessing how age-related skeletal remodeling interacts with deformation-induced constraints, thereby contributing to broader understandings of craniofacial plasticity, skeletal adaptation, and population variability. This study aimed to conduct a comparative craniometric analysis of age-related morphological changes in artificially deformed and non-deformed skulls, focusing on cranial indices, skull shape distributions, and proportional relationships across successive life stages. A total of 254 adult and subadult skulls from the osteological collection of Azerbaijan Medical University were examined, including 200 non-deformed and 54 artificially deformed spec-

imens. Age classification followed an established anthropological age-periodization system. Standard craniometric measurements were obtained, including cranial length, breadth, height, and facial dimensions, from which key cranial and facial indices were calculated. Statistical analysis was performed using IBM SPSS Statistics (v.26.0), with Pearson's Chi-square test applied to assess associations between age, deformation status, and cranial morphology. In non-deformed skulls, brachycranic forms predominated in younger individuals, with a gradual shift toward mesocranic and dolichocranic configurations in later age groups. Elderly individuals exhibited a higher prevalence of euryprosopic facial morphology. In contrast, artificially deformed skulls demonstrated a consistently high frequency of metriocrania across all age categories, indicating relative stabilization of cranial proportions. Younger deformed skulls were characterized by broad and moderately high cranial vaults with predominantly mesoprosopic facial forms. Adult age groups displayed increased variability in cranial indices, particu-

Corresponding author:

Sardar Abdullayev Anar. Department of Human Anatomy and Medical Terminology, Azerbaijan Medical University, Baku, Azerbaijan. E-mail: anarabdullaeva72@mail.ru - ORCID: 0000-0002-7447-5311

Submitted: January 10, 2026 Accepted: February 3, 2026

<https://doi.org/10.52083/HNSP6274>

larly in length–breadth relationships. Statistically significant differences were observed between deformed and non-deformed skulls in the trajectory of age-related cranial index changes ($p \leq 0.05$). Age-related cranial remodeling follows distinct morphological trajectories in artificially deformed and non-deformed skulls. Artificial cranial deformation appears to constrain natural age-dependent variability, resulting in more stable proportional patterns throughout the lifespan. These findings contribute to anthropological, anatomical, and clinical perspectives on craniofacial growth, cultural body-modification practices, and skeletal adaptation.

Key words: Craniometrics – Artificial cranial deformation – Age-related changes – Skull morphology – Cephalic index

INTRODUCTION

The cranial base represents one of the earliest-forming and structurally most complex regions of the human skeleton. Located at the superior aspect of the axial skeleton, it develops through tightly regulated processes of endochondral and intramembranous ossification, and serves as a structural foundation for the cranial vault and facial skeleton (Enlow and Hans, 1996). Functionally, the cranial base protects the central nervous system (CNS), supports sensory organs, and provides passageways for major neurovascular structures, including cranial nerves and arterial vessels (Moore et al., 2018).

Cranial development is closely synchronized with CNS growth, and disturbances in cranial base morphogenesis may lead to significant neurological consequences. Congenital anomalies such as basilar invagination, basilar impression, and platybasia are well-recognized contributors to craniovertebral junction disorders, including Chiari malformation and syringomyelia (Tubbs et al., 2011). Despite advances in imaging and developmental biology, the etiological mechanisms underlying many cranial base anomalies remain incompletely understood, underscoring the importance of morphometric and anthropological approaches (Standring, 2021).

Cranial anomalies are typically defined as per-

sistent deviations from normative skeletal development originating during embryonic or fetal life. These deviations may be diagnosed at birth or identified later in childhood or adulthood. Etiological factors are multifactorial and include endogenous influences such as genetic mutations, advanced or very young parental age, and endocrine disorders, as well as exogenous agents such as ionizing radiation, teratogenic drugs, environmental toxins, and prenatal infections (Sadler, 2019). Genetic mutations, particularly monogenic disorders, account for a significant proportion of congenital craniofacial anomalies.

Clinically, abnormalities of the craniovertebral junction may remain asymptomatic for extended periods or present during adolescence or early adulthood, most commonly between 20 and 40 years of age (Milhorat et al., 2010). Disorders of cranial morphogenesis also represent a substantial cause of perinatal and infant morbidity and mortality, highlighting their clinical and public health significance (Moore et al., 2018).

Beyond pathological variation, the cranial vault undergoes continuous remodeling throughout life. Age-related changes influence cranial dimensions, vault thickness, facial proportions, and cranial indices, reflecting both mechanical and biological adaptation (White et al., 2012). Importantly, some morphological variations coexist with normal neurological function, whereas others are associated with CNS abnormalities (Lieberman, 2011).

Artificial cranial deformation, practised historically by numerous populations worldwide, offers a unique anthropological model for examining the interaction between cultural modification and biological growth. By mechanically altering cranial shape during early development, artificial deformation modifies growth trajectories and long-term cranial proportions (Anton, 1989; Dingwall, 1931).

The present study aimed to analyze age-related cephalometric changes in artificially deformed and non-deformed skulls from the osteological collection of Azerbaijan Medical University, focusing on patterns of cranial adaptation across successive life stages.

MATERIALS AND METHODS

Sample Composition

The study analyzed 254 human skulls curated in the craniological collection of Azerbaijan Medical University. The sample included 200 non-deformed skulls and 54 skulls exhibiting clear morphological evidence of artificial cranial deformation. Sex determination was performed using standard morphological criteria of the cranial vault and base (White et al., 2012).

The non-deformed series consisted of 86 male and 114 female skulls, while the deformed series included 22 male and 32 female specimens.

Age Classification

Age estimation and grouping followed the classification system adopted at the VII All-Union Conference on Age Morphology, Physiology, and Biochemistry (1965). Skulls were categorized into the following age groups:

- Youth
- Early adulthood (Period I)
- Middle adulthood (Period II)
- Elderly

The age distribution comprised 20 skulls from the youth group, 68 from early adulthood, 72 from middle adulthood, and 40 from the elderly group.

Craniometric measurements

Craniometric measurements were obtained according to internationally accepted anthropological standards (Martin and Saller, 1957). The following indices were calculated:

- Cranial (cephalic) index (maximum breadth \times 100 / maximum length)
- Length–height cranial index
- Height–breadth cranial index
- Upper facial index

Measurements were performed using calibrated spreading and sliding calipers to ensure precision and reproducibility.

Statistical analysis

Statistical analysis was conducted using IBM SPSS Statistics (Version 26.0). Descriptive statistics were calculated for all variables. Associations between age group, deformation status, and cranial morphology were evaluated using Pearson's Chi-square test. A significance level of $p \leq 0.05$ was considered statistically significant.

RESULTS

Craniometric classification criteria

In accordance with classical craniometric methodology (Martin and Saller, 1956–1962; Buikstra and Ubelaker, 1994), skull morphology was classified using four principal indices:

- Width–length (cephalic) index: dolichocranial (long), mesocranial (medium), brachycranial (broad);
- Height–length index: chamaecranial (low), orthocranial (medium), hypsicranial (high);
- Height–breadth index: tapeinocranial (low), metriocranial (intermediate), acrocranial (high);
- Upper facial index: wide (euryprosopic), medium (mesoprosopic), and long (leptoprosopic) facial types.

These indices provide a standardized framework for evaluating age-related changes in cranial proportions and facial morphology.

Craniometric characteristics of undeformed skulls

Analysis of undeformed skulls revealed pronounced age-related variation across all major cranial indices (Table 1). With respect to the width–length index, dolichocranial skulls were least frequent in youth (5.0%) and reached their highest representation during early adulthood (23.5%), followed by a gradual decline in later age groups. Mesocranial forms similarly peaked in early adulthood (30.9%), and declined markedly in the elderly (10.0%). In contrast, brachycranial skulls showed a clear age-associated increase, reaching their highest prevalence in elderly individuals (72.5%), indicating progressive cranial

Table 1. Age-related distribution of craniometric characteristics in undeformed skulls (N, %)

Index	Skull type	Youth	Early adulthood	Late adulthood	Elderly
Width–length index	Dolichocranial	1 (5.0)	16 (23.5)	10 (13.9)	7 (17.5)
	Mesocranial	6 (30.0)	21 (30.9)	17 (23.6)	4 (10.0)
	Brachycranial	13 (65.0)	31 (45.6)	45 (62.5)	29 (72.5)
Height–length index	Chamaecranial	1 (5.0)	9 (13.2)	10 (13.9)	5 (12.5)
	Orthocranic	3 (15.0)	22 (32.4)	22 (30.6)	9 (22.5)
	Hypsicranial	16 (80.0)	37 (54.4)	40 (55.6)	26 (65.0)
Height–breadth index	Tapeinocranic	5 (25.0)	22 (32.4)	27 (37.5)	17 (42.5)
	Metriocranic	12 (60.0)	30 (44.1)	32 (44.4)	17 (42.5)
	Acrocranial	3 (15.0)	16 (23.5)	13 (18.1)	6 (15.0)
Upper facial index	Wide face (Euryprosopic)	7 (35.0)	27 (39.7)	38 (52.8)	25 (62.5)
	Medium face (Mesoprosopic)	10 (50.0)	24 (35.3)	19 (26.4)	7 (17.5)
	Long face (Leptoprosopic)	3 (15.0)	17 (25.0)	15 (20.8)	8 (20.0)

Values are presented as absolute number (percentage). Percentages are calculated within each age group.

broadening with age.

Height–length index analysis demonstrated a strong predominance of hypsicranial morphology in youth (80.0%). Although hypsicrania remained the dominant type across all age categories, its relative frequency decreased modestly with advancing age, accompanied by incremental increases in orthocranic and chamaecranial forms. This trend suggests gradual vertical remodeling of the cranial vault during adulthood and senescence.

Assessment of the height–breadth index revealed a gradual shift toward tapeinocranic morphology with age, whereas metriocranic forms remained relatively stable across adulthood before declining slightly in the elderly. Acrocranial forms exhibited no consistent age-dependent trend.

Facial index analysis demonstrated a pronounced age-related transformation. Wide-faced (euryprosopic) morphology increased progressively from youth (35.0%) to old age (62.5%), while medium and long facial types declined correspondingly. This finding reflects age-dependent remodeling of the maxillofacial skeleton and corroborates previous osteological studies documenting facial widening in older populations (Brown and Armelagos, 2020; Flament et al., 2022).

Collectively, these results confirm that undeformed skulls undergo dynamic, age-dependent remodeling characterized by increasing cranial

breadth, reduced longitudinal dominance, and progressive facial widening.

Craniometric characteristics of artificially deformed skulls

In contrast with the undeformed series, artificially deformed skulls exhibited a markedly different pattern of cephalometric variation (Table 2). Across nearly all age categories, cranial proportions remained relatively stable, indicating long-term structural constraint imposed by early-life deformation practices.

With respect to the width–length index, brachycranial morphology predominated in all age groups, ranging from 54.8% to 68.0%, while dolichocranial forms were rare or absent, particularly in youth. Mesocranial skulls constituted a secondary but consistent proportion across age categories, suggesting limited post-deformational variability.

Height–length index analysis showed a strong and persistent predominance of hypsicranial morphology, especially in youth (87.5%) and the elderly (80.0%). Unlike undeformed skulls, no clear age-related decline in cranial height was observed. Similarly, the height–breadth index demonstrated sustained dominance of metriocrania, reinforcing the stabilizing effect of artificial deformation on cranial vault proportions.

Facial morphology in deformed skulls displayed

greater heterogeneity than in undeformed specimens. Although wide faces were common, medium and long facial types persisted across all age groups. Notably, the proportion of long faces increased in the elderly (28.0%), suggesting selective remodeling of the facial skeleton despite constrained cranial vault dimensions.

Overall, artificially deformed skulls demonstrated limited age-related morphological change, with early-life mechanical constraints exerting a lasting influence on cranial proportions.

Comparative analysis

Comparative evaluation of undeformed and deformed skulls revealed fundamental differences in age-related cranial remodeling trajectories. Undeformed skulls exhibited substantial morphological variability across age categories, with a clear progression from dolichocranic and mesocranic forms in youth and early adulthood toward brachycranial dominance in old age. In contrast, deformed skulls maintained relatively stable cranial indices throughout life, with persistent dominance of metriocranic and brachycranial configurations.

Facial index comparison further highlighted this divergence. Undeformed skulls demonstrated a strong and consistent trend toward euryprosopia with advancing age, whereas deformed skulls showed a more heterogeneous facial pattern, with wide, medium, and long faces coexisting across age groups. These findings indicate that artificial

cranial deformation modifies the natural age-related trajectory of craniofacial remodeling by constraining growth patterns during early ontogeny and stabilizing cranial proportions thereafter (Anton and Weinstein, 2021; Torres-Rouff and Yablonsky, 2019).

DISCUSSION

The present findings confirm and extend classical anthropological observations regarding age-related transformations of cranial morphology. In undeformed skulls, the gradual shift from dolichocrania to brachyocrania across the lifespan reflects cumulative remodeling processes influenced by biomechanical loading, cranial suture dynamics, and senescent skeletal adaptation (Lieberman, 2011; Kohn and Leigh, 2022). The increasing prevalence of euryprosopic facial morphology in older individuals is consistent with documented age-related changes in the maxillofacial complex and may reflect both genetic predisposition and lifelong functional adaptation.

Artificial cranial deformation, by contrast, exerts a dominant and enduring influence on cranial development. The persistence of stabilized cranial indices across all age categories indicates that deformation practices imposed during infancy and early childhood effectively override natural growth trajectories. This observation aligns with prior studies demonstrating the long-term structural stability of artificially modified skulls across diverse cultural contexts (Cocilovo and Rothham-

Table 2. Age-related distribution of craniometric characteristics in artificially deformed skulls (N, %)

Index	Skull type	Youth	Early adulthood	Late adulthood	Elderly
Width–length index	Dolichocranial	0 (0.0)	2 (6.3)	3 (9.7)	2 (8.0)
	Mesocranial	3 (37.5)	9 (28.1)	11 (35.5)	6 (24.0)
	Brachycranial	5 (62.5)	21 (65.6)	17 (54.8)	17 (68.0)
Height–length index	Chamaecranial	0 (0.0)	3 (9.4)	2 (6.5)	1 (4.0)
	Orthocranic	1 (12.5)	7 (21.9)	8 (25.8)	4 (16.0)
	Hypsicranial	7 (87.5)	22 (68.8)	21 (67.7)	20 (80.0)
Height–breadth index	Tapeinocranic	2 (25.0)	7 (21.9)	9 (29.0)	6 (24.0)
	Metriocranic	5 (62.5)	19 (59.4)	17 (54.8)	13 (52.0)
	Acrocranial	1 (12.5)	6 (18.8)	5 (16.1)	6 (24.0)
Upper facial index	Wide face (Euryprosopic)	4 (50.0)	12 (37.5)	14 (45.2)	10 (40.0)
	Medium face (Mesoprosopic)	3 (37.5)	14 (43.8)	10 (32.3)	8 (32.0)
	Long face (Leptoprosopic)	1 (12.5)	6 (18.8)	7 (22.6)	7 (28.0)

Note. Values are presented as absolute number (percentage). Percentages are calculated within each age group.

mer, 2018; Krenn and Urban, 2019).

From a clinical perspective, these results underscore the importance of distinguishing culturally induced cranial modifications from pathological anomalies when interpreting craniofacial morphology. Understanding the stabilizing effects of early mechanical constraints also provides valuable insight into cranial bone plasticity and the limits of post-developmental remodeling. From an anthropological standpoint, the findings contribute to reconstructing population history, cultural practices, and biological adaptation.

In summary, age-related cephalometric changes follow divergent pathways in undeformed and artificially deformed skulls. While undeformed skulls exhibit progressive remodeling characterized by cranial broadening and facial widening, deformed skulls maintain constrained and relatively stable morphological parameters throughout life. These results highlight the complex interaction between biological aging processes and cultural modification practices, and emphasize the necessity of integrating both dimensions in craniometric and bioarchaeological research.

Age-related variability in artificially deformed skulls

Analysis of artificially deformed skulls revealed limited age-dependent variability across most cephalometric indices, reflecting the long-term stabilizing effects of early mechanical modification. According to the height–length index, chamaecranial (low-vault) morphology was present in several age groups; however, its distribution did not follow a consistent age-related trend. This irregular pattern suggests that vertical cranial dimensions in deformed skulls are largely constrained by early deformation rather than modified progressively with aging (Anton and Weinstein, 2021).

Evaluation of the height–breadth index demonstrated that acrocranial (high-vault) forms reached their highest frequency during the second phase of adulthood (28.0%), while the lowest prevalence was recorded in early adulthood (15.8%). In contrast, metriocrania (intermediate vault proportions) predominated in the youth and

elderly groups, with a relative reduction observed in early adulthood. This pattern indicates minor fluctuations in cranial vault proportions across the lifespan, although without evidence of a systematic remodeling trajectory (Krenn and Urban, 2019; Torres-Rouff and Yablonsky, 2019).

The upper facial index exhibited more pronounced age-related differentiation. Wide-faced (euryprosopic) morphology was most frequently observed among elderly individuals with deformed skulls, whereas it was nearly absent in youth. Conversely, long-faced (leptoprosopic) morphology predominated during early and late adulthood and reached its highest frequency in the elderly group (83.3%). Notably, leptoprosopia was not observed in young individuals with cranial deformation, suggesting that facial proportions may retain some capacity for age-related modification even when cranial vault growth is mechanically constrained (Brown and Armelagos, 2020; Kohn and Leigh, 2022).

Overall, these findings indicate that, while artificial cranial deformation substantially limits age-related variability in cranial vault indices, selective remodeling of the facial skeleton may continue throughout adulthood and senescence.

Statistical interpretation of age–index relationships in deformed skulls

The relationship between age and cranial morphology in deformed skulls was further evaluated using the Pearson Chi-square (X^2) test (Table 4). Statistical analysis demonstrated a marginal association between age and the width–length (cephalic) index ($X^2 = 12.200$, $df = 6$, $p = 0.058$), approaching but not reaching the conventional threshold for statistical significance ($p < 0.05$). This borderline result suggests that longitudinal–transverse cranial proportions may exhibit limited age-related variability even in the presence of early deformation.

In contrast, no statistically significant associations were identified between age and the height–length index ($X^2 = 4.995$, $p = 0.544$), height–breadth index ($X^2 = 9.545$, $p = 0.145$), or upper facial index ($X^2 = 9.387$, $p = 0.153$). These findings indicate that vertical cranial proportions

and overall facial indices remain largely stable across the lifespan once artificial deformation is imposed during early ontogeny.

From a biomechanical and developmental perspective, the absence of significant age-related correlations supports the hypothesis that artificial cranial deformation exerts a dominant and lasting influence on cranial growth patterns, effectively constraining subsequent remodeling processes (Cocilovo and Rothhammer, 2018; Lieberman, 2011). Minor fluctuations observed in facial morphology may reflect adaptive remodeling of the viscerocranium rather than fundamental changes in cranial vault architecture.

In summary, statistical analysis confirms that artificial cranial deformation significantly reduces age-related variability in most cephalometric indices, with only limited evidence of age-dependent change in width–length proportions. These results reinforce the importance of considering early cultural modification practices when interpreting cranial variation in anthropological, forensic, and clinical contexts.

CONCLUSION

The findings of the present craniometric study demonstrate that age-related cranial remodeling follows markedly different morphological trajectories in non-deformed and artificially deformed skulls. In the non-deformed series, brachycranial skull forms were predominant during youth; however, with advancing age, a gradual transition toward mesocranial and dolichocephalic configurations was observed. This pattern reflects the natural processes of cranial growth, biomechanical adaptation, and senescent remodeling that characterize the human skull across the lifespan. In parallel, a statistically significant increase in the prevalence of euryprosopic (broad facial) morphology was identified among older individuals, corroborating previous anthropological investigations conducted on European and Asian populations, which have consistently reported facial widening as a characteristic feature of advanced age (Brown and Armelagos, 2020; Flament et al., 2022).

In contrast, artificially deformed skulls exhib-

ited a notably higher degree of morphological stability across successive age categories. *Metriocrania* remained the dominant cranial type in nearly all age groups, indicating that mechanical constraints imposed during early ontogeny substantially limit the scope of subsequent age-related cranial remodeling. Deformed skulls in youth were characterized by exceptionally broad and moderately high cranial vaults combined with predominantly mesoprosopic facial forms. In intermediate age groups, only minor variability in cranial length and width was detected, suggesting constrained adaptive potential. Among elderly individuals with deformed skulls, wide and elongated facial morphologies were frequently observed, with long-faced forms reaching exceptionally high frequencies.

Comparative analysis clearly indicates that both the percentage distribution of cranial types and the correlation between cranial indices and aging differ significantly between deformed and non-deformed skulls. Whereas non-deformed skulls undergo progressive age-dependent remodeling manifested by cranial shape transitions and facial widening, artificially deformed skulls maintain relatively stabilized morphological parameters throughout life.

From an anthropological perspective, these results provide compelling evidence of the interaction between biological aging processes and culturally mediated cranial modification practices, emphasizing how early-life mechanical interventions permanently reshape cranial growth trajectories. From a clinical and forensic standpoint, the findings enhance the interpretation of craniofacial variation, facilitate differentiation between pathological anomalies and culturally induced modifications, and improve the diagnostic applicability of cranial indices in osteological analysis.

Overall, this study confirms that artificial cranial deformation significantly alters the natural course of age-related cranial morphological change, underscoring the necessity of integrating both biological and cultural determinants in craniometric and bioarchaeological research.

ACKNOWLEDGEMENTS

The author gratefully acknowledges the Department

of Anatomy and Anthropology of Azerbaijan Medical University for granting access to the osteological collections used in this study. Special appreciation is extended to the technical and laboratory staff for their assistance with specimen handling, measurement procedures, and standardization of craniometric data.

REFERENCES

- ANTON SC (1989) Intentional cranial vault deformation and induced changes of the cranial base and face. *Am J Phys Anthropol*, 79(3): 253-267.
- ANTON SC, WEINSTEIN KJ (2021) Artificial cranial deformation and craniofacial growth: A reassessment of long-term effects. *Am J Phys Anthropol*, 174(1): 85-99.
- BANDALIEVA A (2025) The ethical dimensions of medicine and environmental consciousness in the works of Nizami Ganjavi: A historical inquiry into proto-bioethical thought in medieval Azerbaijani culture. *Sci Educ Innovat Context Modern Problems*, 8(11): 1303-1311.
- BROWN KR, ARMELAGOS GJ (2020) Craniometric variation and the biological impact of aging: An osteological perspective. *J Anat*, 236(5): 921-932.
- BUIKSTRA JE, UBELAKER DH (1994) *Standards for data collection from human skeletal remains*. Arkansas Archaeological Survey Research Series, No. 44.
- CAPASSO L, KENNEDY KAR, WILCZAK CA (1999) *Atlas of occupational markers on human remains*. Edigrafital.
- COCILOVO JA, ROTHHAMMER F (2018) Morphometric analysis of cranial deformation in prehistoric Andean populations. *Homo*, 69(6): 325-338.
- COHEN MM (2017) Developmental anomalies of the skull: Embryology and genetics. *Am J Med Gen Part A*, 173(5): 1301-1316.
- DINGWALL EJ (1931) *Artificial cranial deformation: A contribution to the study of ethnic mutilations*. John Bale, Sons & Danielsson.
- ENLOW DH, HANS MG (1996) *Essentials of facial growth*. W. B. Saunders.
- FLAMENT F, JACQUET L, YE C, AMAR D, KEROB D, JIANG R, ZHANG Y, KROELY C, DELAUNAY C, PASSERON T (2022) Artificial intelligence analysis of facial aging in European and Chinese populations. *J Eur Acad Dermatol Venereol*, 36(7): 1136-1142.
- HRDLIČKA A (1912) *Manual of physical anthropology*. Wistar Institute of Anatomy and Biology.
- KENDOULI N, KANDI MA (2025) La digitalisation comme outil de dynamisation de la gouvernance d'entreprise: Étude de cas d'une PME algérienne (CASA Médical). *Sci, Educ Innovat Context Modern Problems*, 8(11): 370-381.
- KOHN LA, LEIGH SR (2022) Craniofacial growth across the lifespan: A morphometric and evolutionary perspective. *Evolut Anthropol*, 31(4): 176-190.
- KRENN V, URBAN M (2019) Artificial cranial deformation in European archaeological contexts: Morphological and cultural aspects. *Int J Osteoarchaeol*, 29(6): 1009-1020.
- LAHR MM (1996) *The evolution of modern human diversity: A study of cranial variation*. Cambridge University Press.
- LIEBERMAN DE (2011) *The evolution of the human head*. Harvard University Press.
- MARTIN R, SALLER K (1956-1962) *Lehrbuch der Anthropologie in systematischer Darstellung* (Vol. 2). Gustav Fischer.
- MILHORAT TH, CHOU MW, TRINIDAD EM, KULA RW, MANDELL M, WOLPERT C, SPEER MC (2010) Chiari I malformation: Redefining the clinical and radiological spectrum. *J Neurosurg*, 90(1): 150-156.
- MOORE KL, PERSAUD TVN, TORCHIA MG (2018) *The developing human: Clinically oriented Embryology* (10th ed.). Elsevier.
- O'BRIEN MJ, HUNT TL (2019) Cranial modification as cultural practice: A bioarchaeological review. *Annl Rev Anthropol*, 48: 309-326.
- RISSECH C, ESTABROOK GF, MALGOSA A (2006) Cranial suture closure as a method for age estimation: A test on a documented Spanish sample. *Am J Phys Anthropol*, 130(1): 51-58.
- SADLER TW (2019) *Langman's medical embryology* (14th ed.). Wolters Kluwer.
- SAOUD A, NOUACER A (2025) Folk medicine practices among the Tuareg of Hoggar through The Tuareg in the North by Henri Duveyrier (1840–1892). *Sci Educ Innovat Context Modern Problems*, 8(7): 400-412.
- STANDRING S (Ed.) (2021) *Gray's anatomy: The anatomical basis of clinical practice* (42nd ed.). Elsevier.
- TORRES-ROUFF C, YABLONSKY LT (2019) *Cranial modification and identity: An integrative approach*. *Curr Anthropol*, 60(5): 679-695.
- TUBBS RS, OAKES WJ, COHEN-GADOL AA (2011) *The Chiari malformations*. Springer.
- WHITE TD, BLACK MT, FOLKENS PA (2012) *Human osteology* (3rd ed.). Academic Press.

Efficacy and wider perspectives on the Rigo-Chêneau Brace in adolescent idiopathic scoliosis: a retrospective perspective

José M. Morales-de-Pando¹, Juan Sánchez-Palacios¹, Gloria González-Medina^{2,3}, José A. Prada-Oliveira⁴

¹ Rehabilitation Services, Puerta del Mar University Hospital, Andalusian Health Service, Cádiz, Spain

² Department of Human Anatomy and Embryology, University of Cadiz, Cádiz, Spain

³ Department of Physiotherapy, University of Cadiz, Cádiz, Spain

⁴ Instituto de Investigación Biomédica de Cádiz, INIBICA, Cádiz, Spain

SUMMARY

This retrospective study evaluates the effectiveness of the Rigo-Chêneau brace, one of the most widely used three-dimensional orthoses in Europe, in the management of adolescent idiopathic scoliosis. Although the literature on brace effectiveness remains limited and clinical protocols vary, our objective was to provide a recent analysis of retrospective results obtained in routine clinical practice. Data from a total of 35 patients seen in rehabilitation services between 2011 and April 2023 were analyzed; all met the Scoliosis Research Society (2005) standardization criteria: age ≥ 10 years, Risser index 0–2, and a curve magnitude of 25° to 40° . The variables studied included Cobb angle magnitude, vertebral rotation according to the Nash and Moe scale, and the need for surgery. The results indicate that the Rigo-Chêneau brace is effective in controlling the magnitude of the curve. Specifically, 80% of patients maintained or improved their curve angulation at the end of treatment. A significant finding was the improvement or maintenance of verte-

bral rotation in 100% of patients, demonstrating its corrective action in the transverse plane. Effectiveness in preventing surgery was 100% in this cohort of selected patients. Consistent brace wear (adherence greater than 18 hours per day) is also associated with significantly lower curve progression. The Rigo-Chêneau brace showed high effectiveness for musculoskeletal immature patients with moderate adolescent idiopathic scoliosis.

Key words: Brace Rigo-Chêneau – Adolescent idiopathic scoliosis – Orthotic treatment – Cobb angle – Musculoskeletal immaturity

INTRODUCTION

Adolescent Idiopathic Scoliosis (AIS) is the most common spinal deformity in otherwise healthy adolescents, with an approximate prevalence of 2% to 4%. It is characterized by a three-dimensional torsion of the spine (Kleinberg, 1922; Negrini et al., 2018a). Early diagnosis and intervention are essential to prevent progression and the potential need for surgical correction. Conservative treatment with brace use remains the main

Corresponding author:

Dr. J.A. Prada-Oliveira. Department of Human Anatomy and Embryology, Facultad de Medicina, Plaza Fragela s/n, Universidad de Cádiz, Cádiz 11003, Spain. E-mail: arturo.prada@uca.es

Submitted: December 31, 2025. **Accepted:** February 16, 2026.

<https://doi.org/10.52083/LMBZ5741>

strategy to halt progression, avoid surgical fusion, and optimize spinal alignment.

The radiological diagnosis requires a complete spine standing image. The superior frontal plane of one affected vertebra together with the inferior border of the vertebra below show the highest relative until the so-called Cobb's angle. A Cobb's angle greater than 10° with a component of vertebral rotation provides the diagnosis of scoliosis (Goldberg et al., 1988; Zmurko et al., 2003). The scoliotic curve can increase its angulation during periods of rapid body growth, mainly during puberty (Grivas et al., 2006a, b). It is well established in the consensus guides that treatment is indicated once it exceeds 20° if progression is observed, or 25° without progression (Cheung et al., 2019). The angle progression tends to decrease clearly after the final vertebral growth and ossification, except in $>50^\circ$ severe scoliosis (Weinstein et al., 2013). The Cobb's angle tend to increase significantly beyond 30° (Zmurko et al., 2003). These conditions are usually associated with pain, respiratory and cardiac alterations, and impaired functional capacity of the spine.

The Rigo-Chêneau brace (RCB) is one of the most widely used three-dimensional orthoses in Europe. Its design is based on principles of three-dimensional correction and the application of asymmetric forces, seeking correction in both the frontal and transverse planes (Rigo et al., 2003; Rigo and Weiss, 2008). This represents an evolution compared to traditional Boston-type braces (Rigo and Jelacic, 2017).

Despite its widespread use, the existing literature on the actual effectiveness of braces is often limited and inconclusive, with significant variations in clinical protocols between different treatment clinical units. Gradual discontinuation of the brace is recommended, with a very low level of evidence and without a standardized process (Rigo et al., 2003). The variability in current medical indications in clinical practice ranges from a 25% reduction in the number of hours of daily use to removal according to the patient's own convenience (Aulisa et al., 2009). Therefore, the present study aimed to assess the clinical effectiveness of the RCB through a retrospective analysis of outcomes in clinical practice. We focused on a com-

prehensive set of variables, which are essential for accurately evaluating the true clinical efficiency of the RCB.

There is no absolute consensus on this issue, nor scientific literature that supports one model over another, beyond the subjective experience and assessment of rehabilitation physicians. Our objective is to determine clinical parameters of improvement that allow early discontinuation, facilitating return to sports and recreational activities, and reducing the emotional burden and impact of brace use. It is important to reduce side effects so that they do not negatively affect posture, cause skin injuries, or cause back pain. Analyzing the effects in a cohort of patients treated with RCB, based on clinical parameters of improvement and quantification of the effectiveness of RCB use, will allow greater increase in its efficacy while minimizing the personal and iatrogenic medical effects of this treatment.

MATERIALS AND METHODS

Study design and patient selection

The study design was a retrospective analysis. Patient selection was carried out through a search in the Diraya System (integrated health information management system of the Andalusian Health Service) in the Rehabilitation Departments of the Puerta del Mar and the Puerto Real Universities Hospitals of the Andalusian Health Service (SAS), covering the period from 2011 to April 2023.

Initially, 142 patients treated with the RCB were identified (111 females, 31 males). The inclusion criteria were based on the 2005 standardization of the Scoliosis Research Society (SRS) and included: age equal to or greater than 10 years; Risser index 0 to 2, premenarche or less than one year since menarche; curve magnitude 25° to 40° before starting bracing; and no previous treatment (Negrini et al., 2018a; Shi et al., 2016).

After applying the criteria, 107 patients were excluded, resulting in a main analytical cohort of 35 patients with a diagnosis of AIS and a treatment plan with the RCB. An analysis of a related cohort, composed of 45 adolescents (37 females and 8

males), revealed a mean age of 158,4 months at the beginning of treatment.

Variables and measurements

The study variables included sex, age, duration of treatment, Risser stage (at the beginning and at the end), magnitude of the main and compensatory curves (at the beginning and at the end), vertebral rotation, and whether surgery was necessary.

The variables were defined and measured as follows. The gender, as the biological sex of the patient, was reentered as either male or female. The age at treatment initiation was the patient's chronological age, measured in months, defined at the time the Cheneau brace treatment was prescribed and initiated. Finally, the treatment duration was defined as the total length of time, typically calculated in months, from the initial brace fitting to the formal conclusion of the bracing treatment.

The Risser sign is a critical indicator of skeletal maturity. It is assessed from anteroposterior pelvic radiographs, graded on a scale from 0 (no ossification) to 5 (complete fusion of the iliac apophysis). The two distinct time measurement points were the baseline Risser—as the grade at the initiation of brace treatment—and the final Risser—as the grade at the final treatment discontinuation.

Cobb Angle was used to quantify the severity of scoliosis, measured in degrees on standing posteroanterior spinal radiographs. The main curve (the largest structural one) and the compensatory (secondary) curve were recorded. This angle is essential to understand the maintenance of sagittal and coronal balance. Both curve magnitudes were recorded at the start of treatment (baseline) and at the brace-weaning.

The anatomical reference to vertebral rotation (as Nash and Moe Scale) was assessed as the axial rotation of the vertebra at the apex of the main curve. This rotation was graded (from 0 to 4), based on the position of the pedicle shadow relative to the vertebral body on the anteroposterior radiograph.

RESULTS

35 patients were included in the study (30 females (85.7%) and 5 males (14.3%)). Previously, seventy-five percent of patients in this series were excluded based on SRS criteria, with 40% excluded for advanced maturity indicators. The mean age at the start of brace treatment was 147 months. The average treatment duration was 37.12 months.

The Risser sign values for skeletal maturity were 25 patients at stage 0 (71.4%), 2 at stage 1 (5.7%), 8 at stage 2 (22.8%) at baseline. Adherence was a key factor, since patients with more than 18 hours of daily compliance showed significantly less progression of the curve. When examining the angular outcomes in the main cohort of 35 patients, 80% of the patients maintained or improved the curve angulation at the end of treatment. The RCB appeared effective at containing curve magnitude, as shown by mean Cobb angles before and after treatment. The effect on curve magnitude and rotation was Cobb angle of the main curve of 30.03° (mean \pm SD) at the initial stage, and 28.86° (mean \pm SD) after treatment (Fig. 1).

Regarding the three-dimensional results, the effectiveness of the RCB was remarkable in controlling vertebral torsion. The vertebral rotation was maintained or improved in 100% of patients, with 91.4% showing stabilization of the rotation and 8.6% achieving an improvement (Fig. 2).

About the compensatory curve, 75% of the patients showed no significant changes. Finally, the effectiveness in preventing surgery was 100% within the study's selection parameters (curves of 25-40 degrees). However, it was identified that four patients, who were outside the main cohort and presented with Risser 0 and curves greater than 45 degrees, could not avoid surgery despite the use of the brace.

DISCUSSION

The primary and most fundamental component in the initial management of scoliosis is rigid bracing. The Rigo-Chêneau brace (RCB) is the most frequently utilized orthosis, even within the Spanish public health system. Its widespread use is attributable to the force vectors generated by its

MAIN CURVE ANGLE

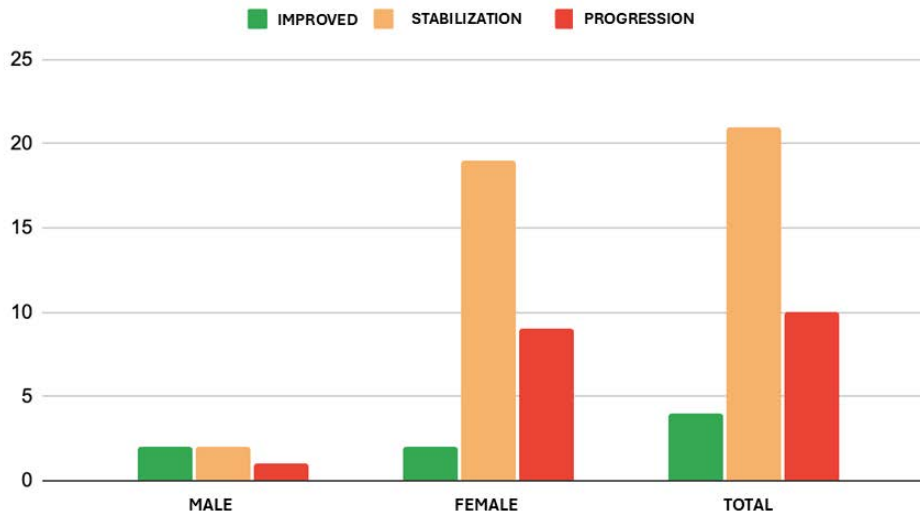


Fig. 1.- Represents the modifications in the main vertebral angle after treatment. The results show the distribution between male, female and total of patients. The X axis represents the number of improved cases (green bar), stabilized cases (orange bar) and progressed to increase angle (red bar); the Y axis represents the number of cases.

specific design, which effectively counteract the vertebral rotational component of the deformity (Rowe et al., 1997; Rigo and Jelacic, 2017). The objective of brace therapy is to halt or mitigate the progression of the scoliotic curve to prevent it from exceeding 50° prior to the attainment of skeletal maturity (Negrini et al., 2018b).

Brace treatment has been associated with substantial psychological and emotional sequelae (Ovadia et al., 2012; Clayson and Levine, 1976), as evidenced by numerous studies reporting nega-

tive alterations in body image, diminished self-esteem (Fällstrom et al., 1986), exposure to bullying, and withdrawal from routine activities, including sports participation and social interactions (Saabye et al., 1986). These psychosocial impacts frequently lead to attempts to conceal the orthosis or to premature discontinuation of the treatment. In a 2002 publication, Andersen proposed that earlier cessation of brace use may mitigate the psychological burden experienced by patients undergoing orthotic management (Andersen et

VERTEBRAL ROTATION

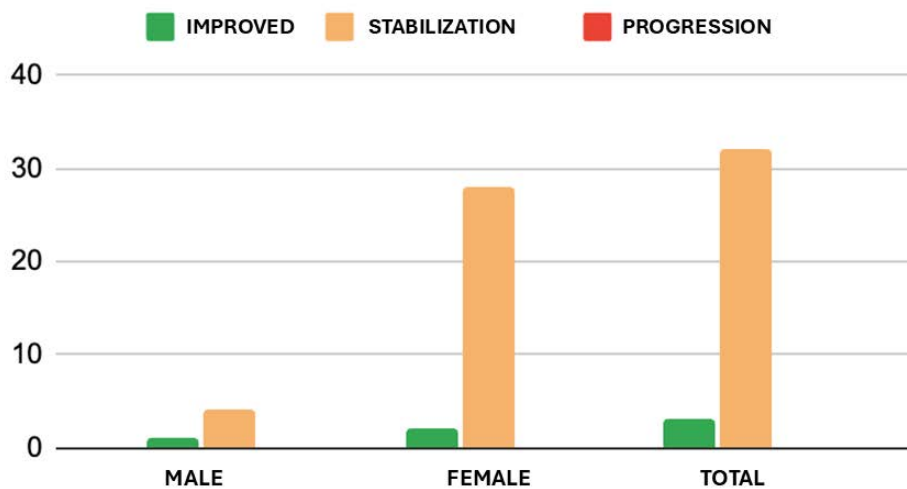


Fig. 2.- Represents the vertebral rotation after treatment. The results show the distribution between male, female and total of patients. The X axis represents the number of improved cases (green bar) and stabilized cases (orange bar); the Y axis represents the number of cases.

al., 2002).

Once prescribed, brace-wearing protocols may include nocturnal use, part-time use, or full-time use (Katz et al., 2010). Nevertheless, the superiority of full-time bracing (23 hours per day) has been extensively documented in the literature (Shi et al., 2016; Piantoni et al., 2018). Consequently, the current clinical recommendation is to initiate treatment with a full-time bracing regimen.

Discontinuation of the brace was recommended to be gradual, although the evidence was poor and the process was not standardized (Isçi et al., 2025). The variability of the medical indications currently applied in clinical practice ranges from a 25% reduction in the number of hours of daily use to withdrawal according to the patient's own convenience (Maruyama et al., 2003; Negrini et al., 2018b). There was no absolute consensus on this issue, nor scientific literature supporting one or another (Canavese and Kaelin, 2011). The objective data were provided by the experience and assessment of rehabilitation physicians themselves.

The findings of this study support the notion that RCB is an effective conservative treatment for AIS. The RCB offers similar or superior results compared to Boston-type braces, especially with three-dimensional spinal realignment. Complete control of vertebral rotation (100% maintained or improved) is a finding that supports the superiority of the RCB's 3D approach for correcting the torsional component of the scoliotic deformity (Fig. 2). Clinical effectiveness is closely linked to compliance; high daily wear times (16-23 hours/day) have been consistently associated with better outcomes. The principle of selecting patients with moderate curves (25-40°) (Fig. 1) and skeletally immature patients was a critical factor for success, as demonstrated by the 100% surgery-avoidance rate in the main cohort.

Nevertheless, certain limitations must be acknowledged. The retrospective design restricts the ability to establish a direct causal relationship and to control for all confounders. Furthermore, the study cohort, although well defined by the SRS criteria, resulted in a limited sample size, which could affect the generalizability of the results.

Finally, reliance on self-reported compliance measures to assess brace adherence introduces potential recall and social desirability bias, underscoring the need to use objective monitoring methods in future research. Prospective studies with objective wear time monitoring are recommended to consolidate the evidence.

The Rigo-Chêneau brace demonstrates clinically significant efficacy in limiting scoliotic curve progression in adolescents with idiopathic scoliosis, particularly when prescribed early and worn consistently in skeletally immature patients. These findings underscore the clinical relevance of timely orthotic intervention and emphasize the necessity of continuous patient and family education to promote optimal treatment adherence. Future investigations should aim to refine brace design through biomechanical and materials research and to develop individualized, evidence-based treatment protocols integrating patient-specific factors such as curve pattern, growth potential, and adherence profiles.

As final considerations, we support a long-term series of results that summarize the improvement of brace treatment in AIS. These results partially coincided with the literature, although we need to increase patient recruitment to prove the importance of different retirement protocols. As mentioned, there is not an absolute consensus around the best brace withdrawal procedure, and we consider that this might be a central point to be discussed to the best patient integration to social, sport and psychological environment. We need to involve other rehabilitation units in order to observe the vertebral correction up until the RCB, nevertheless once was proved to be to the best of our results the best treatment AIS. Our main limitation was related to the recruitment of other treatment unit results, which use to employ different withdrawal procedures.

REFERENCES

- ANDERSEN MØ, ANDERSEN GR, THOMSEN K, CHRISTENSEN SB (2002) Early weaning might reduce the psychological strain of Boston bracing: a study of 136 patients with adolescent idiopathic scoliosis at 3.5 years after termination of brace treatment. *J Pediatr Orthop B*, 11(2): 96-99.
- AULISA AG, GUZZANTI V, GALLI M, PERISANO C, FALCIGLIA F, AULISA L (2009) Treatment of thoraco-lumbar curves in adolescent females affected by idiopathic scoliosis with a progressive action short brace (PASB): assessment of results according to the SRS committee on bracing and nonoperative

management standardization criteria. *Scoliosis*, 4: 21.

CANAVESE F, KAELIN A (2011) Adolescent idiopathic scoliosis: Indications and efficacy of nonoperative treatment. *Indian J Orthop*, 45(1): 7-14.

CHEUNG JPY, CHEUNG PWH, LUK KD (2019) When should we wear bracing for adolescent idiopathic scoliosis? *Clin Orthop Relat Res*, 477(9): 2145-2157.

CLAYSON D, LEVINE DB (1976) Adolescent scoliosis patients. Personality patterns and effects of corrective surgery. *Clin Orthop Relat Res*, 116: 99-102.

FÄLLSTRÖM K, COCHRAN T, NACHEMSON A (1986) Long-term effects on personality development in patients with adolescent idiopathic scoliosis. Influence of type of treatment. *Spine*, 11(7): 756-758.

GOLDBERG MS, POITRAS B, MAYO NE, LABELLE H, BOURASSA R, CLOUTIER R (1988) Observer variation in assessing spinal curvature and skeletal development in adolescent idiopathic scoliosis. *Spine*, 13(12): 1371-1377.

GRIVAS TB, VASILIADIS E, MOUZAKIS V, MIHAS C, KOUFOPOULOS G (2006a) Association between adolescent idiopathic scoliosis prevalence and age at menarche in different geographic latitudes. *Scoliosis*, 1: 9.

GRIVAS TB, VASILIADIS E, SAVVIDOU O, MOUZAKIS V, KOUFOPOULOS G (2006b) Geographic latitude and prevalence of adolescent idiopathic scoliosis. *Stud Health Technol Inform*, 123: 84-89.

ISÇI H, ÖZDEMİR GÖRGÜ S (2025) Understanding bracing outcomes in adolescents with idiopathic scoliosis: a mixed-methods approach. *Front Rehabil Sci*, 6: 1625736.

KATZ DE, HERRING JA, BROWNE RH, KELLY DM, BIRCH JG (2010) Brace wear control of curve progression in adolescent idiopathic scoliosis. *J Bone Joint Surg Am*, 92(6): 1343-1352.

KLEINBERG S (1922) The operative treatment of scoliosis. *Arch Surg*, 5(3): 631-645.

MARUYAMA T, KITAGAWA T, TAKESHITA K, MOCHIZUKI K, NAKAMURA K (2003) Conservative treatment for adolescent idiopathic scoliosis: can it reduce the incidence of surgical treatment? *Pediatr Rehabil*, 6: 215-219.

NEGRINI S, DONZELLI S, AULISA AG, CZAPROWSKI D, SCHREIBER S, DE MAUROY JC, DIERS H, GRIVAS TB, KNOTT P, KOTWICKI T, LABELLE A, MARTI C, MARUYAMA T, O'BRIEN J, PRICE N, PARENT E, RIGO M, ROMANO M, STIKELATHER L, WYNNE J, ZAINA F (2018a) 2016 SOSORT guidelines: orthopaedic and rehabilitation treatment of idiopathic scoliosis during growth. *Scoliosis Spinal Disord*, 13: 3.

NEGRINI S., DONZELLI S, DI FELICE F, ZAINA F, CARONNI A (2018b) Brace treatment for idiopathic scoliosis: State of the art and review of the literature. *Eur J Phys Rehabil Med*, 54(3): 383-392.

OVADIA D, EYLON S, MASHIAH A, WIENTROUB S, LABELLE ED (2012) Factors associated with the success of the Rigo System Chêneau brace in treating adolescent idiopathic scoliosis. *Scoliosis*, 7: 16.

PIANTONI L, TELLO CA, REMONDINO RG, FRANCHERI WILSON IA, GALARETTO E, NOEL MA (2018) When and how to discontinue bracing treatment in adolescent idiopathic scoliosis: results of a survey. *Scoliosis Spinal Disord*, 13: 23.

RIGO M, JELAČIĆ M (2017). Brace technology thematic series: the 3D Rigo Chêneau-type brace. *Scoliosis Spinal Disord*, 12: 1-46.

RIGO M, REITER CH, WEISS HR (2003) Effect of conservative management on the prevalence of surgery in patients with adolescent idiopathic scoliosis. *Pediatr Rehabil*, 6(3-4): 209-214.

RIGO M, WEISS HR (2008) The Chêneau concept of bracing—biomechanical aspects and clinical results. *Stud Health Technol Inform*, 135: 303-319.

ROWE DE, BERNSTEIN SM, RIDDICK MF, ADLER F, EMANS JB, GARDNER-BONNEAU D (1997) A meta-analysis of the efficacy of non-operative treatments for idiopathic scoliosis. *J Bone Joint Surg Am*, 79(5): 664-674.

SAABYE J, CHRISTOFFERSEN H, LUND K (1986) Efterundersøgelse af 46 patienter med idiopatisk adolescent skoliose. Fysiske, psykiske og sociale aspekter. *Ugeskr Laeger*, 148(20): 1230-1231.

SHI B, GUO J, MAO S, WANG Z, YU FW, LEE KM, NG BK, ZHU Z, QIU Y, CHENG JC, LAM TP (2016) Curve progression in adolescent idiopathic scoliosis

with a minimum of 2 years' follow-up after completed brace weaning with reference to the SRS standardized criteria. *Spine Deform*, 4(3): 200-205.

WEINSTEIN SL, DOLAN LA, WRIGHT JG, DOBBS MB (2013) Effects of bracing in adolescents with idiopathic scoliosis. *N Engl J Med*, 369(16): 1512-1521.

ZMURKO MG, MOONEY JF, PODESZWA DA, MINSTER GJ, MENDELOW MJ, GUIRGUES A (2003) Inter- and intraobserver variance of Cobb angle measurements with digital radiographs. *J Surg Orthop Adv*, 12(4): 208-213.

Adverse effects of zinc oxide nanoparticles on the prostate gland of adult albino rat and the possible protective role of rutin C: histological, immunohistochemical and biochemical study

Mohamed Z. Kotb, Afaf A. Mohamed, Amany E. Hamoud, Fayza A.R.A. Gawad, Reda I. Amer

Anatomy and Embryology Department, Faculty of Medicine, Cairo University, Egypt

SUMMARY

The unavoidable and intangible human exposure to zinc oxide nanoparticles (ZnONPs) carries a great risk of toxicities to different organs. Nanoparticles (NPs) are widely applied in many foods, water, medicine, cosmetics, agricultural, and industrial fields. The current study aimed to evaluate ZnONPs-induced histopathological and biochemical changes on the prostate of rats and investigate the possible prophylaxis by combined Rutin and vitamin C against these changes. Four equal groups of total forty adult male albino rats were randomly assigned (control, vehicle control, ZnONPs, and ZnONPs + Rutin C groups). Histological examination was done using hematoxylin and eosin and Masson's trichrome stains. Proliferating cell nuclear antigen (PCNA) and prostatic specific antigen (PSA) were used in an immunohistochemical analysis. Measurements of serum PSA, oxidation marker malondialdehyde (MDA) and reduced glutathione (GSH) were also performed.

ZnONPs group revealed distorted prostatic acini with thickened inter-acinar stroma exhibiting

congested blood vessels and inflammatory cells, in addition to disturbed oxidative-antioxidative balance with elevated serum PSA. ZnONPs and Rutin C group showed marked improvement of the prostatic architecture with restoration of the oxidative-antioxidative balance and serum PSA. Our study concluded that the administration of ZnONPs to rats injured their prostates both histologically and biochemically. Rutin C has a protective role against the toxic effect of ZnONPs.

Key words: Zinc oxide nanoparticle – Prostate gland – Rutin C – Rat – Histological

INTRODUCTION

The prostate plays an essential role in reproduction via its vital secretions carrying and feeding sperms. Prostatic inflammation will inevitably impair male fertility and reproductive ability (Mortrich et al., 2018).

Nanoparticles (NPs) are widely applied in many foods, water, medicine, cosmetic, agricultural, and industrial fields (Pinho et al., 2020). The

Corresponding author:

Mohamed Zakaria Kotb. 10 Wali al Ahd street- Hadayek al Qoba – Cairo, Egypt. Phone: +2/01001082011. E-mail: mohamed_zakaria@kasralainy.edu.eg

Submitted: January 13, 2026. **Accepted:** February 26, 2026

<https://doi.org/10.52083/SCYJ5230>

unavoidable and intangible human exposure to NPs carries a great risk of toxicities to different organs (Mabrouk et al., 2021). NPs' toxicity was documented to be more invasive compared to large-sized materials' toxicity, as they can readily access the circulation and bypass different biological barriers to enter the cells and cause variable toxic effects (Xie et al., 2022).

Zinc oxide nanoparticles (ZnONPs) are among different types of NPs that are widely employed in nanotechnology, and have gained considerable attention recently. Several studies reported that the administration of ZnONPs to experimental animals induced a remarkable oxidative stress and significant histopathological changes, and led finally to cell death (Rehman et al., 2024).

Rutin (RT), an important flavonoid used in pharmaceutical industry, prevented tissue damage by directly scavenging free radicals, activating antioxidant enzymes and preventing lipid peroxidation (Yong et al., 2020).

Vitamin C (VC) also played an integral part in the cellular antioxidative defenses. RT was documented to enhance the reducing power of VC against reactive oxygen species (ROS) (He et al., 2021). Thus, combining RT with VC has a synergistic effect on the cytoprotective ability of both compounds through the inhibition of inflammatory processes (Omar et al., 2022).

Our work was designed to clarify the ZnONPs-induced histopathological and biochemical changes on the rats' prostate, and to investigate the likely prophylactic outcome of RT and VC against these changes.

MATERIALS AND METHODS

Experimental animals

Forty adult male Wistar rats weighing 180-200g were acquired from the animal house of the Faculty of Medicine, Cairo University, and acclimated in the lab for 15 days before the experiment. Each five rats were placed in a metal cage in accordance with the Institutional Animal Care and Use Committee's (IACUC) normal operating procedures and following Institutional Review Board approval (approval number: CU-III-F-85-23). Rats

were given unlimited access to normal food and water.

Chemicals

Zinc oxide nanoparticles: obtained from Plant Physiology Department, Faculty of Agriculture Cairo University. ZnONPs appeared as a grey nano-powder with a molecular weight of 65.39g/mol. Its Chemical Abstract Service Registration Number (CAS No) is 7440-66-6, and the product number is 578002.

Characterization of ZnONPs is done to study their size and shape. The water emulsion of ZnONPs was dropped into an air-dried carbon-coated copper grid at room temperature (Ghosh et al., 2016), and examined by Transmission Electron Microscope (JEOL JEM-2100, Jeol Ltd, Tokyo, Japan) at the National Research Center, Cairo, Egypt (Fig. 1). ZnONPs was dissolved in distilled water and rats were given a dose of 100 mg/kg body weight by oral gavage (Hashem and Amin, 2022).

Rutin C: purchased as Rutin C capsules (PHARCO Pharmaceuticals Company, Egypt). Each capsule contained 50 mg Rutin and 100 mg Vitamin C. Rutin C was dissolved in distilled water.

Experimental design

The weight of each rat was checked weekly to adjust the doses accordingly. All chemicals were given via oral gavage and rats of all groups were sacrificed 4 weeks after the beginning of the experiment. The forty rats were divided into ten rats groups as follows:

Group I (normal control): its rats received nothing.

Group II (vehicle control): its rats were given 1ml/kg distilled water, the solvent for ZnONPs and Rutin C.

Group III (ZnONPs group): its rats were given ZnONPs in a dose of 100 mg/kg body weight (Hashem and Amin, 2022).

Group V (ZnONPs and Rutin C group): its rats were given the same dose of ZnONPs as group III with concomitant administration of Rutin and Vitamin C at a dose of 50 mg/kg and 100 mg/kg body weight respectively (Alsaif, 2009).

Sampling

At the end of the fourth week from beginning of the experiment and after overnight fasting and anesthesia by ether inhalation, blood sampling from the tail vein of each rat was done. Sacrifice of the rats was then carried out by intra-peritoneal injection of lethal dose of 100 mg/kg of phenobarbitone sodium (Shin et al., 2012). The abdomen and pelvis of each rat was incised in order to excise the prostate, which was then processed for further assessments. Previous studies have demonstrated that zinc oxide nanoparticles administered at a dose of 100 mg/kg induce diffuse histopathological alterations affecting all lobes of the rat's prostate; therefore, separate selection or comparison of individual prostatic lobes was considered unnecessary. Moreover, nanoparticle size and surface area have been shown to markedly influence reactive oxygen species generation, resulting in cellular toxicity across all prostatic lobes. The relatively greater susceptibility observed in the ventral lobe is attributable to inherent lobe-specific characteristics, including differences in vascularization, metabolic activity, and secretory function, rather than to a differential effect of the administered compound (Mesallam et al., 2019; Pinho et al., 2020; Vassal et al., 2021; Hashem and Amin, 2022).

Tissue preparation of the prostate gland (Bancroft and Gamble, 2008)

Prostate specimens were immediately fixed in 10% buffered formalin. Dehydration was done in ascending grades of ethyl alcohol (50%, 70%, 90 %, absolute alcohol), then cleared in xylol for one day to remove the alcohol. Embedding in liquid paraffin wax was performed overnight in an oven at 50 °C, then cooled in order to prepare paraffin blocks. Prostate sections (5 µm thick) were obtained by a steel knife on a microtome, then mounted on glass slides, and used for both histological and Immunohistochemical studies.

Histological studies

Hematoxylin and eosin stain (Salman et al., 2017).

Masson's trichrome stain (Sheida et al., 2021): to

detect collagen deposition.

Immunohistochemical examination

- Proliferating Cell Nuclear Antigen (PCNA) staining was used as a marker for cell proliferation (Morcos and Afifi, 2011). The primary antibody was anti-PCNA, which is a rat monoclonal antibody (PC10 antibody ab29, 1:200). The antibody was provided as a vial of 0.1 ml at a concentration of 200 µg/ml to be used at 1 µg/ml dilution. PCNA immunopositivity staining appeared as nuclear brown.

- Prostatic specific antigen (PSA) staining (Wang et al., 2024). The mouse monoclonal PSA antibody (Dianova DIA-PSA, clone HAM18) was applied. Slides were deparaffinized and exposed to heat-induced antigen retrieval solution for 15 minutes (Agilent, Santa Clara, CA, USA). Protocol steps include 5 min peroxidase blocking (Agilent REAL), 20 min of primary antibody incubation at room temperature, and visualization of the bound antibody using the EnVision Flex Kit (Agilent), according to the manufacturer's directions. PSA immunopositivity staining appeared as brown cytoplasmic granular stain of the lining epithelium of the Acini (Bonk et al., 2019).

Morphometric study

Quantitative data was gathered using the Leica Qwin 500 Image Analyzer software system (National Institute of Mental Health, Bethesda, Maryland, USA). We looked at distant standard frames of a known area of 11,694 µm². We used the X40 and X20 objective lens (200 and 400x magnification) to examine five sections of 5 randomly chosen rats per group. The following parameters were examined to finally extract quantitative data from the images:

The average area % of collagen fibers in Masson's trichrome stained sections.

The quantity of cells that are PCNA positive.

The area percentage of sections stained with PSA.

Serological examination

The serum separates after spontaneous coag-

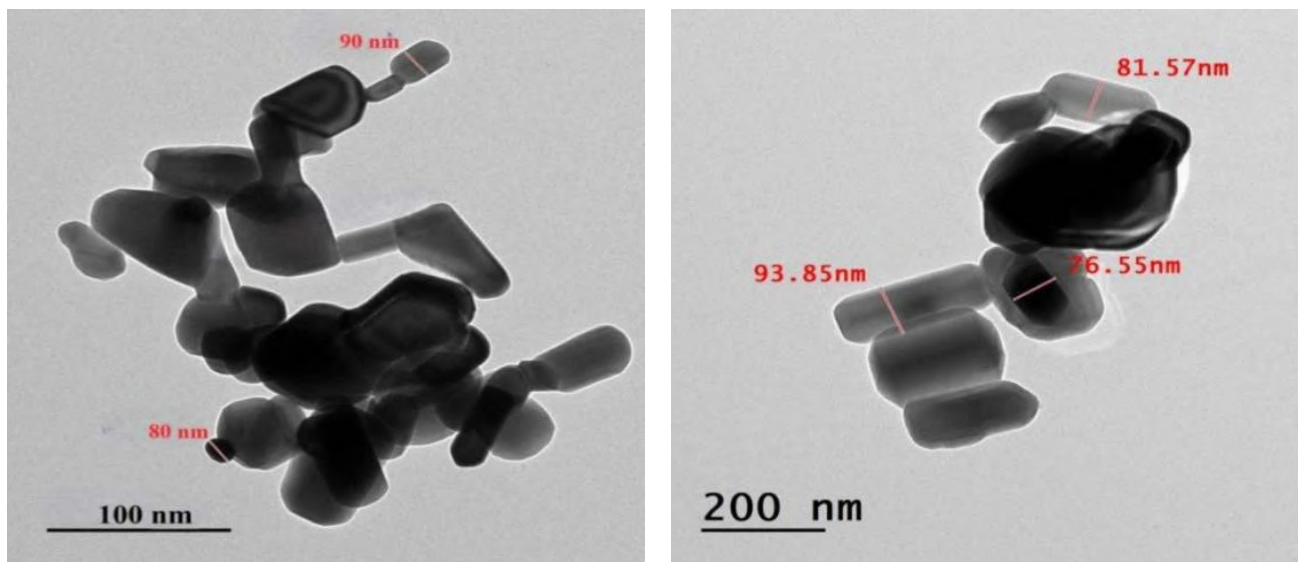


Fig. 1.- Transmission electron micrograph of ZnONPs suspension showing that most of the nanoparticles are spherical with an average size of 13.34 ± 1.6 nm. (TEM, x100,000).

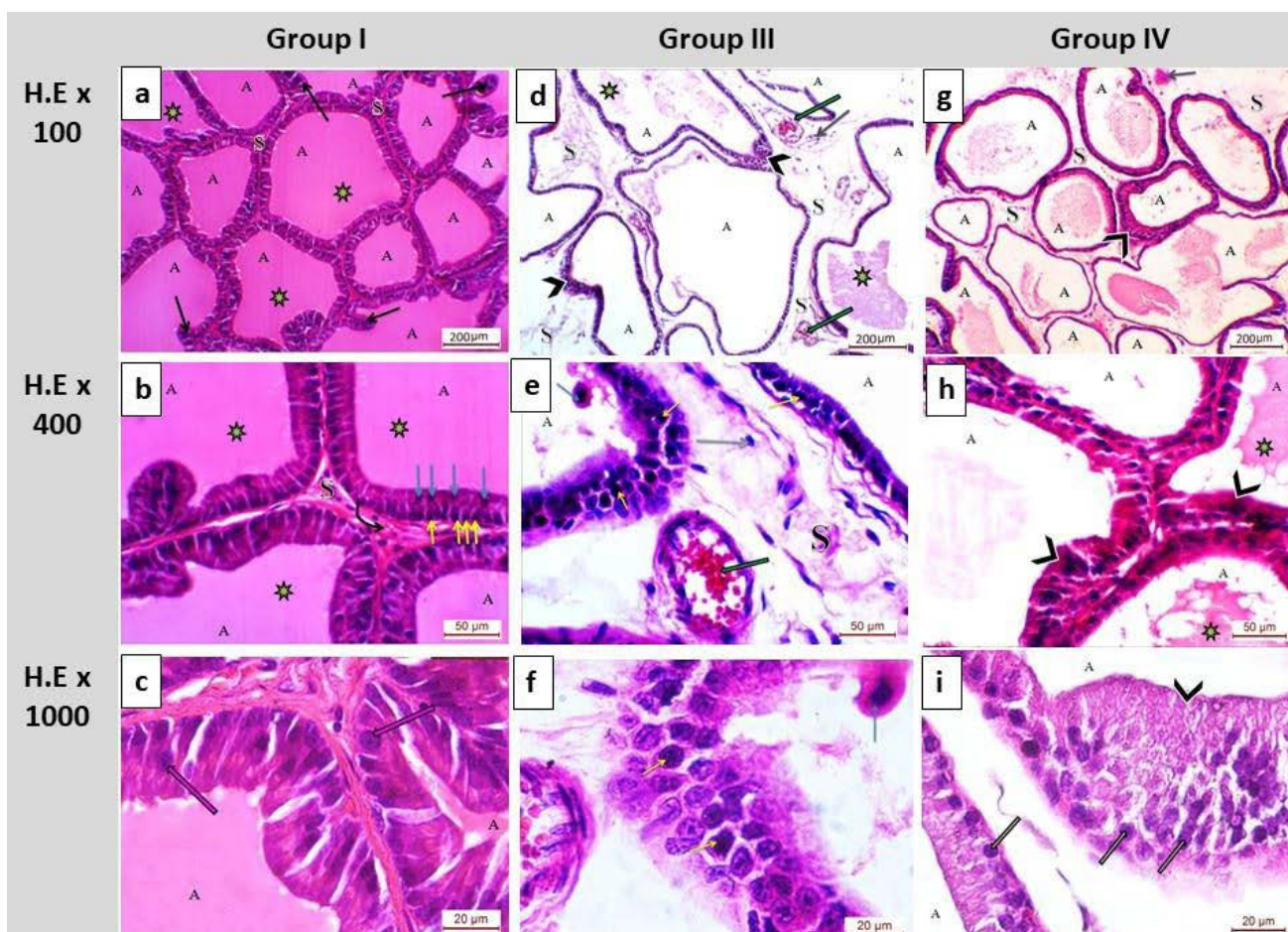


Fig. 2.- H&E-stained sections of prostates of different groups. Group I (a, b, c): regular prostatic acini (A) with papillary projection (black arrows), filled with abundant homogenous eosinophilic secretion (green asterisks), intervened by stroma (S) showing blood capillaries (curved arrow). The acinar lining epithelium is arranged into two layers: basal layer of low cuboidal (yellow arrows) and luminal layer of tall columnar cells (blue arrows). Some nuclei of the lining epithelium are vesicular with prominent nucleoli (thick arrows) and eosinophilic cytoplasm. Group III (d, e, f): irregular distorted prostatic acini (A) with thin epithelial lining and area of hyperplasia (arrowhead), diminished prostatic secretion (green asterisks) with some degenerated cell inside the lumens (blue arrow), thickened stroma (S) with congested blood vessels (green arrows) and inflammatory cell infiltration (purple arrow). Nuclear pyknosis is observed in some lining epithelial cells (yellow arrows). Group IV (g, h, i): prostatic acini (A) variable in size and shape, areas of hyperplastic lining epithelium (arrowhead) showing moderate prostatic secretions (green asterisks). The inter-acinar stroma looks apparently normal (S) with minimal inflammatory cell infiltration (purple arrow). Most of nuclei are pale basophilic (thick arrows) with eosinophilic cytoplasm.

ulation of blood samples. It is then centrifuged for 15 minutes and kept at -80°C for applying the next biochemical studies.

The serum level of Malondialdehyde (MDA) (Hassan et al., 2021) was measured by a standard kit (Biodiagnostic, Giza, Egypt), following the procedure of Ruiz-Larrea et al. (1994).

The serum level of Reduced glutathione (GSH) was measured by a standard kit (Biodiagnostic, Giza, Egypt), following the procedure of Moatamed et al., (2019).

Serum prostatic specific antigen (PSA) (Shahin and Mohamed, 2017) was measured using an ELISA kit from CUSABIO BIOTECH (Wuhan, China), following the manufacturer's procedure.

Statistical analysis

The Statistical Package for Social Sciences version 16 (SPSS Inc., Chicago, USA) was used in order to evaluate the mean and standard deviation (SD) for each of the variables under study. Analysis of variance (ANOVA) was used to compare groups, and Tukey's Post Hoc test was performed for multiple comparisons between each pair of groups. P-values < 0.05 were deemed statistically significant, whereas P-values < 0.001 were deemed extremely statistically significant.

RESULTS

Groups I & II (normal & vehicle controls respectively) showed nearly similar histological, immunohistochemical, and serological results.

Histological results of H & E-stained sections (Fig. 2)

Groups I & II revealed the normal prostate architecture, consisting of regular prostatic acini with papillary projection. The acini contained homogenous pale eosinophilic secretion and were separated by fibromuscular stroma containing blood capillaries. The lining epithelium of acini showed two layers of cells: a basal layer that appeared low cuboidal, and a luminal layer that appeared tall columnar. Some of the lining epithelial nuclei were vesicular, with prominent nucleoli and eosinophilic cytoplasm.

Group III revealed irregular distorted prostatic acini with thin epithelial lining and some areas of hyperplasia and contained diminished prostatic secretion in their lumen. The inter-acinar stroma was thickened with congested vasculature and inflammatory cell infiltration. Some lining epithelium showed pyknotic nuclei, and the lumen of acini contained degenerated cells.

Rats of group IV exhibited considerable improvement of the histological architecture of the prostate, consisting of prostatic acini of variable size and shape with few areas of epithelial hyperplasia. The prostatic acini contained moderate amounts of homogenous secretions. The inter-acinar stroma appeared thin with few inflammatory cell infiltrations. Most of the epithelial nuclei are pale basophilic with eosinophilic cytoplasm.

Histological results of Masson's trichrome sections (Fig. 3)

Groups I & II showed minimum collagen deposition in the fibromuscular stroma. Group III showed abundant collagen deposition in the fibromuscular stroma. Group IV showed slight collagen deposition in the fibromuscular stroma.

Immunohistochemical results of PCNA-stained sections (Fig. 3)

In Groups I & II, only few acinar cells showed dark brown nuclei expressing minimal positive PCNA immunoreaction. In Group III, multiple acinar cells showed dark brown nuclei expressing marked positive PCNA immunoreaction. In Group IV, moderate number of acinar cells showed brown nuclei expressing moderate positive PCNA immunoreaction.

Immunohistochemical results of PSA-stained sections (Fig. 3)

Groups I & II revealed strong immunoreactivity. Group III revealed weak immunoreactivity. Group IV revealed strong immunoreactivity.

Histomorphometric results (Table 1, Fig. 4)

Area percentage of collagen fibers in Masson's trichrome stained sections: Group III showed significantly larger area percentage of collagen

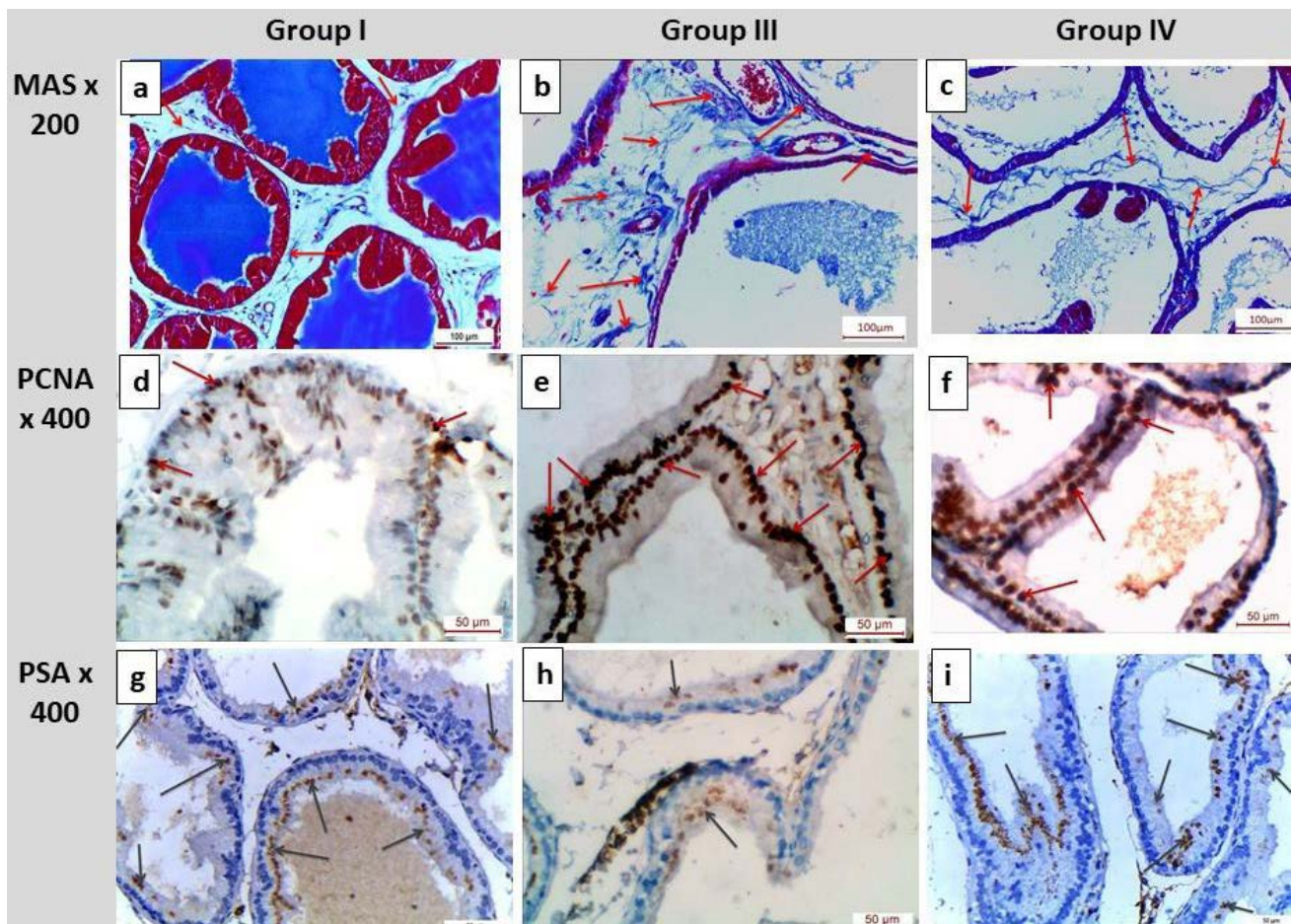


Fig. 3.- a, b, c: Masson's trichrome prostatic sections of different groups. Group I: minimum collagen deposition in the fibromuscular stroma (arrows). Group III: abundant collagen deposition in the fibromuscular stroma (arrows). Group IV: slight collagen deposition in the fibromuscular stroma (arrows). d, e, f: PCNA prostatic sections of different groups. Group I: express mild positive PCNA immunoreaction having few acinar cells with dark brown nuclei (arrows). Group III: expresses marked positive PCNA immunoreaction having multiple acinar cells with dark brown nuclei (arrows). Group IV: expresses moderate positive PCNA immunoreaction having moderate number of acinar cells with dark brown nuclei (arrows). g, h, i: PSA prostatic sections of different groups. Group I: Show deep staining of the cytoplasm with PSA (arrows). Group III: Shows light staining of the cytoplasm with PSA (arrows). Group IV: Show deep staining of the cytoplasm with PSA (arrows).

deposition than groups I & II. However, this area percentage was smaller in group IV than group III.

Number of positive nuclei in PCNA-stained sections: Group III exhibited significantly larger number of PCNA positive nuclei than group I & II. However, this number was significantly smaller in Group IV than Group III.

Area percentage of PSA-stained sections in different groups: Group III showed significantly larger area percent of PSA reaction than groups I & II. However, this area percent was significantly smaller in Group IV than Group III.

Serological results (Table 2, Fig. 5)

Prostatic Specific Antigen level (PSA): Serum level of PSA of group III was noticeably greater than that of Groups I and II. But compared to Group III, this level was much lower in group IV.

Malondialdehyde level (MDA): Serum MDA level of Group III was noticeably higher than in Groups I and II. But compared to Group III, this level was noticeably lower in Group IV.

Decreased Glutathione Level (GSH): Compared to groups I and II, serum GSH was noticeably lower in group III. But compared to Group III, this level was noticeably higher in Group IV.

DISCUSSION

Nowadays, ZnONPs are widely used in several aspects of life, but they are suspected to induce cytotoxic effects on the prostate gland that impair male fertility. The daily intangible human exposure to ZnONPs evokes a great challenge to human health and safety. The present study investigates ZnONPs-induced prostate toxicity in rats and assesses the potential prophylactic role of Rutin C.

Table 1. The area percent of collagen fibers, the number of PCNA positive cells and the area percent of PSA-stained sections in all groups.

Group	Area percentage of collagen fibers (Mean)	Area percentage of collagen fibers (SD)	Compared to group	p-value
I	3.32	1.07	---	----
II	3.14	0.53	I	0.98
III	13.91	1.85	I	0.001**
			II	0.001**
IV	6.18	0.81	III	0.001**
Group	Number of PCNA positive cells (Mean)	Number of PCNA positive cells (SD)	Compared to group	p-value
I	15.7	4.85	----	-----
II	17.5	3.24	I	0.79
III	32.9	5.36	I	0.001**
			II	0.001**
IV	18.8	3.58	III	0.001**
Group	Area percentage of PSA immuno-stained (Mean)	Area percentage of PSA immuno-stained (SD)	Compared to group	p-value
I	2.87	0.56	----	-----
II	2.9	0.47	I	1.000
III	0.81	0.06	I	0.001**
			II	0.001**
IV	3.47	0.78	III	0.001**

* Significant p-value ≤ 0.05 . ** Extremely statistically significant < 0.001 .

In our study, histological examination of group III (ZnONPs treated group) showed irregular distorted prostatic acini with thin epithelial lining

and diminished prostatic secretion in their lumen. The acini were separated by thick fibromuscular stroma containing congested blood vessels

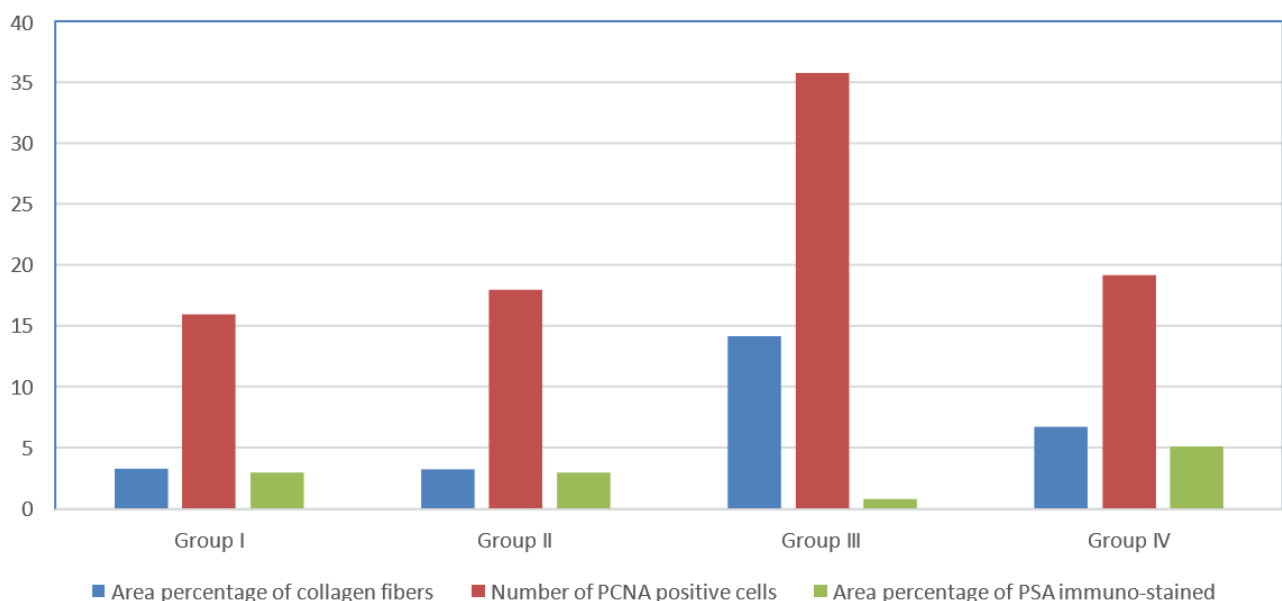


Fig. 4.- Mean area percent of collagen fibers, number of PCNA positive immuno-stained cells and area percent of PSA-stained sections in all groups.



Fig 5.- Mean serum levels of MDA, GSH, and PSA in all groups.

and inflammatory cells. These findings agreed with Hashem and Amin (2022).

A study of Kim et al. (2014) documented similar findings, but at a lower dose of ZnONPs (31.5mg/kg) compared to the present study. Tolba et al. (2018) rationalized the vascular congestion of prostatic stroma to the cellular attempts to restore a normal oxygen ratio through production of adenosine, which causes the arteries to dilate and congest.

In our study, Group III showed shrunken pyknotic nuclei of the prostatic epithelium. This was in accordance with Salianni et al. (2016) who attributed this to the ability of nanoparticles to diffuse through the nuclear pores leading to nuclear damage. Pinho et al. (2020) added that ROS pushed the endoplasmic reticulum to produce unfolded or misfolded proteins in its lumen, leading to cell apoptosis and cell destruction.

In the current study, Group III showed epithelial detachment and patchy areas of hyperplasia. These findings agreed with Tolba et al. (2018), who attributed these findings to the oxidative injury to the lining epithelium causing its proliferations and differentiation through mitosis, which results in the development of new spots of hyperplastic epithelium in some areas and epithelial detachments.

In the present study, Group III showed thickening of the inter-acinar prostatic stroma with inflammatory cellular infiltration. These results were consistent with Cao et al. (2019), who explained that the increased ROS damaged the endothelial cells of the capillaries, resulting in increased microvascular permeability and extravasation of fluid.

In our study, Group IV (ZnONPs and Rutin C treated group) revealed an improvement of prostatic architecture compared to Group III. These findings concurred with Blaszczyk et al. (2019) and Hashem and Amin (2022), who confirmed the antioxidant efficiency of Rutin and vitamin C against free radicals.

In the present study, histological and histomorphometric examination of the collagen fibers in Group III was significantly higher when compared to control groups. Tolba et al. (2018) attributed the increased collagen synthesis to ROS-induced increase in nuclear transcription factor kappa (NF- κ B), which is associated with fibrotic and inflammatory processes. Genah et al. (2021) showed that increased production of cytokines resulted in increased fibroblast activation, with subsequent increased collagen synthesis.

In the current research, Group IV showed a significant decrease in the area percent of collagen

when compared to Group III. This agreed with Gul et al. (2018), who reported a significant downregulation in NF- κ B expression, which encountered excessive collagen production caused by ZnONPs administration.

In the current study, immunohistochemical and histomorphometric analysis of Group III revealed a markedly higher number of PCNA-positive nuclei in comparison to the control group. However, compared to Group III, Group IV showed a marked decline in PCNA-positive nuclei. This was consistent with Hashem and Amin's (2022) findings that ZnONPs caused cellular proliferation and glandular hyperplasia, which in turn led to an increase in PCNA-positive nuclei. They also mention that the elevation of PCNA expression brought on by ROS generation was decreased by rutin's antioxidant function.

In the current work, immunohistochemical and histomorphometric examination of Group III revealed a significant decrease in the area percent of PSA when compared to the control group. While Group IV revealed a significant increase in the area percentage of PSA when compared

to Group III. This agreed with Satari et al. (2021), who explained these findings by the breakdown of the basement membrane of the prostatic acini in ZnONPs-treated group, leading to PSA leakage into the serum, while in the ZnONPs- and-Rutin-treated group there was a restoration of the integrity of the basement membrane preventing the leakage of PSA.

In the current work, serological examination of Group III showed a significant increase in the serum PSA when compared to control group. This agreed with Shahin and Mohamed (2017), who rationalized that to the breakdown of the cellular basement membrane of the prostatic acini and ducts, allowing PSA to leak into the prostatic parenchyma and ultimately into serum. Group IV in our study revealed a significant decrease in PSA compared to Group III. This was in agreement with Hashem and Amin (2022), who attributed that reduction of PSA to the restoration of the integrity of the basement membrane, which keeps PSA from passing into the serum.

According to Weir et al. (2000), the various PSA complexes detected in the serum might or might

Table 2. Mean \pm SD of the serum level of MDA, GSH and PSA levels in all groups

Group	MDA (nmol/ml) Mean	MDA (nmol/ml) SD	Compared to group	p-value
I	42.60	4.32	---	---
II	42.65	4.06	I	1.000
III	124.05	7.37	I	<0.001**
			II	<0.001**
IV	55.75	13.79	III	<0.001**
Group	GSH (mmol/ml) Mean	GSH (mmol/ml) SD	Compared to group	p-value
I	227.1	18.06	----	----
II	223.1	17.05	I	1.000
III	104.95	4.38	I	<0.001**
			II	<0.001**
IV	216.2	10.79	III	<0.001**
Group	PSA (g/ml)	PSA (g/ml)	Compared to group	p-value
I	Mean	SD	----	----
II	2.35	0.31	I	0.98
III	2.3	0.19	I	<0.001**
			II	<0.001**
IV	3	0.15	III	<0.001**

* Significant p-value \leq 0.05. ** Extremely statistically significant $<$ 0.001

not be present in the tissue, and if they are, they might not be responsive to anti-PSA antibodies. Since there was no link between tissue PSA and serum PSA, the authors showed a difference between the immuno-expression of tissue PSA and the serum PSA level in the ZnONPs group.

In the current study, serological examination of Group III showed a significant increase in MDA and a decrease in GSH when compared to control group. Such changes could be attributed to oxidative stress and production of ROS that led to DNA damage, lipid peroxidation, inflammatory reactions and organelle dysfunction as mentioned by Hosseini et al. (2020) and Mesallam et al. (2019), who added that ZnONPs' toxicity was inversely correlated with their size, so that the nanoparticles' surface area and size had an impact on their capacity to generate ROS and, in turn, their cellular toxicity.

In the present work, serological examination of Group IV showed a significant decrease in MDA and increase in GSH as compared to Group III. This was in accordance with Khan et al. (2017), who stated that Rutin acted as a scavenger of ROS through giving hydrogen atoms to peroxy radicals, superoxide anions, and hydroxyl radicals. Ziamajidi et al. (2023) confirmed the role of vitamin C in elimination of free radicals.

Our results showed that vitamin C and Rutin have potent antioxidant qualities against oxidative stress in the rats given ZnONPs. According to previous studies, nutritional molecules can interact with nanoparticles and influence their toxicity; however, this varies depending on the kind of nanoparticle and nutrient molecule. Furthermore, food molecules may modify Zn ion release, which impacts ZnONPs toxicity (Ekhlasian et al., 2023).

Attia et al. (2018) suggested that nanoparticles-induced ROS production hinders the production of antioxidant enzymes, such as superoxide dismutase, catalase, peroxidases, reductase and transferases. Therefore, cells try to stimulate nuclear transcription factor kappa B, which participates in the mRNA transcription of these antioxidant enzymes, but cells are still unable to re-establish the usual balance when soluble NPs are

present, which causes cytotoxicity and ultimately cell death. Sewelam and Shehata (2021) showed that the genes that encode cytokines, chemokines, and other inflammatory mediators like IL-1, IL-6, IL-8, and tumor necrosis factor- α were up-regulated as a result of the increased oxygen free radicals brought on by ZnONPs. The polymorph nuclear leukocytes (PMNLs), which generate more ROS, are then activated, and invaded as a result of these chemicals.

In contrast to the results of our work, Salman (2017) claimed that only a high dose of ZnONPs (350 mg/kg/day) had toxic effects on the prostate and testis, while lower dose (150 mg/kg/day) caused only delirious effect on seminal vesicles. Such a difference might be related to shortening the duration of ZnONPs administration to fifteen days only.

Our study concluded that administration of zinc oxide nanoparticles had deleterious effects on the biochemical and histological architecture of the prostate. Rutin C has protective effects against the toxic effect of ZnONPs.

Our study recommended to consume Rutin-C-rich food and supplements. Further studies are required to study the long-time exposure to ZnONPs, to know the impact of NPs on fertility in males.

REFERENCES

- ALSAIF M (2009) Beneficial effects of rutin and vitamin C coadministration in a streptozotocin-induced diabetes rat model of kidney nephrotoxicity. *Pak J Nutr*, 8: 745-754.
- ATTIA H, NOUNOU H, SHALABY M (2018) Zinc oxide nanoparticles induced oxidative DNA damage, inflammation and apoptosis in rat brain after oral exposure. *Toxics*, 6(2): 29.
- BANCROFT JD, GAMBLE M (2008) Theory and practice of histological techniques. 6th ed. Churchill Livingstone, Elsevier, China.
- BLASZCZAK W, BARCZAK W, MASTERNAK J, KOPCZYŃSKI P, ZHITKOVICH A, RUBIŚ B (2019) Vitamin C as a modulator of the response to cancer therapy. *Molecules*, 24(3): 453.
- BONK S, KLUTH M, HUBE-MAGG C, POLONSKI A, SOEKELAND G, MAKROPIDI-FRAUNE G, MÖLLER-KOOP C, WITT M, LUEBKE AM, HINSCH A, BURANDT E, STEURER S, CLAUDITZ TS, SCHLOMM T, PEREZ D, GRAEFEN M, HEINZER H, HULAND H, IZBICKI JR, WILCZAK W, MINNER S, SAUTER G, SIMON R (2019) Prognostic and diagnostic role of PSA immunohistochemistry: a tissue microarray study on 21,000 normal and cancerous tissues. *Oncotarget*, 10: 5439-5453.
- CAO C, DAI L, MU J, WANG X, HONG Y, ZHU C, JIN L, LI S (2019) S1PR2 antagonist alleviates oxidative stress-enhanced brain endothelial permeability by attenuating p38 and Erk1/2-dependent cPLA2 phosphorylation. *Cell Signal*, 53: 151-161.
- EKHLASIAN A, EFTEKHAR E, DAEI S, ABBASALIPOURKABIR R,

- NOURIAN A, ZIAMAJIDI N (2023) The antioxidant and anti-apoptotic properties of vitamins A, C and E in heart tissue of rats exposed to zinc oxide nanoparticles. *Mol Biol Rep*, 50: 2357-2365.
- GENAH S, CIALDAI F, CICCONE V, SERENI E, MORBIDELLI L, MONICI M (2021) Effect of NIR laser therapy by MLS-MiS source on fibroblast activation by inflammatory cytokines in relation to wound healing. *Biomedicines*, 9: 307.
- GHOSH M, SINHA S, JOTHIRAMAJAYAM M, JANA A, NAG A, MUKHERJEE A (2016) Cyto-genotoxicity and oxidative stress induced by zinc oxide nanoparticles in human lymphocytes in vitro and Swiss albino male mice in vivo. *Food Chem Toxicol*, 97: 286-296.
- GULA, KUNWAR B, MAZHAR M, FAIZI S, AHMED D, SHAH MR, SIMJEE SU (2018) Rutin and rutin-conjugated gold nanoparticles ameliorate collagen-induced arthritis in rats through inhibition of NF- κ B and iNOS activation. *Int Immunopharmacol*, 59: 310-317.
- HASHEM H, AMIN M (2022) Effect of zinc nanoparticles on adult rat prostate gland and the possible protective role of rutin: histological and biochemical study. *Egypt J Histol*, 45: 372-385.
- HASSAN R, ELSAYED M, KHOLIEF T, HASSANEN N, GAFER J, ATTIA Y (2021) Mitigating effect of single or combined administration of zinc oxide, chromium oxide and selenium nanoparticles on genotoxicity and metabolic insult in diabetic rats. *Environ Sci Pollut Res*, 28: 48517-48534.
- HE J, XU W, ZHENG X, ZHAO B, NI T, Yu P, DENG S, PAN X, CHEN E, MAO E, BIAN X (2021) Vitamin C reduces vancomycin-related nephrotoxicity through the inhibition of oxidative stress, apoptosis and inflammation in mice. *Ann Transl Med*, 9: 1319.
- HOSSEINI S, AMANIR, MOSHREFIA, RAZAVIMEHR S, AGHAJANIKHAH M, SOKOUTI Z (2020) Chronic zinc oxide nanoparticles exposure produces hepatic and pancreatic impairment in female rats. *Iran J Toxicol*, 14: 145-154.
- KHAN R, KHAN M, AHMED M, SHAH M, REHMAN S, et al. (2017) Effects of rutin on testicular antioxidant enzymes and lipid peroxidation in rats. *Indian J Pharm Educ Res*, 51: 412-417. <https://doi.org/10.5530/IJPER.51.3.69>.
- KIM Y, PARK J, LEE E, PARK S, SEONG N, KIM JH, KIM GY, MEANG EH, HONG JS, KIM SH, KOH SB, KIM MS, KIM CS, KIM SK, SON SW, SEO YR, KANG BH, HAN BS, AN SS, YUN HY, KIM MK (2014) Toxicity of 100 nm zinc oxide nanoparticles: a report of 90-day repeated oral administration in Sprague Dawley rats. *Int J Nanomedicine*, 9: 109-126.
- MABROUK M, DAS D, SALEM Z, BEHEREI H (2021) Nanomaterials for biomedical applications: production, characterisations, recent trends and difficulties. *Molecules*, 26: 1077.
- MESALLAM D, DERAZ R, ABDEL AAL A, AHMED S (2019) Toxicity of subacute oral zinc oxide nanoparticles on testes and prostate of adult albino rats and role of recovery. *J Histol Histopathol*, 6: 2-12.
- MOATAMED E, HUSSEIN A, EL-DESOKY M, KHAYAT A (2019) Comparative study of zinc oxide nanoparticles and its bulk form on liver function of Wistar rat. *Toxicol Ind Health*, 35: 627-637.
- MORCOS M, AFIFI N (2011) Effect of doxazosin on experimentally induced prostatic hyperplasia in adult male albino rats: a histological and immunohistochemical study. *Egypt J Histol*, 34: 870-882.
- MOTRICH R, SALAZAR F, BRESER M, MACKERN-OBERTI J, GODOY G, OLIVERA C, PAIRA DA, RIVERO VE (2018) Implications of prostate inflammation on male fertility. *Andrologia*, 50: e13093.
- OMAR S, EL BOROLOSSY R, ELSAID T, SABRI N (2022) Evaluation of the combination effect of rutin and vitamin C supplementation on oxidative stress and inflammation in hemodialysis patients. *Front Pharmacol*, 13: 961590.
- PINHO A, REBELO S, PEREIRA M (2020) The impact of zinc oxide nanoparticles on male (in)fertility. *Materials*, 13: 849.
- REHMAN N, JABEEN F, ASAD M, NIJABAT A, ALI A, KHAN SU, LUNA-ARIAS JP, MASHWANI ZU, SIDDIQA A, KARTHIKEYAN A, AHMAD A (2024) Exposure to zinc oxide nanoparticles induced reproductive toxicities in male Sprague Dawley rats. *J Trace Elem Med Biol*, 83: 127411.
- RUIZ-LARREA M, LEAL A, LIZA M, LACORT M, DE GROOT H (1994) Antioxidant effects of estradiol and 2-hydroxyestradiol on iron-induced lipid peroxidation of rat liver microsomes. *Steroids*, 59(6): 383-388.
- SALIANI M, JALAL R, GOHARSHADI E (2016) Mechanism of oxidative stress involved in the toxicity of ZnO nanoparticles against eukaryotic cells. *Nanomed J*, 3(1): 1-14.
- SALMAN R (2017) The influence of ZnO nanoparticles on reproductive system tissues of albino male mice: histopathological study. *Int J Sci Res*, 6: 2021-2025.
- SATARIA, GHASEMI S, HABTEMARIAM S, ASGHARIAN S, LORIGOOINI Z (2021) Rutin: a flavonoid as an effective sensitizer for anticancer therapy. *Evid Based Complement Alternat Med*, 2021: 9913179.
- SEWELAM A, SHEHATA M (2021) Nano-zinc oxide induced pancreatic toxicity and the ameliorating role of naringenin. *Egypt J Histol*, 44: 1081-1097.
- SHAHIN N, MOHAMED M (2017) Nano-sized titanium dioxide toxicity in rat prostate and testis. *Toxicol Appl Pharmacol*, 334: 129-141.
- SHEIDA F, HAMZEHPUR M, SOHRABI M, ALIZADEH A (2021) Histological modifications of the rat prostate following oral administration of silver nanoparticles. *J Shahrekord Univ Med Sci*, 23: 51-55.
- SHIN I, LEE M, HA H, SEO C, SHIN H (2012) Inhibitory effect of Yukmijihwang-tang against testosterone-induced benign prostatic hyperplasia in rats. *BMC Complement Altern Med*, 12: 48.
- TOLBA A, MANDOUR D (2018) Histological effects of bisphenol-A on the reproductive organs of the adult male albino rat. *Eur J Anat*, 22: 89-102.
- VASSAL M, REBELO S, PEREIRA ML (2021) Metal oxide nanoparticles: evidence of adverse effects on the male reproductive system. *Int J Mol Sci*, 22(15): 8061.
- WANG H, LIU C, DONG Z, CHEN X, ZHANG P (2024) Prostate-specific antigen and steroid hormone receptors in benign prostatic hyperplasia. *Aging Male*, 27: 2391380.
- WEIR E, PARTIN A, EPSTEIN J (2000) Correlation of serum prostate specific antigen and quantitative immunohistochemistry. *J Urol*, 163: 1739-1742.
- XIE D, HU J, WU T, XU W, MENG Q, CAO K, LUO X (2022) Effects of flavonoid supplementation on nanomaterial-induced toxicity. *Front Nutr*, 9: 929343.
- YONG D, SAKER S, CHELLAPPAN D, MADHESWARAN T, PANNEERSELVAM J, CHOUDHURY H, PANDEY M, CHAN YL, COLLET T, GUPTA G, OLIVER BG, WARK P, HANSBRO N, HSU A, HANSBRO PM, DUA K, ZEESHAN F (2020) Molecular and immunological mechanisms underlying the pharmacological properties of rutin. *Endocr Metab Immune Disord Drug Targets*, 20: 1590-1596.
- ZIAMAJIDI N, KHAJVAND-ABEDINI M, DAEI S, ABBASALIPOURKABIR R, NOURIAN A (2023) Ameliorative effects of vitamins A, C and E on sperm parameters and testis histopathology in zinc oxide nanoparticle-treated rats. *Biomed Res Int*, 2023: 4371611.

Anatomical variation of the prostatic artery and the impact of its embolization on IPSS in benign prostatic hyperplasia

Ahmed F. AlDomairy¹, Gamal-eldine M. Niazi², Radwa M. Elsabban¹

¹ Department of Anatomy and Embryology, Faculty of Medicine, October 6 University, Giza, Egypt

² Department of Radiology, Faculty of Medicine, Ain Shams University, Cairo, Egypt

SUMMARY

The prostate gland is known for its potential implications, particularly prostate cancer and benign prostatic hyperplasia. It is supplied by the prostatic artery, which shows considerable anatomical variation, directly implicating prostatic artery embolization, an emerging minimally invasive therapy for benign prostatic hyperplasia. Identifying prostatic artery origin variation is essential in order to optimize embolization and improve clinical outcomes. The objective was to investigate the anatomical variation of the prostatic artery using cadaveric dissection and angiographic evaluation, and to assess the impact of this variation on clinical outcomes following prostatic artery embolization. A bilateral cadaveric dissection was conducted on five male pelvis specimens to identify prostatic artery origin. The radiological arm included 54 symptomatic benign prostatic hyperplasia patients undergoing prostatic artery embolization, with prostatic artery origin variation and symmetry documented. IPSS recorded pre-procedure and at 3 and 6 months post-embolization, and statistical analysis was

performed.

Cadaveric analysis showed that the prostatic artery most commonly originated from vesical arteries (60%), followed by the obturator (20%) and internal pudendal arteries (20%). Radiologically, vesical origin was also the most frequent (41.7%), followed by obturator (23.1%), internal pudendal (21.3%), and internal iliac artery (13.9%). Symmetrical prostatic artery origin was observed in 83.3% of patients. Prostatic artery embolization produced a significant reduction in mean IPSS, from 24.53 pre-procedure to 16.31 and 11.56 after 3 and 6 months respectively ($p < 0.001$). Neither patient age nor prostatic artery origin impacted clinical improvement. The prostatic artery shows marked anatomical variability, with vesical arteries representing the most frequent origin. Prostatic artery embolization is an effective treatment for benign prostatic hyperplasia, producing significant improvement regardless of prostatic artery origin or patient age.

Key words: Prostatic artery – Cadaver – Benign prostatic hyperplasia – Embolization

Corresponding author:

Dr. Ahmed F. AlDomairy. Department of Anatomy and Embryology, Faculty of Medicine, October 6 University, 6th of October city, Giza, Egypt 12566. Phone: 00201005208027. E-mail: aaldomairy@o6u.edu.eg / aaldomairy@hotmail.com

Submitted: January 25, 2026. **Accepted:** February 26, 2026

<https://doi.org/10.52083/JAWR8576>

INTRODUCTION

The human prostate is a pyramidal gland located below the bladder, comprising distinct anatomical, histological, and pathological regions. Historically, Lowsley (1912) led the initial anatomical division of the prostate gland into five lobes: the middle (median), anterior, posterior and two lateral lobes, with the lateral lobes containing most glandular tissue. Histologically, the gland consists of compound tubuloalveolar glands embedded in a dense fibromuscular stroma, with a two-layered epithelium and occasional corpora amylacea within the lumina (De Marzo et al., 2007). Historically, the posterior lobe was considered the primary site of prostate cancer and the median lobe of benign prostatic hyperplasia. However, the widely accepted zonal classification by McNeal (1988) describes peripheral, central, and transitional zones. The peripheral zone contains about 70% of glandular tissue, and is the most frequent site of cancer; the transitional zone surrounds the urethra and enlarges in older men with BPH; and the central zone, surrounding the ejaculatory ducts, is rarely affected primarily, but may be secondarily involved in malignancy (Ittmann, 2018).

The pelvic region is primarily supplied by the internal iliac artery, which exhibits considerable variability in its branching pattern, with recognized differences related to sex. Awareness of these anatomical variations is of particular importance in pelvic and urological surgeries. Early attempts to classify the branching pattern of the internal iliac artery relied on a simplified division into anterior and posterior trunks from which the smaller branches arise (Carter, 1867; Sharpey et al., 1867; Wilson, 1868). A more detailed and widely adopted classification was later proposed by Adachi (1928), who described five types based on the origin of the gluteal and internal pudendal arteries, whether arising independently or from common trunks. This classification did not consider variations in the origin of the obturator artery previously described by Lipshutz (1918), and was subsequently refined by Ashley and Anson (1941), who incorporated the umbilical artery into the classification scheme. According to Yamaki et al. (1998), the most frequent branching pattern (60–80%) consists of the internal iliac

artery branching into the superior gluteal artery, and a common trunk giving rise to both the inferior gluteal and internal pudendal arteries. Less commonly, a common trunk for the superior and inferior gluteal arteries or for the superior gluteal and internal pudendal arteries may be observed, while in some cases all three arteries originate independently.

Lipshutz (1918) reported that the prostatic artery most frequently originated from the anterior division of the internal iliac artery (30%), followed by the obturator artery (15%), the middle rectal artery (10%), the ischiopudendal trunk (10%), and the inferior gluteal artery (5%). In a later anatomical study, Clegg (1955) examined the origin of the prostatovesical artery, and found that 52.9% arose from the common trunk of the inferior gluteal and internal pudendal arteries, 11.8% originated from the umbilical artery or its origin, 11.8% from a common trunk with the vesicodifferential artery, 5.9% from the internal pudendal artery, and 5.9% from the obturator artery. Roberts and Krishinger (1967) similarly reported the ischiopudendal trunk as the most frequent site of origin (37.7%), followed by the obturator artery (23.3%), superior vesical artery (13.3%), inferior vesical artery (13.3%), internal pudendal artery (10%), and, less commonly, the dorsal artery of the penis (3.3%).

The prostatic vascular system is a crucial factor in the growth and function of the prostate; affection of the blood flow to the prostate gland may be involved in the BPH development and control (Carnevale et al., 2013). The prostate receives its arterial blood supply from prostatic branches of variable anatomical origins. According to Teichgraber et al. (2018), superior and inferior vesical arteries typically arise from the internal iliac artery. The inferior vesical artery runs caudally to reach the base of the bladder, supplying the seminal vesicles and the prostate as well. In some cases, the inferior vesical artery shares a common trunk with either superior vesical artery or middle rectal artery, from which the prostatic artery (PA) may arise. The superior vesical artery supplying the superior surface of the bladder may also contribute to prostatic supply. Additionally, prostatic branches may arise from the common

gluteal–pudendal trunk or directly from the internal pudendal artery (Bilhim et al., 2011).

Moya et al. (2017) reported six possible origins for the PA: internal pudendal artery (29.3%), gluteal-pudendal trunk (27.5%), inferior vesical artery (20.7%), middle rectal artery (15.5%), obturator artery (5.2%), and other less common sources. On the other hand, angiographic classification simplifies the PA origin into four main types: a common vesical trunk dividing into superior and inferior vesical arteries; inferior vesical artery arising separately from the internal iliac artery; obturator artery; and internal pudendal artery. Less common origins include the accessory pudendal artery, anterior division trifurcation of the internal iliac artery, posterior division of the internal iliac artery, and inferior epigastric artery (De Assis et al., 2015).

A number of studies reported that the prostate may, in some cases, receive dual arterial supply, with a cranial anterolateral pedicle mainly supplying the transition zone and a caudal posterolateral pedicle supplying the apex and peripheral zone. The anterolateral pedicle often supplies the central gland and BPH nodules, typically arising from the vesical arteries and commonly targeted in embolization procedures. The posterolateral pedicle supplies the peripheral and caudal prostate and may communicate with rectal branches. Anastomoses with surrounding arteries are common and should be considered during embolization (Bilhim et al., 2012; De Assis et al., 2015; Wang et al., 2017).

Prostate tissue remodelling and degeneration are part of the normal aging process, leading to alterations in smooth muscle function, prostate size, enlargement, and fibrosis, which ultimately disturb prostatic function (Liu et al., 2019). BPH is one of the commonest diseases affecting men after the age of forty, with the risk of onset and progression increasing with advancing age. Genetics, diet, and lifestyle also influence the prevalence of the disease (Lim, 2017).

Benign prostate syndrome (BPS) refers to lower urinary tract symptoms and bladder outlet obstruction secondary to BPH (Liu et al., 2019). BPH is regarded as a nodular disease, typically affect-

ing the transition zone rather than the whole prostate. Bladder outlet obstruction does not correlate solely with prostate size but is largely influenced by the location of the adenoma, particularly if situated near the bladder neck or urethra (Nickel et al., 2016). Thus, prostate size and symptom severity are not necessarily correlated. Even small prostates may cause significant symptoms if the adenoma is strategically positioned. Symptoms of BPS typically include delayed initiation of micturition, prolonged voiding time, weak urinary stream, a sensation of incomplete bladder emptying, increased nocturia, frequency, urgency, and dysuria – all of which significantly impact the quality of life in older men (Carnevale et al., 2013).

Treatment decisions for BPS are primarily guided by the impact of symptoms on patients' quality of life. First-line management typically involves pharmacological therapy. Drug therapies for BPH can improve urine flow, but they do not reduce the size of the prostate and can contribute to sexual dysfunction or hypotension as side effects (Bilhim et al., 2012). If medical management fails, surgical intervention may be required. Transurethral resection of the prostate has been for decades the gold-standard surgical treatment for symptomatic BPH, although it carries a morbidity rate of up to 20% (Capdevila et al., 2021).

Prostatic artery embolization has emerged since 2000 as a minimally invasive alternative technique for symptomatic patients, offering comparable clinical outcomes with faster recovery and fewer complications (De Assis et al., 2015). Advantages of PAE include avoiding hospitalization, general anesthesia, and surgery, and reducing the risk of sexual side-effects such as retrograde ejaculation or erectile dysfunction (Franco et al., 2023). PA embolization involves selective embolization of intraprostatic vessels and precapillary arterioles, resulting in irreversible ischemia and an inflammatory response that leads to complete tissue anoxia. Subsequent gland shrinkage occurs following edema resorption and scar formation. Accurate identification of PA vasculature and its origins during embolization is essential to avoid nontarget embolization and to recognize small anastomoses between intraprostatic branches or adjacent arteries (Zhang et al., 2015; Teichgra-

ber et al., 2018). Misinterpretation of the vascular anatomy of the PA and its variations could result in nontarget embolization of periprostatic organs and other structures such as the bladder, rectum, and penis (Pilan et al., 2022).

The International Prostate Symptom Score (IPSS) is a validated and widely used tool for assessing lower urinary tract symptoms related to benign prostatic hyperplasia (BPH). The questionnaire comprises seven questions, each scored from 0 to 5 according to symptom severity. These items assess key urinary symptoms including incomplete emptying, frequency, intermittency, urgency, weak stream, straining, and nocturia, the maximum total score is 35 (Barry et al., 2017). It is designed to assess the severity of symptoms, identify patients who may benefit from intervention, and monitor response to treatment over time. With scores interpreted as follows: 0–7 indicating mild symptoms, 8–19 moderate symptoms, and ≥ 20 severe symptoms (Naidu et al., 2021). This simple tool remains a core component of both clinical assessment and research in BPH (Zhu et al., 2024).

The aim of the work was to study the anatomical variations of the prostatic artery (PA) using both cadaveric dissection and angiography, and

to evaluate the impact of these variations, as well as embolization outcomes on IPSS, through the angiography.

MATERIALS AND METHODS

Cadaveric study

This cadaveric study was conducted in accordance with applicable ethical standards and institutional regulations. Cadaveric specimens were obtained through recognized body donation programs. Specimens were prepared and preserved in 10% formalin solution according to institutional protocols, ensuring proper fixation, ethical compliance, and suitability for anatomical study.

The study was conducted in accordance with the guidelines of the Declaration of Helsinki and approved by the Ethics Committee of October 6 University (protocol code O6U-ERC-0055).

The authors sincerely thank those who donated their bodies to science so that anatomical research and teaching could be performed. Results from such research can potentially increase scientific knowledge and can improve patient care. Therefore, these donors and their families deserve our highest respect.

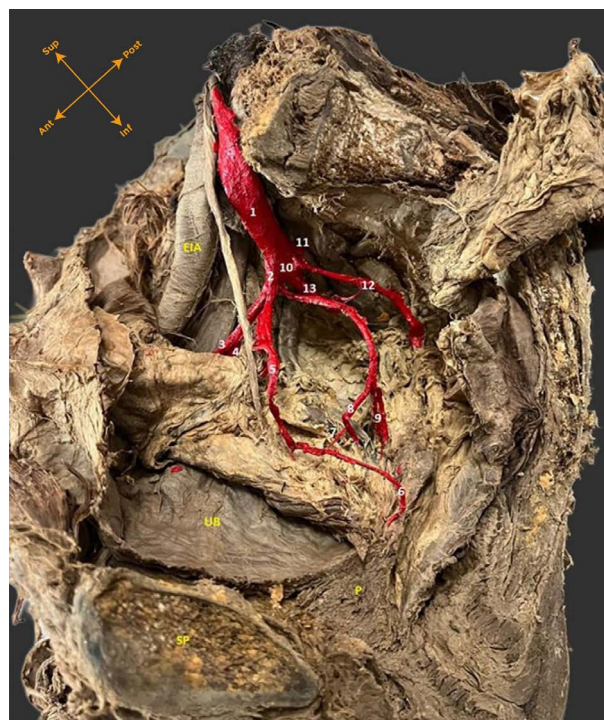


Fig. 1.- Cadaveric dissection of a right pelvic side showing the PA originating from the vesical artery. 1: Internal iliac artery; 2: Anterior division; 3: Superior vesical artery; 4: Obturator artery; 5: Inferior vesical artery; 6: Prostatic artery; 7: anastomotic branch; 8: Middle rectal artery; 9: Internal pudendal artery; 10: Posterior division; 11: Iliolumbar artery; 12: Lateral sacral artery; 13: Gluteal branches. EIA: External iliac artery; UB: Urinary bladder; SP: Symphysis pubis; P: Prostate.

The cadaveric study was performed bilaterally on five adult male pelvis specimens. Dissection started with the identification, delineation, and separation of both common iliac arteries and their bifurcation into the external and internal iliac arteries. All branches of the internal iliac artery were carefully dissected, with particular attention paid to the origin and course of the PA.

Radiological study (Patients)

The radiological study included 54 patients clinically diagnosed with BPH, aged over 50 years, with an IPSS greater than 19. All patients provided written informed consent to participate in the study. Exclusion criteria included suspicion of prostate cancer, active urinary tract infection, abnormal coagulation profile, or known allergy to contrast media. These criteria were previously applied by Basiouny et al. (2022).

Prostatic artery embolization procedure

Prostatic artery embolization was performed according to standard techniques under intravenous sedation, targeting the PA. All procedures were performed by the second author using a Siemens Monoplane angiography machine (Siemens Inc., Germany). Right femoral artery puncture was performed under local anesthesia, and a catheter was advanced through the femoral artery to the internal iliac artery and its anterior division, using digital subtraction angiography (DSA). Selective catheterization of the PA was performed using a microcatheter. Selective PA angiography was done to assess the arterial course, related anastomoses, and to avoid non-target embolization. Embolic material was introduced into the PA in order to achieve stasis of blood flow and complete occlusion of the prostatic parenchymal supply (Basiouny et al., 2022; Bilhim, 2023). Technical success is identified as successful embolization of all angiographically and/or cone-beam-computed-tomography visible arterial supply to the prostate and stasis in the PA with no contrast uptake in images taken in intraoperative imaging.

It is worth noting that the radiological classification of the PA, as described by Carnevale et al. (2017), shows a slight variation from the traditional anatomical descriptions. Radiologists, for

instance, often refer to a common vesical trunk as type I, whereas anatomists usually differentiate between the superior and inferior vesical arteries as separate branches. According to the radiological classification, the PA can arise from the vesical artery (type I), directly from the internal iliac artery (type II), the obturator artery (type III), the internal pudendal artery (type IV), or from less common origins (type V). In this study, we use the term vesical origin more broadly, to refer to any origin involving vesical arteries, allowing for a practical alignment between both anatomical and radiological viewpoints.

Outcome measures

Changes in IPSS were recorded before the procedure, at 3 months and 6 months postoperatively.

Statistical analysis

SPSS version 22.0 software was used for data analysis. Continuous data were presented as mean \pm standard deviation, and categorical data were presented as percentages. The t-test was used for pairwise comparisons of continuous variables between groups, and analysis of variance (ANOVA) was applied for comparisons among multiple groups. A p-value < 0.05 was considered statistically significant, and < 0.001 was considered highly significant.

RESULTS

Cadaveric results

In all cadaveric pelvic sides (No = 10), the internal iliac artery exhibited anterior and posterior divisions, but with variable branching patterns. The PA, being the specifically examined vessel, was identified as a direct branch from the vesical artery in six pelvic sides as it passed to supply the urinary bladder (Fig. 1). In two specimens, the PA originated from the obturator artery, and in another two, it originated from the internal pudendal artery. No cases demonstrated a direct origin from the internal iliac artery or other branches. There was no difference in PA origin between both sides in any of the examined specimens (Table 1).

Table 1. Distribution of PA origins observed in cadaveric specimens

PA origin	Number of specimens	Percentage
Vesical artery	6	60%
Obturator artery	2	20%
Internal pudendal artery	2	20%

Radiological results

Anatomical variations of the origin of PA were observed during angiography of all the cases treated with PA embolization included in the current study.

The PA originated from the vesical artery in 45 sides (18 bilateral, 4 from the right side, and 5 from the left). It arose from the obturator artery in 25 sides (11 bilateral, one from the right side only, and two from the left). The PA was found to originate from the internal pudendal artery in 23 sides (bilaterally in 10 cases, from the right in 2, and from the left in 1 case). It originated from the internal iliac artery in 15 sides (bilaterally in 6 cases, from the right in 2, and from the left in 1). Out of the 54 cases, 45 (83.3%) demonstrated symmetrical PA origin on both sides, while 9 cases showed an asymmetrical origin (Table 2 and Fig. 2).

All patients were followed for IPSS measurement before procedure, and at 3 and 6 months after the procedure. A progressive improvement in IPSS was observed at both time points. The mean pre-procedure IPSS score of 24.53 dropped to 16.31 after 3 months and to 11.56 after 6 months. This improvement was statistically analyzed and showed highly significant differences between the three measurements (Tables 3-4 and Fig. 3).

The impact of the origin of PA (after excluding patients with asymmetrical origin) as well as patient age, on the IPSS was also tested and no statistically significant differences were detected

(Tables 5-6).

It is to be noted that all specimens included in the study contributed to the statistical analysis. However, only representative images from cadaveric dissections and radiological studies were selected to illustrate key anatomical findings. Images of lower quality or preservation status were excluded from publication to maintain clarity and scientific rigor.

DISCUSSION

In the present study, the main origin of the PA was found to be from the vesical arteries. There is an obvious variation in the description of the vesical artery origin. The classical anatomical classification points to distinct origins of both superior vesical artery and inferior vesical artery, both originating from the anterior division of the internal iliac artery. The superior vesical represents the post foetal fate of the umbilical artery, with its terminal part obliterated forming the medial umbilical ligament. While the inferior vesical artery—also referred to as the vaginal artery in females—descends caudally to supply the pelvic genital organs. However, different studies have shown variable origins of the vesical arteries including a common trunk, multiple superior vesical arteries or a shared origin of inferior vesical artery with other pelvic branches such as middle rectal or obturator arteries (Bilhim et al., 2011; Mamatha et al., 2015; De Treigny et al., 2017). That is why we adopted the term “vesical origin” in the present work, to bypass the origin dilemma.

Table 2. Distribution of PA origins observed in patients

Origin	Symmetrical origin	Right side	Left side	Total	Percentage
Vesical	18 cases (36 sides)	4 sides	5 sides	45 sides	41.7 %
Obturator	11 cases (22 sides)	1 side	2 sides	25 sides	23.1%
Internal pudendal	10 cases (20 sides)	2 sides	1 sides	23 sides	21.3%
Internal iliac	6 cases (12 sides)	2 sides	1 sides	15 sides	13.9%
Total	45 cases (90 sides)	9 cases (18 sides)		54 cases (108 sides)	100%

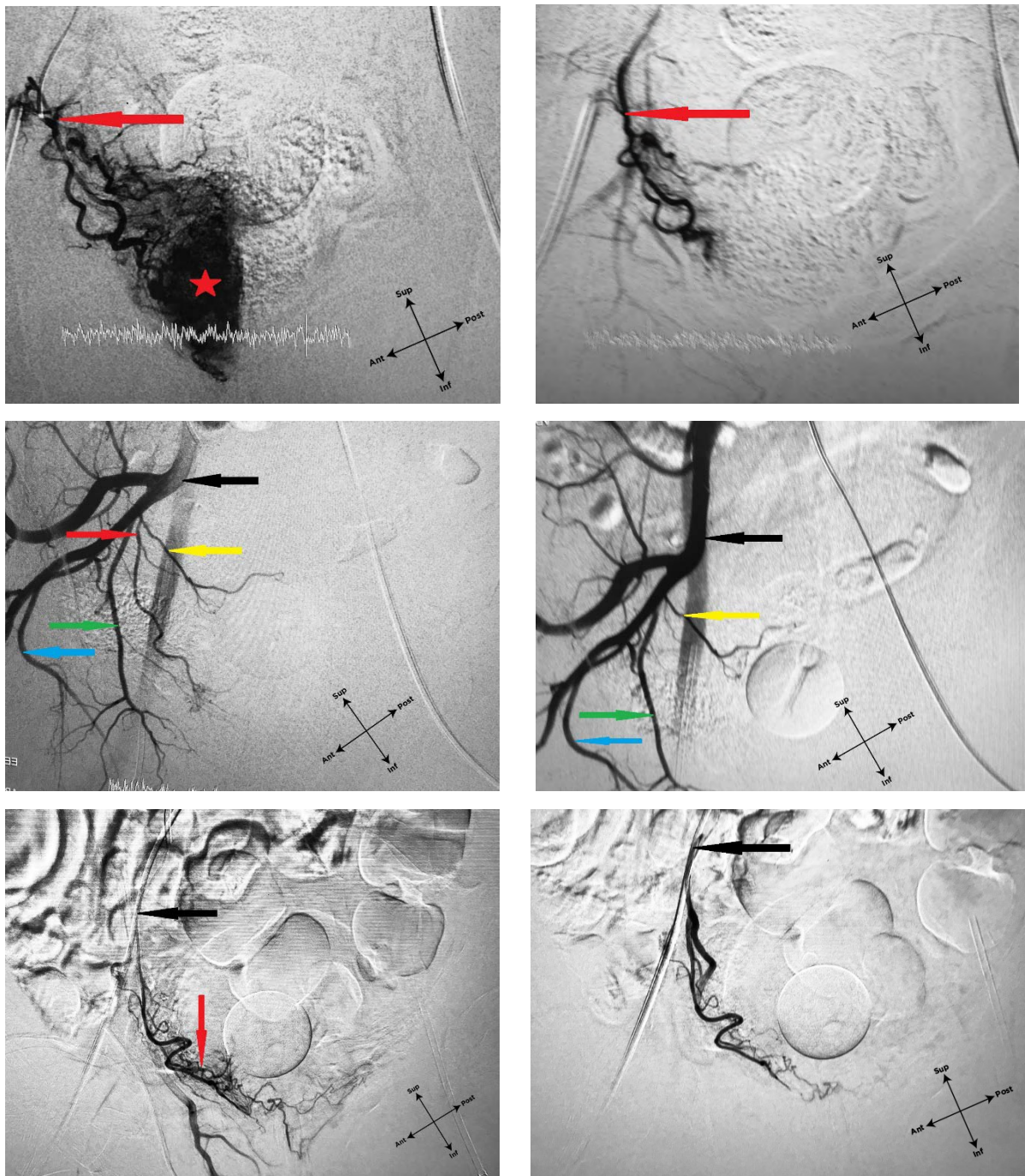


Fig. 2.- Digital subtraction angiography images demonstrating different origins of right prostatic arteries before and after embolization. In all images Black arrow points to the internal iliac artery or the microcatheter inside it. Yellow arrow points to the vesical artery, Green artery points to the obturator artery. Blue artery points to the internal pudendal artery. Red arrow points to the prostatic artery. a) Pre-embolization blush (*) of prostatic artery. b) The same patient following embolization. c) Pre-embolization prostatic artery originating from vesical trunk. d) The same patient following embolization. e) Pre-embolization prostatic artery originating from internal iliac artery. f) The same patient following embolization.

The PA originated from the vesical artery in 60% of the cadaveric arm of the study and in 41.7% of the radiological arm. These cadaveric results strongly correspond to those of Garcia-Monaco et al. (2014) who reported the vesical artery as the most common origin of the PA in 56.5% of cases. The similarity between the results along with the rarity of cadaveric studies highlights the important implication of the study.

On the other hand, the radiological findings strongly support our previous results (Basiouny et al., 2022). They also correspond to the findings of Carnevale et al. (2017), Du Pisanie et al. (2019), Enderlein et al. (2020) and Moschouris et al. (2023), who reported the superior vesical artery as the most common origin of the PA in 33.9%, 34.3%, 27.5% and 31% of cases respectively. The cumulative consideration of the vesical origin in

Table 3. Showing the mean and standard deviation (SD) of IPSS before the procedure and 3 and 6 months post-embolization in all patients (N = 54)

IPSS Before		IPSS after 3 months		IPSS after 6 months		ANOVA	P value
Mean	SD	Mean	SD	Mean	SD		
24.53	2.91	16.31	2.57	11.56	2.83	252.03	0.0001

Table 4. Multiple comparison between IPSS before the procedure, 3 months, and 6 months post-procedure in all patients (N = 54)

Groups		P value	Lower bound of 95% CI	Upper bound of 95% CI
IPSS Before	IPSS after 3 months	0.0001	7.0653	9.3792
IPSS Before	IPSS after 6 months	0.0001	11.8208	14.1347
IPSS after 3 months	IPSS after 6 months	0.0001	3.5986	5.9125

Table 5. Mean and standard deviation of IPSS scores before, and at 3 and 6 months after the procedure, according to the origin of the PA (symmetrical bilateral cases only, N = 45)

IPSS	Vesical A (N = 18 = 40%)		Obturator A (N = 11 = 24.5%)		IPA (N = 10 = 22.2%)		IIA (N = 6 = 13.3%)		ANOVA	P value
	Mean	SD	Mean	SD	Mean	SD	Mean	SD		
Before	24.389	3.16	24.818	2.44	23.700	3.09	25.833	2.79	0.707	0.553
after 3 months	16.500	2.90	16.182	2.14	15.400	2.80	17.500	1.64	0.885	0.457
after 6 months	11.944	3.06	11.182	2.52	10.400	2.59	13.000	2.83	1.275	0.296

No statistically significant difference between the groups

Table 6. Mean and standard deviation (SD) of IPSS scores before, and at 3 and 6 months after the procedure, according to the age groups (N = 54)

IPSS	50-60 (N = 16 = 29.6%)		60-70 (N = 26 = 48.2%)		Above 70 (N = 12 = 22.2 %)		ANOVA	P value
	Mean	SD	Mean	SD	Mean	SD		
Before	24.29	3.07	25.40	2.62	23.27	2.94	2.062	0.140
after 3 months	15.71	2.73	17.35	2.01	16.18	2.75	3.424	0.132
after 6 months	11.07	3.27	12.45	2.61	10.55	2.34	1.986	0.150

No statistically significant difference between the groups

the present work may contribute to the higher levels observed. Conversely, variability in reported prevalence has been described in other reviews. Some studies have reported a higher frequency of origins from the internal pudendal artery or from a common trunk with superior vesical artery (Xuan et al., 2019; Şerbanoiu et al., 2023). These discrepancies are likely related to differences in study design, imaging technique and classification criteria, rather than true inconsistencies. Importantly, such studies primarily address overall clinical efficacy of prostate artery embolization, and do not specifically analyze the impact of arterial origin variability on clinical outcomes.

The present study was conducted on 54 patients, all over 50 years old, diagnosed with BPH and presenting with an IPSS score of 19 or higher. All the patients demonstrated improvement in IPSS score 3 and 6 months following the procedure. The mean IPSS score of the patients dropped from 24.53 before the procedure to 16.31 at three months and 11.56 six months after the procedure. The study revealed a highly significant difference as regards the IPSS progress, indicating a high treatment efficacy. These findings confidently confirm the suitability of this procedure for the treatment of BPH.

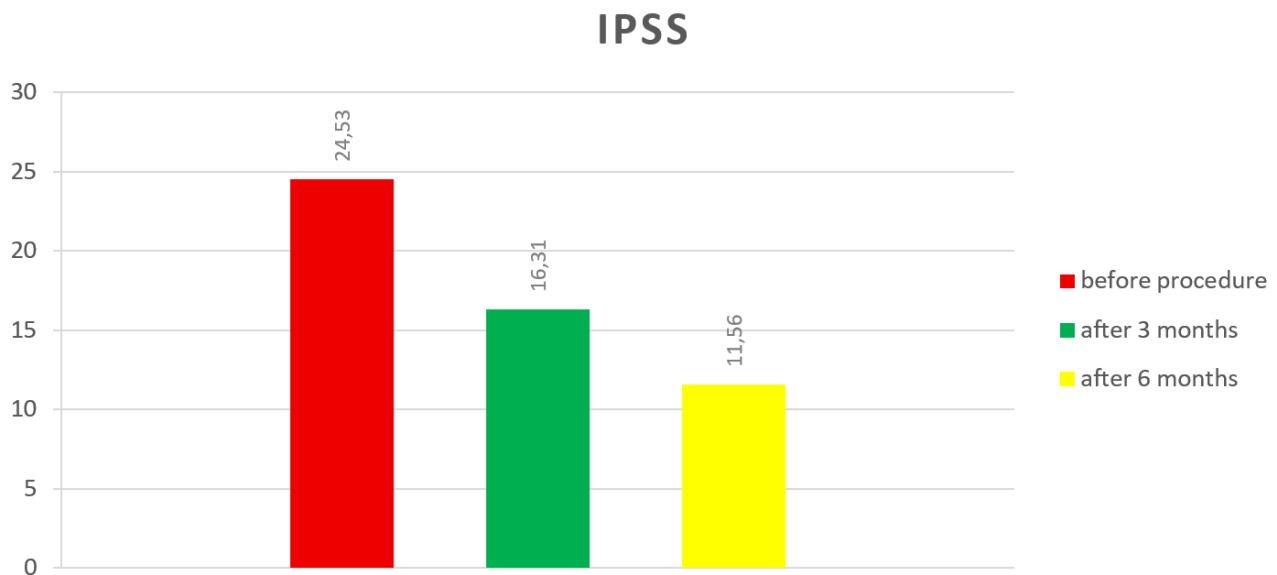


Fig. 3.- A chart illustrating the progression of IPSS scores before, and at 3 and 6 months after the procedure.

Recent meta-analyses and large clinical series have demonstrated that prostate artery embolization (PAE) results in significant improvement in IPSS and quality of life in patients with BPH, supporting its role as an effective, minimally invasive treatment option (Wang et al., 2018). Although comparative analyses have shown that certain functional outcomes, such as maximum urinary flow rate and prostate volume reduction, may be more pronounced following transurethral resection of the prostate (Xu et al., 2021), these studies primarily evaluate overall clinical efficacy and do not address the potential influence of anatomical variations in the origin of the prostatic artery. In this context, the present study adds specific anatomical insight by demonstrating that clinical improvement, as reflected by IPSS reduction, is achieved irrespective of the arterial origin pattern.

Neither the patient's age nor the origin of his PA affected the outcomes of the study. There was no statistically significant difference between patient groups when stratified by age. Although some studies have reported an inverse relationship between age and the success of the procedure (Bilhim et al., 2016), this was attributed later by the same author to arterial sclerosis and impaired bladder physiology (Bilhim, 2023). Enderlein et al. (2020) found that arterial tortuosity increases with age, resulting in longer procedure times and technical difficulties. The findings of the present

work are consistent with this explanation. On the other hand, Loffroy et al. (2024) and Zorzi et al. (2025) denied the effect of the age as an influencing factor of IPSS improvement. Overall, it seems that age may influence the technical aspects of the procedure rather than its results.

In the present work, we examined both cadaveric and clinical findings as concerning the PA origin; we also monitored IPSS scores in order to establish a robust conclusion regarding the efficacy of PA embolization as a therapeutic procedure. However, the modest sample size—particularly in the cadaveric arm, where ethical considerations limited its use—and the single center design were obstacles that should be addressed in future work.

CONCLUSION

We conclude that the PA exhibits variable origins among the population, with the vesical arteries being the most common source. We also conclude that PA embolization is an effective therapeutic management of BPH, regardless of the patient's age or PA origin.

ACKNOWLEDGEMENTS

We gratefully acknowledge the invaluable contribution of the body donors, as well as their families, whose generosity made the anatomical research and the advancement of medical science possible.

AUTHORS CONTRIBUTION

Conceptualization, Ahmed F. AlDomairy, Gamal-el-

dine M. Niazi and Radwa M. Elsabban; Methodology, Gamal-eldine M. Niazi; Validation, Gamal-eldine M. Niazi; Data Curation, Ahmed F. AlDomairy and Radwa M. Elsabban; Writing – Original Draft Preparation, Radwa M. Elsabban Ahmed F. AlDomairy; Writing – Review & Editing, Ahmed F. AlDomairy; Supervision and Project Administration, Ahmed F. AlDomairy. All authors shared the literature search and revision, commented on previous versions of the manuscript and approved the final manuscript. They all agree to be personally accountable for their own contribution and for the accuracy and integrity of all parts of the work.

Institutional review board statement and compliance with ethical standards

The study was conducted according to the guidelines of the Declaration of Helsinki and approved by the Ethics Committee of October 6 University (protocol code O6U-ERC-0055).

Consents and privacy rights

A written informed consent was obtained from the patients included in this study. The privacy rights of the subjects were preserved.

REFERENCES

- ADACHI B (1928) Das Arteriensystem der Japaner. Vol. II. Kyoto: Maruzen Publishing Co.
- ASHLEY FL, ANSON BJ (1941) The hypogastric artery in American whites and negroes. *Am J Phys Anthropol*, 28: 381-395.
- BARRY MJ, FOWLER FJ, O'LEARY MP, BRUSKEWITZ RC, HOLTGREWE HL, MEBUST WK, CALKINS DR (2017) The American Urological Association symptom index for benign prostatic hyperplasia (BPH). *J Urol*, 197(2S): S189-S197.
- BASIOUNY KE, GHAZI MS, NIAZI M ALLAM AE (2022) Anatomical variants in prostatic artery embolization in treatment of benign prostatic hyperplasia: *Egypt J Radiol Nucl Med*, 53: 120.
- BILHIM T (2023) Prostatic artery embolization: an update. *Korean J Radiol*, 24(4): 313-323.
- BILHIM T, CASAL D, FURTADO A, PAIS D O'NEIL JEG, PISCO JM (2011) Branching patterns of the male internal iliac artery: imaging findings. *Surg Radiol Anat*, 33: 151-159.
- BILHIM T, PISCO JM, TINTO HR, FERNANDES L, PINHEIRO LC, FURTADO A, CASAL D, DUARTE M, PEREIRA J, OLIVEIRA AG, O'NEILL JE (2012) Prostatic arterial supply: anatomic and imaging findings relevant for selective arterial embolization. *J Vasc Interv Radiol*, 23(11): 1403-1415.
- BILHIM T, PISCO J, PEREIRA JA, COSTA NV, FERNANDES L, PINHEIRO LC, DUARTE M, OLIVEIRA AG (2016) Predictors of clinical outcome after prostate artery embolization with spherical and non-spherical polyvinyl alcohol particles in patients with benign prostatic hyperplasia. *Radiology*, 281(1): 289-300.
- CAPDEVILA F, INSAUSTI I, GALBETE A, SANCHEZ-IRISO E, MONTESINO M (2021) Prostatic artery embolization versus transurethral resection of the prostate: a post hoc cost analysis of a randomized controlled clinical trial. *Cardiovasc Interv Radiol*, 44(11): 1771-1777.
- CARNEVALE FC, DA MOTTA LEAL FILHO JM, ANTUNES AA, BARONI RH, MARCELINO ASZ, CERRI LMO, YOSHINAGA EM, CERRI GG, SROUGI M (2013) Quality of life and clinical symptom improvement support prostatic artery

embolization for patients with acute urinary retention caused by benign prostatic hyperplasia. *J Vasc Interv Radiol*, 24(4): 535-542.

CARNEVALE FC, SOARES GR, DE ASSIS AM, MOREIRA AM, HARWARD SH, CERRI GG (2017) Anatomical variants in prostate artery embolization: a pictorial essay. *Cardiovasc Interv Radiol*, 40(9): 1321-1337.

CARTER H (1867) *Anatomy Descriptive and Surgical*. London, Philadelphia, pp 429-446.

CLEGG EJ (1955) The arterial supply of the human prostate and seminal vesicles. *J Anat*, 89: 209-216.

DE ASSIS AM, MOREIRA AM, RODRIGUES VCD, HARWARD SH, ANTUNES AA, SROUGI M, CARNEVALE FC (2015) Pelvic arterial anatomy relevant to prostatic artery embolization and proposal for angiographic classification. *Cardiovasc Interv Radiol*, 38(4): 855-861.

DE MARZO AM, PLATZ EA, SUTCLIFFE S, XU J, GRÖNBERG H, DRAKE CG, NAKAI Y, ISAACS WB, NELSON WG (2007) Inflammation in prostate carcinogenesis. *Nat Rev Cancer*, 7(4): 256-269.

DE TREIGNY OM, ROUMIGUIE M, DEUDON R DE BONNECAZE G, CARFAGNA L, CHAYNES P, RIMAILBO J, CHANTALAT E (2017) Anatomical study of the inferior vesical artery: is it specific to the male sex. *Surg Radiol Anat*, 39(9): 961-965.

DU PISANIE J, ABUMOUSSA A, DONOVAN K, STEWART J, BAGLA S, ISAACSON A (2019) Predictors of prostatic artery embolization technical outcomes: patient and procedural factors. *J Vasc Interv Radiol*, 30(2): 233-240.

ENDERLEIN GF, LEHMANN T, VON RUNDSTEDT FC, ASCHENBACH R, GRIMM MO, TEICHGRABER U, FRANIEL T (2020) Prostatic artery embolization - anatomic predictors of technical outcomes. *J Vasc Interv Radiol*, 31(3): 378-387.

FRANCO JVA, TESOLIN P, JUNG JH (2023) Update on the management of benign prostatic hyperplasia and the role of minimally invasive procedures. *Prostate Int*, 11(1): 1-7.

GARCIA-MONACO R, GARATEGUI L, KIZILEVSKY N, PERALTA O, RODRIGUEZ P (2014) Human cadaveric specimen study of the prostatic arterial anatomy: implications for arterial embolization. *J Vasc Interv Radiol*, 25(2): 315-322.

ITTMANN M (2018) Anatomy and histology of the human and murine prostate. *Cold Spring Harb Perspect Med*, 8(5): a030346.

LIM KB (2017) Epidemiology of clinical benign prostatic hyperplasia. *Asian J Urol*, 4(3): 148-151.

LIPSHUTZ B (1918) A composite study of the hypogastric artery and its branches. *Ann Surg*, 67: 584-608.

LIU TT, THOMAS S, MCLEAN DT, ROLDAN-ALZATE A, HERNANDO D, RICKE EA, RICKE WA (2019) Prostate enlargement and altered urinary function are part of the aging process. *Aging*, 11(9): 2653-2669.

LOFFROY R, QUIRANTES A, GUILLEN K, MAZIT A, COMBY PO, AHO-GLELE LS, CHEVALLIER O (2024) Prostate artery embolization using n-butyl cyanoacrylate glue for symptomatic benign prostatic hyperplasia: A six-month outcome analysis in 103 patients. *Diagn Interv Imaging*, 105(4): 129-136.

LOWSLEY OS (1912) The development of the human prostate gland with reference to the development of other structures at the neck of the urinary bladder. *Am J Anat*, 13(3): 299-346.

MAMATHA H, HEMALATHA B, VINODINI P, SOUZA ASD, SUHANI S (2015) Anatomical study on variations in the branching pattern of internal iliac artery. *Indian J Surg*, 77(2): 248-252.

MCNEAL JE (1988) Normal histology of the prostate. *Am J Surg Pathol*, 12(8): 619-633.

MOSCHOURIS H, STAMATIOU K, TZAMARIAS S, FRIGKAS K, SPANOMANOLIS N, ISAAKIDOU I, DIMITROULA E, SPILIOPOULOS S, BROUNTZOS E, MALAGARI K (2023) Angiographic imaging of prostatic artery origin in a Greek population and correlation with technical and clinical aspects of prostatic artery embolization. *Cureus*, 15(9): e44520.

MOYA C, CUESTA J, FRIERA A, SEDO JMGV, VALDERRAMA-CANALES FJ (2017) Cadaveric and radiologic study of the anatomical variations of the

prostatic arteries: A review of the literature and a new classification proposal with application to prostatectomy. *Clin Anat*, 30(1): 71-80.

NAIDU SG, NARAYANAN H, SAINI G, SEGARAN N, ALZUBAIDI SJ, PATEL IJ, OKLU R (2021) Prostate artery embolization-review of indications, patient selection, techniques and results. *J Clin Med*, 10(21): 5139.

NICKEL JC, ROEHRBORN CG, CASTRO-SANTAMARIA R, FREEDLAND SJ, MOREIRA DM (2016) Chronic prostate inflammation is associated with severity and progression of benign prostatic hyperplasia, lower urinary tract symptoms and risk of acute urinary retention. *J Urol*, 196(5): 1493-1498.

PILAN BF, DE ASSIS AM, MOREIRAAM, RODRIGUES VCD, CARNEVALE FC (2022) Protection of nontarget structures in prostatic artery embolization. *Radiol Bras*, 55(1): 6-12.

ROBERTS WH, KRISHINGER GL (1968) Comparative study of human internal iliac artery based on Adachi classification. *Anat Rec*, 158: 191-196.

SERBANOIU A, NECHIFOR R, MARINESCU AN, IANA G, BRATU AM, SALCIANU IA, ION RT, FILIPOIU FM (2023) Prostatic artery origin variability: five steps to improve identification during percutaneous embolization. *Medicina*, 59(12): 2122.

SHARPEY W, THOMSON A, CLELAND J (1867) *Quain's Elements of Anatomy*. 7th ed. Longmans, Green and Co., London, pp 418-442.

TEICHGRABER U, ASCHENBACH R, DIAMANTIS I, VON RUNDSTEDT F, GRIMM, M, FRANIEL T (2018) Prostate artery embolization: indication, technique and clinical results. *Rofo*, 190(9): 847-855.

WANG M, ZHOU S, ZHANG Y, LI C, LI H (2018) Prostate artery embolisation for benign prostatic hyperplasia: a systematic review and meta-analysis. *BJU International*, 121(5): 706-713.

WANG MQ, DUAN F, YUAN K, ZHANG G, YAN J, WANG Y (2017) Benign prostatic hyperplasia: Cone-beam CT in conjunction with DSA for identifying prostatic arterial anatomy. *Radiology*, 282(1): 271-280.

WILSON E (1868) *A System of Human Anatomy, General and Special*. 7th ed. London, Philadelphia, pp 323-333.

XU L, ZHOU Z, MU Y, CAI T, GAO Z, LIU L (2021) An updated meta analysis of the efficacy and safety of prostatic artery embolization vs transurethral resection of the prostate in the treatment of benign prostatic hyperplasia. *Front Surg*, 15(8): 779571.

XUAN HN, HOANG DH, NGUYEN NTB, PHAN GH, LE VAN K, NGUYEN TD, TRAN TA (2019) Anatomical characteristics and variants of prostatic artery in patients with benign hyperplasia prostate by digital subtraction angiography. *Open Access Maced J Med Sci*, 7(24): 4204-4208.

YAMAKI K, SAGA T, DOI Y, AIDA K, YOSHIZUKA M (1998) A statistical study of the branching of the human internal iliac artery. *Kurume Med J*, 45(4): 333-340.

ZHANG G, WANG M, DUAN F, YUAN K, LI K, YAN J, CHANG Z, WANG Y (2015) Radiological findings of prostatic arterial anatomy for prostatic arterial embolization: preliminary study in 55 chinese patients with benign prostatic hyperplasia. *PLoS One*, 10(7): e0132678.

ZHU D, MALI K, BANDARI J, JAIN RK, QUARRIER SO (2024) Enhancing the management of benign prostatic hyperplasia: the role of electronic health record patient portal distribution of the International Prostate Symptom Score. *Urol Pract*, 11(4): 709-715.

ZORZI F, ROSSIN G, DIGREGORIO M, LAVECCHIA S, PIASENTIN A, TRAUNERO F, MORREALE C, RIZZO M, CAI T, TROMBETTA C, ZUCCHI A, LIGUORI G (2025) Prostatic artery embolization in elderly comorbid patients with benign prostatic hyperplasia: safety, efficacy, and predictive factors of clinical failure. *J Pers Med*, 15(1): 23.

Relationship between dorsal digit ratio and hand grip strength in young adult Nigerian population

Smart I. Mbagwu, Chidiebere A. Nnajeze, Kelechi E. Ichie

Department of Anatomy, Faculty of Basic Medical Sciences, Nnamdi Azikiwe University, PMB 5025, Awka, Anambra State, Nigeria

SUMMARY

Digital ratio, particularly the second-to-fourth digit ratio (2D:4D), has been explored as a non-invasive marker of prenatal hormone exposure and a potential predictor of Hand Grip Strength (HGS). While previous studies have linked lower 2D:4D ratios to enhanced physical strength, evidence from African populations remains limited. This study investigated the relationship between dorsal digit ratios (2D:4D and 3D:5D) and handgrip strength (HGS) in a sample of young adult Nigerians aged between 18 and 30 years. A total of 249 participants (124 males and 125 females) were randomly selected. Dorsal digit lengths were measured using a digital vernier caliper, and HGS was assessed using a modified sphygmomanometer.

Results showed clear sexual dimorphism in both digit ratios and hand grip strength. Females had significantly higher right-hand 2D:4D ratios than males, while males exhibited significantly greater HGS and longer digits across all measured fingers. Notably, the 2D:4D ratio was a significant predictor of left-hand grip strength across sexes. In males, the right-hand 2D:4D ratio did not cor-

relate with grip strength, whereas the 3D:5D ratio proved a better predictor. Among females, both 2D:4D and 3D:5D ratios showed significant associations with grip strength in both hands.

These findings suggest that dorsal digit ratios, particularly 2D:4D and 3D:5D, may serve as useful indicators of grip strength, with hand-specific and sex-specific variations in predictive value. This pattern reinforces the relevance of digit ratio variation as a potential anatomical marker of functional performance.

Key words: Digit ratio – Humans – Nigeria – Hand strength – Sex factors

INTRODUCTION

The 2D:4D digit ratio, defined as the ratio between the lengths of the second (index) and fourth (ring) digits, has emerged as a non-invasive biomarker of prenatal sex hormone exposure, particularly the balance between fetal testosterone and estrogen levels (Lutchmaya et al., 2004; Manning et al., 1998; Zheng and Cohn, 2011). This sexually dimorphic trait is established early in development and remains relatively stable across the

Corresponding author:

Smart Ikechukwu Mbagwu. Department of Anatomy, Faculty of Basic Medical Sciences, Nnamdi Azikiwe University, PMB 5025, Awka, Anambra State, Nigeria. E-mail: si.mbagwu@unizik.edu.ng - Orcid: 0000-0003-4297-6303

Submitted: January 9, 2026 **Accepted:** March 10, 2026

<https://doi.org/10.52083/UOLA3192>

lifespan (Manning and Fink, 2023). Typically, lower 2D:4D ratios, where the ring finger is longer than the index finger, indicate higher exposure to prenatal testosterone and are more common in males, while higher ratios are associated with greater prenatal estrogen exposure and are more frequently observed in females (Manning et al., 2007; Zhao et al., 2013). Though most commonly measured on the ventral surface, the dorsal digit ratio has gained traction as a more anatomically reliable indicator, due to reduced interference from fingertip fat and flexion creases (Kumar et al., 2017).

Beyond its developmental implications, digit ratio has been associated with a range of behavioral, cognitive, and physiological traits. Prenatal androgen exposure is known to influence the development of systems essential for physical fitness, such as the musculoskeletal, cardiovascular, and central nervous systems (Zheng and Cohn, 2011), which could confer performance-related advantages to individuals with lower 2D:4D ratios (Klimek et al., 2014). As such, digit ratio has been associated with a range of physical and behavioral traits, including facial morphology (Meindl et al., 2012), athletic performance (Honekopp and Watson, 2010; Kim and Kim, 2016), sexual orientation (Grimbos et al., 2010), and personality features (Bailey and Hurd, 2005; Bağcı Uzun and İnceoğlu, 2024). Likewise, higher ratios have been associated with anxiety and emotional vulnerability, particularly in females (Manning et al., 2014; Rinella et al., 2022). From a physiological standpoint, the digit ratio has been correlated with measures of physical strength and muscle development, suggesting that prenatal androgen exposure may influence long-term musculoskeletal outcomes (Pasanen et al., 2022).

Hand grip strength (HGS) is a widely accepted, practical, and non-invasive measure of muscular fitness and overall physical function. It serves as a reliable indicator of general health and strength capacity across diverse populations. (Vaishya et al., 2024). Given testosterone's role in muscle development, a link between prenatal hormone exposure (reflected by 2D:4D) and adult HGS is biologically plausible. Supporting this, studies have shown that men with lower digit ratios ex-

hibit higher HGS while women exhibited an inconsistent pattern (Longman et al., 2011; Zhao et al., 2013; Nanda and Samanta, 2017). This relationship appears consistent across various ethnic populations, including European, East Asian, and Indian groups (Fink et al., 2006; Zhao et al., 2012; Nanda and Samanta, 2017). In addition, it has been shown to predict a variety of health outcomes, including bone mineral density, frailty, cardiovascular disease, and mortality risk (Vaishya et al., 2024).

Given the ethnic variation in 2D:4D ratios, and the evidence linking lower digit ratios to enhanced physical strength in males, it is important to investigate this association in diverse populations, especially the African population, which is understudied. Cultural, genetic, and environmental variations may influence both digit ratio and physical strength outcomes (Isen et al., 2014), underscoring the need for population-specific investigations. Furthermore, while most prior studies have examined ventral digit ratios, few have evaluated the dorsal measurement (Kumar et al., 2017; Voracek, 2009)—despite its proposed anatomical advantages.

Given these gaps, this study investigated the relationship between dorsal digit ratio and hand grip strength in a sample of young adult Nigerians. By exploring these associations, the study aimed at contributing to a growing body of literature on the predictive value of digit ratio as a biomarker of physiological capacity and to providing baseline data relevant to health screening, athletic profiling, and developmental research in West African populations.

MATERIALS AND METHODS

Participants

This study was conducted at the College of Health Sciences, Nnamdi Azikiwe University, Nnewi Campus, Anambra State, Nigeria. A total of 249 healthy Nigerian young adults, comprising 124 males and 125 females, participated in the study. All participants were between 18 and 30 years of age and of Nigerian parentage, with both parents being of Nigerian descent. Participants were randomly selected from the student popula-

tion of the College of Health Sciences to ensure a representative sample.

Eligibility criteria included individuals aged 18 to 30 years with no visible or non-visible musculoskeletal disorders, hand deformities, or long fingernails that could interfere with measurement accuracy. Individuals outside the specified age range or with any condition affecting the fingers or upper limbs were excluded from participation.

The sample size was determined using the standard formula for population-based sample estimation, with a population size of 425, a 99% confidence level ($z = 2.582$), a margin of error of 0.05, and an estimated proportion of 0.5. The calculated sample size was 259.39, and 249 participants were ultimately recruited for the study.

Procedure

Participants were invited to individual assessment sessions during which demographic data, including age and sex, were recorded. All measurements were conducted with participants seated in a standardized position to ensure consistency. Digit lengths were measured using a digital vernier caliper and recorded in centimeters (cm), with the hand placed flat on a table and fingers extended at a 90-degree angle to the palm. Measurements were taken from the tip of each finger to the dorsal base of the proximal phalanx for the second (2D), third (3D), fourth (4D), and fifth (5D) digits of both hands.

Hand grip strength was assessed using a modified sphygmomanometer. Participants were seated with their shoulder adducted, elbow flexed at 90 degrees, and both forearm and wrist in a neutral position. The sphygmomanometer cuff was rolled into a cylindrical shape and inflated to 20 mmHg. Participants were instructed to grip the cuff maximally, and grip strength was recorded for both hands. The average of the two measurements was taken as the final hand grip strength. Prior to data collection, participants were familiarized with the procedure to ensure accurate and consistent performance.

All assessments were conducted in accordance with standardized protocols. Health conditions or pain that could compromise strength measure-

ment were monitored and used as exclusion criteria during the session.

Materials

Digit lengths were measured using a 6-inch (150 mm) digital vernier caliper with an accuracy of 0.02 mm and a resolution of 0.01 mm. The caliper was a stainless-steel precision instrument, calibrated to ensure reliable data collection. Hand grip strength was measured using a modified sphygmomanometer calibrated in millimeters of mercury (mmHg), which has been validated as a reliable tool for assessing maximal voluntary grip force.

The parameters measured in this study included age, sex, dorsal digit lengths (2D, 3D, 4D, 5D), and hand grip strength. Two digit ratios were calculated for each participant: the second-to-fourth digit ratio (2D:4D), defined as the length of the index finger divided by the length of the ring finger, and the third-to-fifth digit ratio (3D:5D), defined as the length of the middle finger divided by the length of the little finger.

Statistical Analysis

Statistical analyses were performed using SPSS® version 29.0 (IBM Corporation, Armonk, NY, USA). Descriptive statistics were computed for all variables. Independent t-tests were used to assess sex differences in digit lengths, digit ratios, and hand grip strength. Pearson correlation coefficients were calculated to examine associations between digit ratios and grip strength. Partial correlation analyses were conducted to control potential confounding variables such as age and sex. Statistical significance was defined at $p \leq 0.05$.

Ethical Considerations and Informed Consent

This study was conducted in accordance with the ethical principles outlined in the Declaration of Helsinki for research involving human participants (World Medical Association, 2013). Ethical approval for the study was obtained from the Research Ethics Committee of the Faculty of Basic Medical Sciences, Nnamdi Azikiwe University, Nnewi Campus, Anambra State, Nigeria with approval number NAU/REC/FBMS/03569.

All participants were adequately informed about the purpose, procedures, benefits, and potential risks of the study before enrollment. Participation was entirely voluntary, and written informed consent was obtained from each participant prior to data collection. Participants were assured of their right to decline participation or withdraw from the study at any point without penalty or loss of benefits.

Confidentiality and anonymity were strictly maintained throughout the study. Personal identifiers were not recorded, and all data were coded and stored securely, accessible only to the researchers. Standardized procedures were employed to ensure participant safety and comfort during digit measurement and hand grip strength assessment.

No financial incentives were provided, and the study did not involve any form of coercion.

RESULTS

Dorsal Digit Ratio

Descriptive statistics presented in Table 1 show that males had longer dorsal digit lengths than females across all measured fingers (2D, 3D, 4D, and 5D) on both the right and left hands. Standard deviations were notably higher for the female right hand 4D and left hand 5D measurements, indicating greater anatomical variability within these digits.

Males showed tightly clustered 2D:4D ratios (≈ 0.90 – 0.91) and consistent 3D:5D ratios around

1.28 across both hands (Table 2). Female participants showed greater variability in dorsaldigit lengths, particularly in the 4D and 5D measurements, which corresponded with higher 2D:4D ratios (0.92–0.97) and slightly elevated left hand 3D:5D ratios (1.34 ± 0.33) (Table 2).

Hand Grip Strength (HGS)

Descriptive statistics for handgrip strength are presented in Table 3. Across both hands, males demonstrated significantly higher grip strength than females. For the right hand, males recorded a mean value of 364.89 ± 21.83 mmHg compared with 261.78 ± 25.75 mmHg in females. A similar pattern was observed in the left hand, where males averaged 359.50 ± 30.99 mmHg and females 249.44 ± 32.70 mmHg. In both sexes, right hand grip strength was slightly higher than left hand values.

Association between Dorsal Digit Ratios and Hand Grip Strength

Males

Among male participants, the correlation between the right hand 2D:4D ratio and right hand grip strength was weak and not statistically significant ($p = 0.298$), indicating no meaningful association. In contrast, the righthand 3D:5D ratio showed a significant negative correlation with grip strength ($r_h = -0.27$, $p = 0.002$), suggesting that lower 3D:5D ratios were associated with greater right hand grip strength (Table 4).

For the left hand, the 2D:4D ratio showed a pos-

Table 1. Descriptive statistics (Mean \pm SD) for right and left dorsal digit lengths (2D–5D) in male and female young adult Nigerians, with commutative values for the total sample

Hand	Dorsal digit	Mean \pm SD (cm)		Commutative Mean \pm SD (n = 249)
		Male (n = 124)	Female (n = 125)	
Right	2D	10.3 \pm 0.48	9.8 \pm 0.56	10.1 \pm 0.57
	3D	11.8 \pm 0.76	11.1 \pm 0.60	11.5 \pm 0.76
	4D	11.4 \pm 0.64	10.1 \pm 1.91	10.9 \pm 0.78
	5D	9.2 \pm 0.49	8.7 \pm 0.56	9.0 \pm 0.58
Left	2D	10.3 \pm 0.49	9.7 \pm 0.45	10.1 \pm 0.56
	3D	11.8 \pm 0.79	11.0 \pm 0.61	11.5 \pm 0.78
	4D	11.3 \pm 0.70	10.5 \pm 0.52	10.9 \pm 0.78
	5D	9.2 \pm 0.52	8.2 \pm 1.98	8.7 \pm 1.54

Note: 2D = index finger; 3D = middle finger; 4D = ring finger; 5D = little finger.

Table 2. Digit Ratios of young adults of the Nigerian population in this study

Sex	Hand	2D:4D (\pm SD)	3D:5D (\pm SD)
Male (n = 124)	Right	0.90 \pm 0.06	1.28 \pm 0.10
	Left	0.91 \pm 0.07	1.28 \pm 0.11
Female (n = 125)	Right	0.97 \pm 0.19	1.28 \pm 0.10
	Left	0.92 \pm 0.13	1.34 \pm 0.26

Note: Ratios were computed as 2D/4D and 3D/5D respectively.

Table 3. Descriptive statistics (Mean \pm SD) for Right and Left Hand Grip Strength in male and female young adult Nigerians

Hand	Grip strength (mmHg) Mean \pm SD	
	Male (n = 124)	Female (n = 125)
Right	364.89 \pm 21.83	261.78 \pm 25.75
Left	359.50 \pm 30.99	249.44 \pm 32.70

Table 4. Association between the dorsal digit ratio and hand grip strength (HGS) of male and female population in the study

Sex	Hand	Variables	Correlation coefficient (r_h)	p-value
Male (n = 124)	Right	2D:4D	-0.09	0.298
		3D:5D	-0.27	0.002*
	Left	2D:4D	0.17	0.059
		3D:5D	-0.54	<0.001*
Female (n = 125)	Right	2D:4D	0.267	0.003*
		3D:5D	-0.03	0.719
	Left	2D:4D	-0.27	0.002*
		3D:5D	0.24	0.006*

, statistically significant, p-value \leq 0.05

itive but non-significant association with grip strength ($p = 0.059$), falling just above the conventional threshold for statistical significance. In contrast, the left hand 3D:5D ratio demonstrated a strong and statistically significant negative correlation with grip strength ($r_h = -0.54$, $p < 0.001$), indicating a robust inverse relationship between this digit ratio and left hand muscular strength.

Female

Among the females, the right-hand 2D:4D ratio was positively and significantly correlated with right-hand grip strength ($r_h = 0.267$, $p = 0.0026$), indicating that higher digit ratios were associated with stronger grip performance. Conversely, the right-hand 3D:5D ratio showed no significant association with grip strength ($p = 0.719$), suggesting limited predictive value (Table 4).

For the left hand, the 2D:4D ratio demonstrated a statistically significant negative correlation with

grip strength ($r_h = -0.274$, $p = 0.002$), while the 3D:5D ratio showed a statistically significant positive correlation ($r_h = 0.243$, $p = 0.0062$). These results indicate that both digit ratios are associated with grip strength in the left hand, but in opposite directions (Table 4).

General population

The association between dorsal digit ratios and handgrip strength in the general population of young adult Nigerians is summarized in Table 5. For the right hand, neither digit ratio demonstrated a statistically significant relationship with grip strength. The 2D:4D ratio showed a weak negative correlation ($r = -0.05$, $p = 0.437$), while the 3D:5D ratio exhibited a weak positive correlation ($r = 0.07$, $p = 0.281$), indicating minimal predictive value for righthand strength.

For the left hand, a statistically significant negative correlation was observed between the 2D:4D

Table 5. Summary of associations between Dorsal Digit Ratios and Hand Grip Strength in the general population of young adult Nigerians

Hand	Digit Ratio	Correlation coefficient (r_s)	p-value
Right (n = 249)	2D:4D	-0.05	0.437
	3D:5D	0.07	0.281
Left (n = 249)	2D:4D	-0.27	<0.001*
	3D:5D	-0.04	0.456

, statistically significant, p-value $\leq 0.05^$

ratio and grip strength ($r = -0.27$, $p < 0.001$), indicating that lower digit ratios were associated with greater left hand strength. In contrast, the left hand 3D:5D ratio showed a weak and non significant negative correlation ($r = -0.04$, $p = 0.456$), suggesting minimal predictive value for this ratio.

Sexual dimorphism on digit ratios and its effect on grip strength

Table 6 presents the comparative analysis of hand grip strength between male and female participants, highlighting the presence of sexual dimorphism. The results show that males exhibited significantly higher grip strength than females in both hands.

For the right hand, males recorded a mean grip strength of 364.89 ± 21.83 mmHg, while females averaged 261.78 ± 25.75 mmHg. The difference was statistically significant ($t = -34.05$, $p < 0.001$). Similarly, for the left hand, males had a mean grip strength of 359.50 ± 30.99 mmHg compared to 249.44 ± 32.70 mmHg in females, with the difference also reaching statistical significance ($t = -27.26$, $p < 0.001$).

DISCUSSION

This study examined the associations between the 2D:4D ratio, 3D:5D ratios and handgrip strength in a young adult Nigerian population. Our study revealed consistent and statistically significant sexual dimorphism was observed in dorsal finger lengths, with males exhibiting longer dig-

its (2D, 3D, 4D, and 5D) on both hands compared with females. These findings align with previous research (Hone and McCullough, 2012; Kumar et al., 2017), reinforcing the view that finger-length patterns are shaped by sex-linked developmental influences, particularly prenatal androgen exposure. Similarly, males in this study displayed lower 2D:4D ratios than females, a pattern widely reported in the literature and often associated with enhanced athletic performance, greater physical strength, and higher aggression levels (Perciavalle et al., 2013; Zamani Sani et al., 2022).

Sexual dimorphism was also evident in handgrip strength, with males demonstrating significantly higher values in both hands. This finding is consistent with prior studies attributing male strength advantages to prenatal androgen effects, sex specific differences in muscle mass and endocrine profiles (Hone & McCullough, 2012; Kuderer et al., 2025), and evolutionary pressures such as male–male competition (Misiak et al., 2020). Together, these patterns underscore the biological relevance of digit ratios as potential markers for understanding sex linked variation in physical capability.

Our analysis revealed a distinct hand-specific pattern in the relationship between dorsal digit ratios and grip strength. While no significant associations were identified for the right hand, the left-hand 2D:4D ratio emerged as a moderate predictor of grip strength in the general population. This laterality effect suggests that the left hand

Table 6. Comparison of Hand Grip Strength between male and female participants

Variable	Grip Strength (mmHg) (Mean \pm SD)		t-value	p-value
	Male (n = 124)	Female (n = 125)		
Right	364.89 ± 21.83	261.78 ± 25.75	-34.05	<0.001*
Left	359.50 ± 30.99	249.44 ± 32.70	-27.26	<0.001*

, statistically significant, p-value $\leq 0.05^$

may be more sensitive to developmental or anatomical factors reflected in digit ratio variation, a pattern consistent with reports that digit ratio asymmetry can influence functional outcomes.

The absence of significant righthand correlations aligns with previous studies reporting inconsistent findings across populations. Although some authors have attributed such variability to factors like hand dominance, our study did not assess dominance and therefore cannot conclude in this regard. Nonetheless, Gallup et al. (2010) and van Anders (2007) similarly reported no meaningful associations, suggesting that methodological and demographic differences may contribute to inconsistent outcomes. In contrast, Xu and Zheng (2015) observed more pronounced sex differences in right hand digit ratios, highlighting laterality as an important consideration in digit ratio research.

These inconsistencies may stem from methodological differences, including the use of ventral versus dorsal digit measurements, as well as genetic and environmental factors that vary across populations. Future studies should aim to standardize measurement techniques and explore the role of cultural and developmental influences.

This study further examined the sex-specific patterns in the relationship between dorsal digit ratios (2D:4D and 3D:5D) and hand grip strength. In males, the 3D:5D ratio exhibited a significant inverse correlation with grip strength in both hands, indicating that lower 3D:5D ratios are associated with greater muscular strength. Although the present study did not identify a statistically significant correlation between the 2D:4D ratio and handgrip strength (HGS), the broader literature on this relationship remains equivocal.

Several studies have reported significant negative associations between 2D:4D and HGS in male samples (Hone & McCullough, 2012; Açar et al., 2021), suggesting that a lower 2D:4D ratio, reflective of greater prenatal androgen exposure, may confer a muscular strength advantage. In contrast, others have reported positive correlations (Nanda & Samanta, 2017), highlighting the influence of population-specific and methodological factors on observed outcomes. Notably, Fink et al.

(2006) demonstrated a significant negative relationship between 2D:4D and grip strength across both Caucasian and Mizo male populations, lending cross-cultural support to the androgenic

hypothesis. The discrepancy between the present findings and portions of the existing literature may reflect variability in sample demographics, measurement protocols, or the relatively modest statistical power of individual studies.

In females, a significant positive correlation was observed between the right-hand 2D:4D ratio and grip strength, whereas the left-hand 2D:4D ratio demonstrated a significant negative correlation. These lateralized and directionally opposing associations warrant careful interpretation, as they suggest that the relationship between digit ratios and muscular strength in females is neither linear nor uniform across hands. Such findings are partially concordant with prior investigations (Açar et al., 2021; Bäck et al., 2023), which similarly identified negative associations between the 2D:4D ratio and grip strength in female cohorts, though the presence of a concurrent positive association in the contralateral hand introduces an additional layer of complexity that has been insufficiently addressed in the existing literature.

With respect to the 3D:5D ratio, a statistically significant positive correlation was identified exclusively in the left hand among female participants, a pattern that stands in contrast to the findings of Nanda and Samanta (2017), who reported no significant association between this ratio and grip strength. This discrepancy may reflect genuine population-level differences in digit ratio distribution, or alternatively, may be attributable to methodological heterogeneity across studies, including variation in sample size, participant age range, and grip strength assessment protocols.

The opposing directionality of digit ratio correlations between the right and left hands in females, coupled with the sex-differentiated patterns observed throughout this study, suggests that the predictive utility of digit ratios for muscular strength is modulated by both biological sex and upper limb laterality. These observations are consistent with a growing body of evidence indicating that the hormonal and developmen-

tal determinants of digit ratio morphology, most notably the prenatal testosterone-to-estrogen milieu interact differentially with the physiological substrates of grip strength depending on sex (Manning, 2002; Hönekopp & Watson, 2010). The asymmetric and at times paradoxical nature of these correlations further underscores the inherent complexity of digit ratio physiology and cautions against overly deterministic interpretations of digit ratio-strength associations in mixed-sex samples.

CONCLUSION

Digit ratios demonstrated sex-specific and lateralized predictive associations with handgrip strength, with the 3D:5D ratio emerging as a more robust predictor in males, while both the 2D:4D and 3D:5D ratios showed significant associations among females, reflecting sex-specific androgenic programming with implications for musculoskeletal performance. These findings further confirm significant sexual dimorphism in handgrip strength, with males demonstrating superior grip performance and greater absolute digit lengths across all measured digits. Collectively, the present study supports the utility of digit ratios as non-invasive anthropometric markers of muscular strength, with their predictive value modulated by biological sex and hand laterality. Future studies employing larger, ethnically diverse samples and harmonized methodological frameworks will be essential in consolidating these associations and establishing their clinical relevance.

Limitations

Several limitations of the present study warrant acknowledgment. First, the cross-sectional design precludes any causal inference between digit ratios and handgrip strength. Second, hand dominance was not assessed, limiting the interpretation of observed lateralized associations. Third, although the study sample was ethnically mixed, ethnic background was not formally recorded or analyzed, which may have introduced unexamined variability given known population-level differences in digit ratio morphology. Fourth, potential confounding variables – including physical activity level, nutritional status, and occupational

hand use – were not controlled, which may have influenced grip strength measurements. Future studies incorporating longitudinal designs, larger samples with documented ethnic composition, and comprehensive covariate assessment are encouraged to address these limitations.

REFERENCES

- AÇAR G, DIGILLI B, SAĞLAM A, ÇİÇEKÇİBAŞI A (2021) The relationship of the digit ratio (2D:4D) with body fat distribution and handgrip strength in medical students. *Cukurova Med J*, 46(2): 555-556.
- BAĞCI UZUN G, İNCEOĞLU F (2024) Association of 2D:4D finger length ratio of people working in different professions with personality traits. *Heliyon*, 10(11): e32332.
- BAILEY AA, HURD PL (2005) Finger length ratio (2D:4D) correlates with physical aggression in men but not in women. *Biol Psychol*, 68(3): 215-222.
- BÄCK N, SCHAEFER K, WINDHAGER S (2021) Handgrip strength and 2D:4D in women: homogeneous samples challenge the (apparent) gender paradox. *Proc Biol Sci*, 288(1964): 20212328.
- FINK B, THANZAMI V, SEYDEL H, MANNING JT (2006) Digit ratio and hand-grip strength in German and Mizos men: cross-cultural evidence for an organizing effect of prenatal testosterone on strength. *Am J Hum Biol*, 18(6): 776-782.
- GALLUP AC, WHITE DD, GALLUP GG (2007) Handgrip strength predicts sexual behavior, body morphology, and aggression in male college students. *Evol Hum Behav*, 28: 423-429.
- GRIMBOS T, DAWOOD K, BURRIS RP, ZUCKER KJ, PUTS DA (2010) Sexual orientation and the second to fourth finger length ratio: a meta-analysis in men and women. *Behav Neurosci*, 124(2): 278-287.
- HONE LSE, MCCULLOUGH ME (2012) 2D:4D ratios predict hand grip strength (but not hand grip endurance) in men (but not in women). *Evol Hum Behav*, 33: 780-789.
- HÖNEKOPP J, WATSON S (2010) Meta-analysis of digit ratio 2D:4D shows greater sex difference in the right hand. *Am J Hum Biol*, 22(5): 619-630.
- ISEN J, MCGUE M, IACONO W (2014) Genetic influences on the development of grip strength in adolescence. *Am J Phys Anthropol*, 154(2): 189-200.
- KIM TB, KIM KH (2016) Why is digit ratio correlated to sports performance? *J Exerc Rehabil*, 12(6): 515-519.
- KLIMEK M, GALBARCZYK A, NENKO I, ALVARADO LC, JASIENSKA G (2014) Digit ratio (2D:4D) as an indicator of body size, testosterone concentration and number of children in human males. *Ann Hum Biol*, 41(6): 518-523.
- KUDERER S, ROTTER C, KIRCHENGAST S (2025) Associations between 2D:4D digit ratio and handgrip strength in a Central European population. *Early Hum Dev*, 208: 106315.
- KUMAR S, VORACEK M, SINGH M (2017) Sexual dimorphism in digit ratios derived from dorsal digit length among adults and children. *Front Endocrinol (Lausanne)*, 8: 41.
- LONGMAN D, WELLS JCK, STOCK JT (2015) Can persistence hunting signal male quality? A test considering digit ratio in endurance athletes. *PLoS One*, 10(4): e0121560.
- LUTCHMAYA S, BARON-COHEN S, RAGGATT P, KNICKMEYER R, MANNING JT (2004) 2nd to 4th digit ratios, fetal testosterone and estradiol. *Early Hum Dev*, 77(1-2): 23-28.
- MANNING JT, FINK B (2023) Digit ratio (2D:4D) and its relationship to foetal and maternal sex steroids: A mini-review. *Early Hum Dev*, 183: 105799.
- MANNING JT, SCUTT D, WILSON J, LEWIS-JONES DI (1998) The ratio of 2nd to 4th digit length: a predictor of sperm numbers and concentrations of testosterone, luteinizing hormone and oestrogen. *Hum Reprod*, 13(11): 3000-3004.

MANNING JT, CHURCHILL AJ, PETERS M (2007) The effects of sex, ethnicity, and sexual orientation on self-measured digit ratio (2D:4D). *Arch Sex Behav*, 36(2): 223-233.

MANNING JT, KILDUFF L, COOK C, CREWETHER B, FINK B (2014) Digit ratio (2D:4D): A biomarker for prenatal sex steroids and adult sex steroids in challenge situations. *Front Endocrinol (Lausanne)*, 5: 9.

MEINDL K, WINDHAGER S, WALLNER B, SCHAEFER K (2012) Second-to-fourth digit ratio and facial shape in boys: the lower the digit ratio, the more robust the face. *Proc Biol Sci*, 279(1737): 2457-2463.

MISIAK M, BUTOVSKAYA M, OLESZKIEWICZ A, SOROKOWSKI P (2020) Digit ratio and hand grip strength are associated with male competition outcomes: a study among traditional populations of the Yali and Hadza. *Am J Hum Biol*, 32(2): e23321.

NANDA B, SAMANTA PP (2017) The second to fourth digit ratio: a measure of hand grip strength? *Int J Adv Med*, 4(5): 1250-1254.

PASANEN BE, TOMKINSON JM, DUFNER TJ, PARK CW, FITZGERALD JS, TOMKINSON GR (2022) The relationship between digit ratio (2D:4D) and muscular fitness: A systematic review and meta-analysis. *Am J Hum Biol*, 34(3): e23657.

PERCIVALLE V, DI CORRADO D, PETRALIA MC, GURRISI L, MASSIMINO S, COCO M (2013) The second-to-fourth digit ratio correlates with aggressive behavior in professional soccer players. *Mol Med Rep*, 7(6): 1733-1738.

RINELLA S, MASSIMINO S, SORBELLO A, PERCIVALLE V, COCO M (2022) Cognitive performances: The role of digit ratio (2D:4D) with a protective factor for anxiety. *Front Neuroergon*, 3: 870362.

VAISHYA R, MISRA A, VAISH A, URSINO N, D'AMBROSI R (2024) Hand grip strength as a proposed new vital sign of health: a narrative review of evidences. *J Health Popul Nutr*, 43(1): 7.

VAN ANDERS SM (2007) Grip strength and digit ratios are not correlated in women. *Am J Hum Biol*, 19(3): 437-439.

VORACEK M, REIMER B, DRESSLER SG (2010) Digit ratio (2D:4D) predicts sporting success among female fencers independent from physical, experience, and personality factors. *Scand J Med Sci Sports*, 20(6): 853-860.

WORLD MEDICAL ASSOCIATION (2013) World Medical Association Declaration of Helsinki: ethical principles for medical research involving human subjects. *JAMA*, 310(20): 2191-2194.

XU Y, ZHENG Y (2015) The digit ratio (2D:4D) in China: A meta-analysis. *Am J Hum Biol*, 27(3): 304-309.

ZAMANI SANI SH, SADEGHI-BAHMANI D, FATHIREZAIIE Z, AGHDASI MT, ABBASPOUR K, BADICU G, BRAND S (2022) Gender differences and relationship of 2D:4D-ratio, mental toughness and dark triad traits among active young adults. *Biology (Basel)*, 11(6): 864.

ZHAO D, YU K, ZHANG X, ZHENG L (2013) Digit ratio (2D:4D) and handgrip strength in Hani ethnicity. *PLoS One*, 8(11): e77958.

ZHENG Z, COHN MJ (2011) Developmental basis of sexually dimorphic digit ratios. *Proc Natl Acad Sci USA*, 108(39): 16289-16294.

Correlation of p53 expression with morphological features in complete and partial hydatidiform moles

Melisa Lelić¹, Emin Grbić², Daniel Petrovič³, Suada Ramić¹, Jasminka Mustedanagić-Mujanović⁴, Adna Mujkić¹

¹ Department for Histology and Embryology, University of Tuzla, Medical Faculty, Bosnia and Herzegovina

² Department of Physiology, University of Tuzla, Medical Faculty, Bosnia and Herzegovina

³ Institute of Histology and Embryology, University of Ljubljana, SI, Medical Faculty, Slovenia

⁴ Department of Pathology, University Clinical Center Tuzla, Bosnia and Herzegovina

SUMMARY

Hydatidiform mole, the most common form of gestational trophoblastic disease, presents as complete or partial form. Complete hydatidiform mole (CHM) usually presents with prominent histological criteria, whereas partial hydatidiform mole (PHM) shows a wide spectrum of presentations depending on gestational age. Molecular markers enhance the understanding of the variation and heterogeneous presentation of molar pregnancies, as well as their biological potential and behavior. This retrospective study included 50 CHM and 50 PHM specimens, terminated in first trimester via suction curettage. A second histopathological review of slides stained with hematoxylin and eosin was conducted, as well as a selection of representative tissue slides for p53 immunostaining. This study aimed to determine the precise correlation between specific morphological criteria and the patterns of p53 immun-expression.

Semi-quantitative analysis of samples for both

pathological criteria and p53 immunostaining was performed. p53 positivity was defined as follow: the percentage of positive cells/nuclei: + (10-40%); ++ (40-70%); +++ (>70%); and staining intensity was scored as: 1 – weak, 2 – moderate, and 3 – strong intensity. P53 expression was estimated on at least 200 nuclei of cytotrophoblasts per slide. Significant difference in p53 expression exist between CHM and PHM in staining intensity. CHM shows significant correlation of p53 positivity with hydrops, central cisterns and atypia. In PHM trophoblast pseudoinclusions demonstrate strong significant correlation with p53 positivity. The irregular pseudoinclusions demonstrate lower expression compared with round or oval, being consistent with benign behavior of PHM. Prominent morphological criteria strongly correlate with p53 immunoexpression for both CHM and PHM.

Key words: Hydatidiform mole – p53 expression – Trophoblast – Pseudoinclusions

Corresponding author:

Prof. Dr Melisa Lelić. Univerzitetska 1, Medical Faculty, University of Tuzla, Bosnia.
Phone: +387 35 320 640. E-mail: melisa.lelic@untz.ba

Submitted: February 11, 2026. **Accepted:** March 12, 2026

<https://doi.org/10.52083/OQTE8844>

INTRODUCTION

Gestational trophoblastic disease (GTD) represents a rare spectrum of conditions arising from trophoblastic tissue. Hydatidiform mole (HM) is the most common form of GTD, presenting as either complete (CHM) or partial (PHM) molar pregnancies. Typically, HM is a unique event during a woman's reproductive period, developing as a result of disturbed conception characterized by extreme aneuploidy and an imbalance of maternal and paternal genes. Although uncommon, recurrence of HM suggests a potential genetic predisposition (Altieri et al., 2003; Ngan et al., 2018; Smith, 2003). Despite differences in cytogenetics, pathology, and clinical presentation, the management of CHM and PHM is similar (Soper, 2021).

Prominent histological criteria are sufficient for distinguishing molar pregnancies from non-molar specimens, as well as for differentiating CHM from PHM. Diffuse stromal edema and generalized trophoblast proliferation characterize the majority of complete moles. In contrast, the partial form demonstrates variable, focal edema of the villi, with scalloped edges, trophoblastic inclusions, and pseudoinclusions. Trophoblastic proliferation is less pronounced and more focal compared to complete moles (Ngan et al., 2018). Routine histological examination is fundamental for the diagnosis and differentiation of molar entities. Molar specimens evacuated during early and very early pregnancy often exhibit poorly developed histological features. This is particularly relevant for PHM, leading to potential misdiagnosis and significant intra- and inter-observer variability, with a wide spectrum of presentations depending on gestational age (Seckl et al., 2013). Histological characteristics similar to PHM can also be observed in case of single or combined trisomies (Sebire et al., 2016; Wilson et al., 2016). The well-known aberrant genomic composition of HM is recognized as the foundation for precise diagnosis, supported by several effective and powerful ancillary techniques that enable prognostic stratification of molar gestations (Hui et al., 2017; Buza, 2022).

Immunohistochemistry (IHC) is useful for confirming the diagnosis and predicting the biological potential of molar specimens. Studies have

provided data on molecular markers using the IHC method, enhancing the understanding of the variation and heterogeneous presentation of HM, as well as their biological potential and behavior (Fukunaga, 2002; McConnell et al., 2009; Sebire & Seckl, 2008). p53 is a tumor suppressor gene that plays a critical role in maintaining genomic stability and serves as a marker of proliferative activity. It ensures that cells repair DNA damage before undergoing cell division by inducing cell cycle arrest, thereby allowing time for DNA repair. If the damage is irreparable, p53 can trigger apoptosis to prevent the propagation of defective cells. Due to its central role in cellular integrity, p53 is the most frequently disrupted gene in neoplastic processes (Levine, 2020; Levine & Oren, 2009).

However, the analysis of p53 immunohistochemical staining can be challenging due to varying methodologies, such as differences in cut-off values, staining intensity, and the use of scoring systems like the H-score. These inconsistencies can sometimes make the results less clear and more difficult to interpret.

p53 has consistently been found to exhibit increased expression in CHM compared to PHM. Invasive nature of hydatidiform moles is elucidated with overexpression of p53 in villous cytotrophoblasts and dysregulation of its modulators (Ali et al., 2017; Erol et al., 2016; Bahutair et al., 2024). This study aimed to determine the precise correlation between specific morphological criteria and the patterns of p53 immunoeexpression.

MATERIAL AND METHODS

This retrospective study included 50 CHM specimens and 50 PHM specimens, all of which were obtained during the first trimester via suction curettage. To ensure diagnostic accuracy, a second histopathological review of hematoxylin-and-eosin- (H&E)-stained slides was conducted by a single, experienced pathologist.

The study was approved by the Medical Ethics Committee University Clinical Center Tuzla (Ref. No: 279/15; date: December 23, 2014, and Ref. No 04-912-74/15; date: October, 8,2015). The written consent was provided before inclusion in the study. The study adhered to the principles of the

Declaration of Helsinki, 2013.

Patohistological analysis

Semi-quantitative analysis of samples was performed in order to estimate: hydrops of villi (focal or generalized) trophoblast proliferation (focal or diffuse), trophoblast pseudoinclusions (absent, round, irregular), and nuclear atypia in villous cytotrophoblast (absent, mild, moderate, strong).

Immunostaining

Following semiquantitative analysis, representative tissue blocks/slides were selected for p53 immunostaining. The immunohistochemistry staining procedure was performed on formalin-fixed, paraffin-embedded tissue samples cut at 4µm, using monoclonal mouse antihuman antibody (DAKO, monoclonal mouse antihuman p53 protein, Clone DO-7) with a 1:400 dilution. Prior to staining, 1mM citric buffer (pH 8.0 at 100°C, 10-minute duration) was used for antigen retrieval. The Immunostaining Center, Shandon Sequenza, was used for all incubation stages. After 30 minutes of incubation with the primary antibody, samples were treated with the secondary antibody (biotin, streptavidin, and peroxidases). The sections were counterstained with Mayer's hematoxylin, and Canada balsam was used for mounting the slides. Breast cancer tissue was applied to every slide, which were treated with the same procedure that served as external positive control. A Nikon ECLIPSE E400 microscope, with magnifications of 20x and 40x, was used for the analysis of p53 expression.

p53 positivity was defined as the presence of brown color immunoexpression of the villous cytotrophoblasts nuclei, and described as negative with less than 10% positive nuclei. Semi-quantitative analysis was used in order to estimate the percentage of positive cells/nuclei: + (10-40%); ++

(40-70%); +++ (>70%), and staining intensity was scored as follows: 1 – weak, 2 – moderate, and 3 – strong intensity. p53 expression was estimated on at least 200 nuclei of cytotrophoblasts per slide.

Statistical analysis

One-factor multivariate analysis of variance (MANOVA) was used for statistical analysis and performed using the IBM SPSS software version 25. P values ≤ 0.05 were considered statistically significant.

RESULTS

The results of the semi-quantitative analysis of morphological criteria for both CHM and PHM are summarized in Table 1. Mean gestational age was estimated at 8 and 9,2 gestational weeks for CHM and PHM, respectively.

The reaction of IHH staining on the p53 protein was analyzed at the nuclear level of the villous cytotrophoblasts. The reaction appeared as varying shades of brownish color, ranging from ochre to dark brown. Although cytoplasmic reaction in the form of yellow staining was observed in most samples, it was not analyzed. In addition to the reaction at the cytotrophoblast level, a similar reaction in terms of shade was observed in the nuclei of extravillous trophoblast (internal positive control). The most common staining pattern was moderate nuclear staining (39% of all samples). The staining results for CHM and PHM are presented in Figs. 1 and 2.

Out of the total number, there were 94% positive complete and 66% positive partial molar specimen (Chi: 12,25, p<0,0005). The results of distribution of p53 expression in CHM and PHM (Table 2 and Table 3.) reveals insignificant differences in percentage of positive cells (Chi: 0.057, p>0,05), as it is recorded in staining intensity (chi:8,44; p<0,01).

Table 1. Morphological criteria in CHM and PHM

	H		TP		TPI		TA				
	F**/**	D	F	D	A	R	I	A	W	M	S
CHM (%)	6	94	2	98	74	2	24	6	28	36	30
PHM (%)	62/33*	5	100	-	42	10	48	82	16	2	0

Abbreviations: H - hydrops; TP - trophoblast proliferation; TPI - trophoblast pseudoinclusions; TA - trophoblast atypia; focal* - F* - focal hydrops with central cisterns; F ** - focal hydrops without central cisterns; F - focal; D - diffuse; A - absent; R - round; I - irregular; W - weak; M - moderate; S - strong.



Fig. 1.- p53 expression in CHM (>70%). Magnification: x40.

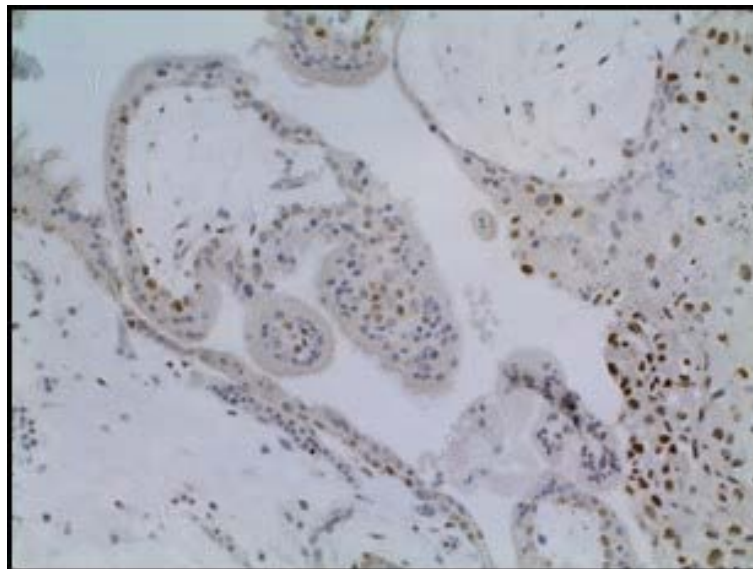


Fig. 2.- p53 expression in PHM. Magnification: x20.

Correlation of each diagnostic criteria on p53 percentage positive cells and expression intensity are presented in Table 4 to Table 8. Correlation of single diagnostic criteria and percentage of p53 positive cells in CHM. In complete moles, significant correlation of percentage of positive cells demonstrated hydrops with central cisterns (positive correlation, $p=0.028$) and atypia (negative correlation, $p=0.012$) (Table 4). In partial moles, trophoblast pseudoinclusions demonstrates strong significant positive correlation with percentage of positive cells ($p=0.003$) (Table 5).

In complete moles, significant correlation of p53 staining intensity demonstrated hydrops with central cisterns (positive correlation, $p=0.042$)

and atypia (negative correlation, $p=0.010$) (Table 6). In partial moles, trophoblast pseudoinclusions demonstrates strong significant positive correlation with p53 staining intensity ($p=0.037$) (Table 7). In partial moles, significant differences in p53 staining pattern are observed between round and irregular pseudoinclusions: irregular ones demonstrate lower p53 expression (Table 8).

DISCUSSION

Molar pregnancies develop as a result of an extreme genetic composition, which can lead to several clinical complications, such as persistence of trophoblast and progression to gestational trophoblast neoplasia. Poorly developed mor-

Table 2. Distribution of p53 positivity in CHM and PHM

% of positive ctb nuclei	CHM (n)	PHM (n)	Sig.
10-40%	36	26	p>0,05
40-70%	8	5	
>70%	3	2	
Total	47	33	

Abbreviations: ctb - cytotrophoblast

Table 3. Distribution of p53 intensity of expression in analyzed specimen

Staining intensity	CHM (n)	PHM (n)
Mild	14	14
Moderate	20	19
Intense	13	0
Total	47	33

Table 4. Correlation of single diagnostic criteria and percentage of p53 positive cells in CHM

Variables	%PC	HCC	TP	PI	AT
%PC	1.000	0.271*	.	0.069	-0.319*
HCC	0.271*	1.000	.	0.247*	-0.226
TP	.	.	1.000	.	.
PI	0.069	0.247*	.	1.000	-0.028

Abbreviations: %PS - percentage of positive cells; HCC - hydrops with central cisterns; TP - trophoblast proliferation; PI - pseudo-inclusions; AT - atypia; Values are Pearson correlation coefficients; * - statistical significance (p<0.05).

Table 5. Correlation of individual diagnostic criteria and p53 positive cells in PHM

Variables	%PC	HCC	TP	PI	AT
%PS	1.000	0.087	0.049	0.383**	-0.031
HCC	0.087	1.000	-0.036	0.148	-0.028
TP	0.049	-0.036	1.000	0.084	0.302*
PI	0.383**	0.148	0.084	1.000	0.221
AT	-0.031	-0.028	0.302*	0.221	1.000

Abbreviations: %PS - percentage of positive cells; HCC - hydrops with central cisterns; TP - trophoblast proliferation; PI - pseudo-inclusions; AT - atypia; Values are Pearson correlation coefficients; * - statistical significance (p<0.05); ** - statistical significance (p<0.01).

Table 6. Correlation of single diagnostic criteria and p53 staining intensity in CHM

Variables	IE	HCC	TP	PI	AT
IE	1.000	0.250*	-	-0.027	-0.332*
HCC	0.250*	1.000	-	0.237	-0.222
TP	-	-	1.000	-	-
PI	-0.027	0.237*	-	1.000	-0.020
AT	-0.332*	-0.222	-	-0.020	1.000

Abbreviations: IE - intensity of expression; HCC - hydrops with central cisterns; TP - trophoblast proliferation; PI - pseudo-inclusions; AT - atypia; Values are Pearson correlation coefficients; * - statistical significance (p<0.05)

Table 7. Correlation of single diagnostic criteria and p53 staining intensity in PHM

Variables	IE	HCC	TP	PI	AT
IE	1.000	0.056	0.141	0.255*	0.008
HCC	0.056	1.000	-0.036	0.148	-0.028
TP	0.141	-0.036	1.000	0.084	0.302*
PI	0.255*	0.148	0.084	1.000	0.221
AT	0.008	-0.028	0.302*	0.221	1.000

Abbreviations: IE - intensity of expression; HCC - hydrops with central cisterns; TP - trophoblast proliferation; PI - pseudoinclusions; AT - atypia; Values are Pearson correlation coefficients; * - statistical significance ($p < 0.05$)

phological criteria underlie misdiagnosis or, in case of partial mole, more often, overdiagnosis of molar pregnancies (Buza and Hui, 2013; Nagy et al., 2024). The molecular ground of molar pregnancies exposes a wide and complex genetic and epigenetic interaction, resulting from a spectrum of expression patterns of several genes and their products that influence final diagnosis, as well as understanding the disease progression and clinical outcome (Fisher and Maher, 2021; Xing et al., 2022; Bahutair et al., 2024).

This study was performed in order to identify the relationship of diagnostic criteria and p53 staining pattern. Our findings disclose that the leading criteria are sufficient for the diagnosis and distinction of both complete and partial molar specimen in the first trimester, even with CHM samples evacuated in average one week earlier than partial ones. Immunostaining results for p53 revealed significant differences between CHM and PHM. Differences in correlation of single diagnostic criteria were observed as well. We found that, in complete moles, p53 expression strongly positively correlates with hydrops with central cisterns. Furthermore, negative correlation is observed with nuclear atypia of proliferated trophoblast for both criteria. In partial moles, only trophoblast pseudoinclusions significantly correlates with p53 immunoeexpression. The irregular form of pseudoinclusions disclose lower p53 expression compared with the round/regular ones.

Analyzing morphological criteria to distinguish PHM from nonmolar trisomic gestation, Wilson et al. (2016) found that the presence of two of the following three criteria (cisterns, multifocal trophoblastic proliferation, and large trophoblastic inclusions) lead to an accurate diagnosis of PHM in 93% of cases. Irregular trophoblastic pseudoinclusions seen in PHM are presentation of villi with irregular, fjord-like indentations of proliferating trophoblast into stroma, most likely due to slower rate of change from normal to hydatidiform placental morphology (Joyce et al., 2022).

Similar to our results, immunoexpression of p53 is detected in both molar forms, and studies disclosed significant higher p53 expression in CHM compared to PHM, suggesting its potential usefulness in distinguishing CHM from PHM (Chen et al., 2011; Kheradmand et al., 2017; Misraoui et al., 2019), and rare opposite results are reported (Khooei et al., 2019).

The majority of complete moles arise from total androgenetic conception with lack of maternal genes. One of the observations in this study renders a broad spectrum of immunostaining results, from p53 negative to strongly positive CMH samples, with more than 70% of intensively stained cytrotrophoblast nuclei, leading to the conclusion that moles' complex genetic composition may underlie complete molar specimen. In our previous study, with p57 expression we confirmed the diag-

Table 8. Correlation of trophoblast pseudoinclusions and p53 expression

	MD	SE	p	95% CI - LB	95% CI - UP
Absent vs. Present Round	0.67	0.298	0.071	-0.04	1.38
Absent vs. Present Irregular	-0.19	0.147	0.388	-0.55	0.16
Present Round vs. Present Irregular	-0.86	0.306	0.017*	-1.59	-0.13

Abbreviations: PI - pseudoinclusions; MD - mean difference; SE - standard error; 95% CI - confidence interval; LB - lower bound; UP - upper bound; * - statistically significant ($p < 0.05$)

nosis of CHM for all satisfactory immunostaining result (Lelić et al., 2017). Wide spectrum of p53 immunoexpression is described in previous studies, from overexpression of wild type to non-immunoreactive p53 in nonsense mutations, leading to confounding results in prognostic significance of p53 results (Lax et al., 2000). Therefore, observed staining intensity in CHM is more likely to be due with the significant p53 disturbance.

In correlation with nuclear atypia studies revealed that mutant p53 shows strong positive correlation with nuclear grade of atypic cells (Tang et al., 2021).

Observed negative correlation of p53 expression with nuclear atypia and trophoblast proliferation leads to the conclusion that despite significant genetic disturbance, trophoblast in moles still have well-defined limitation of their invasive growth.

Wild-type p53 protein can repair damaged cells and maintain the stability of genomes, but its half-life is short, its content in cells is low, and it is not generally expressed, while mutant p53 protein loses the ability to repair cells and promotes the development of tumors. p53 mutations found to be involved in progression of numerous proliferative tumours/conditions. Weak positive staining contributes to the p53 wild type, while forming of nontruncated protein may result with the complete lack of staining (Li et al., 2023; Yemelyanova et al., 2011).

Trophoblast pseudoinclusions were recognized as a significant feature of partial moles (Buza and Hui, 2013). However, there are no data considering the significance of their presentation either round or irregular, and our results actualize the significance in p53 immunexpression.

It has been reported that p53 gene mutation is rare in complete hydatidiform mole and trophoblastic tumors (Halperin et al., 2000; Chen et al., 1994). Cheung et al. reported a positive correlation between p53 and Ki-67 proliferation index in trophoblastic tissues of hydatidiform moles (Cheung et al., 1994). Hence, p53 overexpression may be a reflection of the higher proliferation capacity of the trophoblastic cells in molar tissues. A possible role of expression of the p53 protein in proliferative trophoblastic tissues is an attempt

to modulate the excessive proliferative activity in trophoblastic cells (Li et al., 2002). On the other hand, Halperin et al. evaluated the expression of the p53 and apoptosis in GTD and normal placenta and showed that the percentage of apoptotic cells demonstrated a significant increase in HMs compared with normal placenta and also significant overexpression of p53 in HMs compared with normal placenta, they concluded that p53 overexpression in hydatidiform moles could be the result of upregulation of apoptosis (Halperin et al., 2000). Study limitations: unicentric study, small sample size, and incomplete clinical data. Further research would be desirable to monitor complications of molar pregnancy.

CONCLUSION

The p53 immunostaining pattern in molar specimens is a reliable method for distinguishing between CHM and PHM. The leading diagnostic criteria for both CHM and PHM show a strong, statistically significant correlation with p53 staining intensity and the percentage of positive cells.

REFERENCES

- ALI SM, AHMEDI NY, SHALAL TM, ABDULHAMEED TT (2017) Immunoexpression of P53 protein in trophoblastic diseases. *Zanco J Med Sci*, 21: 157863.
- ALTIERI A, FRANCESCHI S, FERLAY J, SMITH J, LA VECCHIA C (2003) Epidemiology and aetiology of gestational trophoblastic diseases. *Lancet Oncology*, 4: 670-678.
- BAHUTAIR SNM, DUBE R, KURUBA MGB, SALAMA RAA, PATNI MAMF, KAR SS, KAR R (2024) Molecular basis of hydatidiform moles—a systematic review. *Int J Mol Sci*, 25(16): 8739.
- BUZA N (2022) Gestational trophoblastic disease: contemporary diagnostic approach. *Surg Pathol Clin*, 15: 197-218.
- BUZA N, HUI P (2013) Partial hydatidiform mole: histologic parameters in correlation with DNA genotyping. *Int J Gynecol Pathol*, 32: 307-315.
- CHEN CA, CHEN YH, CHEN TM, KO TM, WU CC, LEE CN, HSIEH CY (1994) Infrequent mutation in tumor suppressor gene p53 in gestational trophoblastic neoplasia. *Carcinogenesis*, 15: 2221-2223.
- CHEN YX, SHEN DH, YI-QUN GU, ZHONG PP, XIE JL, SONG QJ, ZHANG YL, WEN J (2011) Immunohistochemistry of p57 and p53 protein in differential diagnosis of hydropic abortion, partial and complete hydatidiform mole. *Chin J Pathol*, 40: 694-697.
- CHEUNG ANY, SRIVASTAVA G, CHUNG LP, NGAN HYS, MAN TK, LIU YT, CHEN WZ, COLLINS RJ, WONG LC, MA HK (1994) Expression of the p53 gene in trophoblastic cells in hydatidiform moles and normal human placentas. *J Reprod Med*, 39: 223-227.
- EROL O, SÜREN D, TUTUŞ B, TOPTAŞ T, GÖKAY AA, DERBENT AU, ÖZEL MK, SEZER C (2016) Immunohistochemical analysis of E-cadherin, p53 and inhibin- α expression in hydatidiform mole and hydropic abortion. *Pathol Oncol Res*, 22(3): 515-521.
- FISHER RA, MAHER GJ (2021) Genetics of gestational trophoblastic disease.

Best Pract Res Clin Obstet Gynaecol, 74: 29-41.

FUKUNAGA M (2002) Immunohistochemical characterization of p57KIP2 expression in early hydatidiform moles. *Human Pathol*, 33: 1188-1192.

HALPERIN R, PELLER S, SANDBANK J, BUKOVSKY I, SCHNEIDER D (2000) Expression of the p53 gene and apoptosis in gestational trophoblastic disease. *Placenta*, 21: 58-62.

HUI P, BUZA N, MURPHY KM, RONNETT BM (2017) Hydatidiform moles: genetic basis and precision diagnosis. *Annu Rev Pathol*, 12: 449-485.

Joyce CM, Fitzgerald B, McCarthy TV, Coulter J, O'Donoghue K (2022) Advances in the diagnosis and early management of gestational trophoblastic disease. *BMJ Medicine*, 1: e000321.

KHERADMAND P, GOUDARZI M, TAVAKOLI M (2017) Analysis of p53 expression in partial hydatidiform mole and hydropic abortion. *Front Biol*, 12: 357-360.

KHOOEI A, PASDAR FA, FAZEL A, MAHMOUDI M, NIKRAVESH MR, SHAHBAZIAN SD (2019) P53 expression in various types of hydropic placentas (through ploidy analysis as a complementary tool in diagnosis of samples). *Caspian J Int Med*, 10: 205-210.

LAX SF, KENDALL B, TASHIRO H, SLEBOS RJC, ELLENSON LH (2000) The frequency of p53, K-ras mutations, and microsatellite instability differs in uterine endometrioid and serous carcinoma: Evidence of distinct molecular genetic pathways. *Cancer*, 88: 814-824.

LELIC M, FATUSIC Z, ILJAZOVIC E, RAMIC S, MARKOVIC S, ALICELEBIC S (2017) Challenges in the routine praxis diagnosis of hydatidiform mole: a tertiary health center experience. *Med Arch (Sarajevo, Bosnia and Herzegovina)*, 71: 256-260.

LEVINE AJ (2020) P53: 800 million years of evolution and 40 years of discovery. *Nature Rev Cancer*, 20: 471-480.

LEVINE AJ, OREN M (2009) The first 30 years of p53: growing ever more complex. *Nature Rev Cancer*, 9: 749-758.

LI HW, TSAO SW, CHEUNG ANY (2002) Current understandings of the molecular genetics of gestational trophoblastic diseases. *Placenta*, 23: 20-31.

LI X, LUO D, ZHANG L, LI Q, FAN J, ZHANG J, HUANG B, YANG M, NIE X, CHANG X, PAN H (2023) Accurate interpretation of p53 immunohistochemical patterns is a surrogate biomarker for TP53 alterations in large B-cell lymphoma. *BMC Cancer*, 23(1): 1008.

MCCONNELL TG, MURPHY KM, HAFEZ M, VANG R, RONNETT BM (2009) Diagnosis and subclassification of hydatidiform moles using p57 immunohistochemistry and molecular genotyping: validation and prospective analysis in routine and consultation practice settings with development of an algorithmic approach. *Am J Surg Pathol*, 33: 805-817.

MISSAOUI N, LANDOLSI H, MESTIRI S, ESSAKLY A, ABDESSAYED N, HMISSA S, MOKNI M, YACOUBI MT (2019) Immunohistochemical analysis of c-erbB-2, Bcl-2, p53, p21WAF1/Cip1, p63 and Ki-67 expression in hydatidiform moles. *Pathology - Research and Practice*, 215: 446-452.

NAGY A, NIU N, SUN T, BUZA N, HUI P (2024) Diandric triploid partial mole versus digynic nonmolar triploidy: is morphological assessment sufficient for the diagnostic distinction? *Histopathology*, 85(6): 879-888.

NGAN HYS, SECKL MJ, BERKOWITZ RS, XIANG Y, GOLFIER F, SEKHARAN PK, LURAIN JR, MASSUGER L (2018) Update on the diagnosis and management of gestational trophoblastic disease. *Int J Gynecol Obstet*, 143 Suppl 2: 79-85.

SEBIRE NJ, SECKL MJ (2008) Gestational trophoblastic disease: current management of hydatidiform mole. *BMJ (Clinical Research)*, 337: 453-458.

SEBIRE NJ, MAY PC, KAUR B, SECKL MJ, FISHER RA (2016) Abnormal villous morphology mimicking a hydatidiform mole associated with paternal trisomy of chromosomes 3,7,8 and unipaternal disomy of chromosome 11. *Diagnostic Pathol*, 11: 1-8.

SECKL MJ, SEBIRE NJ, FISHER RA, GOLFIER F, MASSUGER L, SESSA C (2013) Gestational trophoblastic disease: ESMO clinical practice guidelines for diagnosis, treatment and follow-up. *Ann Oncol*, 24: vi39-vi50.

SMITH HO (2003) Gestational trophoblastic disease epidemiology and trends.

Clin Obstet Gynecol, 46: 541-556.

SOPER JT (2021) Gestational trophoblastic disease: current evaluation and management. *Obstet Gynecol*, 137: 355-370.

TANG M, LIU PJ, YUE B, YANG XT, CHEN GY (2021) The correlation between mutant P53 protein expression and cell atypia in early differentiated gastric adenocarcinoma. *Cancer Manag Res*, 13: 4129-4134.

WILSON Y, BHARAT C, CROOK ML, KEE AR, PEVERALL J, RUBA S, STEWART CJR (2016) Histological comparison of partial hydatidiform mole and trisomy gestation specimens. *Pathology*, 48(6): 550-554.

XING D, MILLER K, BEIERL K, RONNETT BM (2022) Loss of p57 Expression in conceptions other than complete hydatidiform mole: a case series with emphasis on the etiology, genetics, and clinical significance. *Am J Surg Pathol*, 46: 18-32.

YEMELYANOVA A, VANG R, KSHIRSAGAR M, LU D, MARKS MA, SHIH IM, KURMAN RJ (2011) Immunohistochemical staining patterns of p53 can serve as a surrogate marker for TP53 mutations in ovarian carcinoma: an immunohistochemical and nucleotide sequencing analysis. *Mod Pathol*, 24: 1248-1253.

Variations of the anterior belly of the digastric muscle: a cadaveric and meta-analysis study

Marcelo Prado¹, José Neto¹, Carolina Basto¹, Iapunira Aragão², Felipe Aragão³, Francisco Reis⁴, José Aragão⁵

¹Department of Medicine, Federal University of Sergipe (UFS), Aracaju, SE, Brazil

²Municipal Hospital Munir Rafful (MHMR), Volta Redonda, Rio de Janeiro, Brazil

³Heart Institute of the Hospital das Clínicas, Faculty of Medicine, University of São Paulo (INCOR), São Paulo, SP, Brazil

⁴Medical School of Tiradentes University (UNIT), Aracaju, SE, Brazil

⁵Clinical Anatomy, Department of Morphology, Federal University of Sergipe (UFS)

SUMMARY

Variations of the anterior belly of the digastric muscle are frequently reported in adult populations; however, the developmental timing of their appearance remains insufficiently understood. This study aimed to describe the morphology and prevalence of anterior digastric belly variations and to contextualize these findings through a meta-analysis of published anatomical studies. Twenty-six formalin-fixed human fetuses (13 male, 13 female) were dissected and analyzed morphologically. Variations were classified according to De-Ary-Pires, Ary-Pires and Pires-Neto. A systematic review and meta-analysis of observational studies reporting the prevalence of anterior belly variations was conducted following PRISMA guidelines. The mean gestational age was 29.4 ± 3.58 weeks. Variations were observed in six fetuses (23.1%), all classified as type II, with no association with sex or gestational age. The meta-analysis of 16 studies ($n = 787$) yielded a pooled prevalence of 25.1% (95% CI: 15.5–35.9;

$I^2 = 90.6\%$), with variation across geographical regions and sexes. Variations of the anterior belly of the digastric muscle are established during fetal development and occur at frequencies comparable to those reported in postnatal populations. These findings support a developmental origin for this anatomical variability and provide a morphological framework for future embryological and anatomical investigations of the suprahyoid region.

Key words: Anatomic variation – Fetal development – Meta-analysis – Neck muscles – Prevalence

INTRODUCTION

The digastric muscle is a suprahyoid muscle characterized by two muscular bellies, anterior and posterior, connected by an intermediate tendon. The posterior belly originates from the mastoid notch of the temporal bone and runs anteroinferiorly, whereas the anterior belly arises

Corresponding author:

Marcelo Lucas de Lima Prado. Federal University of Sergipe (UFS), Aracaju, SE, Brazil. Avenida Marechal Rondon, S/N, Rosa Elze, São Cristóvão – SE, Brazil. Phone: +55 75 981489152. E-mail: marcelolucas953@gmail.com

Submitted: December 26, 2025. **Accepted:** March 15, 2026

<https://doi.org/10.52083/OWLI7144>

from the digastric fossa of the mandible, near the symphysis, and extends posteroinferiorly. The intermediate tendon passes through the stylohyoid muscle and attaches to the body and greater horn of the hyoid bone via a fibrous loop (Standring, 2008). This anatomical configuration contributes to several functions, including mandibular depression, elevation of the hyoid bone, and stabilization of the larynx during swallowing and speech (Kim and Loukas, 2019).

Several anatomical studies have reported the presence of accessory bellies of the digastric muscle, consisting of additional muscular bundles that may follow ipsilateral, contralateral, or even midline-crossing trajectories (Mangalagiri et al., 2009). De-Ary-Pires et al. (2003) proposed a classification system comprising five types, ranging from a single belly (type I) to multiple accessory bellies or the presence of an independent mentohyoid muscle (type V). Singular cases include trapezoid-shaped accessory bellies connecting both sides or multiple heads with atypical insertions (Aragão et al., 2022).

Although variations of the anterior belly of the digastric muscle generally have no direct pathological significance, they represent a source of anatomical diversity that may complicate anatomical interpretation, particularly in imaging-based or surgical contexts when unrecognized (Kim and Loukas, 2019). Most available evidence describing these variations is anatomical in nature, and their developmental origin remains incompletely understood (Gross et al., 2023). Therefore, the study of the digastric muscle and its variations, especially of the anterior belly, is essential not only to expand classical anatomical knowledge but also to improve clinical and surgical practice through more accurate interpretation of imaging and safer approaches to the cervical region.

Despite extensive documentation of anterior digastric belly variations in adults, limited data exist regarding the timing of their emergence during human development. Whether these variants represent congenital anatomical patterns established during early myogenesis or postnatal modifications remains unclear. Examination of fetal specimens offers a unique opportunity to clarify this issue by directly assessing the presence and

morphology of these variants during gestation.

Accordingly, the present study combines a fetal anatomical investigation with a meta-analysis of published prevalence data in order to test the hypothesis that variations of the anterior belly of the digastric muscle are established early in development and persist throughout life.

MATERIAL AND METHODS

Anatomical study

The study included 26 human fetuses (13 male and 13 female) fixed in formalin, without macroscopic deformities, belonging to the Human Anatomy Laboratory of the Federal University of Sergipe (Brazil). All specimens were obtained in accordance with Brazilian Law No. 8.501/1992, which regulates the use of unclaimed cadavers for teaching and research purposes. The authors hereby confirm that every effort was made to comply with all local and international ethical guidelines and laws concerning the use of human cadaveric donors in anatomical research. Gestational age (GA) was estimated using the equation $GA = 8.2982 + (0.38764 \times F)$, where F represents the heel-to-great-toe length (Goldstein, Reece and Hobbins, 1988). Measurements were performed with a digital caliper accurate to 0.01 mm.

Morphological and morphometric analysis

The components of the digastric muscle were analyzed through careful dissection under natural light. Measurements were taken using a 0.01 mm precision digital caliper. The morphology of the anterior belly was classified according to De-Ary-Pires, Ary-Pires and Pires-Neto (2003), as follows:

Type I: Single belly originating from the inferior border of the mandible near the symphysis.

Type II: Two bellies, with additional bundles connected to the mandible or mylohyoid muscle, either ipsilaterally or contralaterally.

Type III: Three bellies, with additional bundles connected to the mandible or mylohyoid muscle, either ipsilaterally or contralaterally.

Type IV: Four bellies, with additional bundles

connected to the mandible or mylohyoid muscle, either ipsilaterally or contralaterally.

Type V: Often described as an independent muscle, a rare variation known as the mentohyoid (Macalister's) muscle.

The length of the anterior belly was measured from its insertion on the mandible (anterior point) to its connection with the intermediate tendon on the hyoid bone (posterior point). The length of the posterior belly was measured from its insertion on the temporal bone (posterior point) to its connection with the intermediate tendon (anterior point). The width of these bellies was measured at their respective points according to the mentioned insertion.

Statistical analysis

Data normality was assessed using the Shapiro-Wilk test to determine the use of parametric or non-parametric tests (Royston, 1992). Associations between quantitative variables were analyzed using Pearson's correlation for normally distributed data and Spearman's correlation for non-normal data, with correlation strength classified as weak (0–0.4), moderate (0.4–0.7), or strong (0.7–1).

Comparisons between sides were performed using a paired t-test for normal data or the Wilcoxon test for non-normal data (Rosner, Glynn and Lee, 2006). Comparisons between sexes used an independent-sample t-test when normality was met or the Mann-Whitney test otherwise. Statistical analyses were performed using JAMOVI 2.6.26, adopting a significance level of 5% ($p < 0.05$).

Meta-analysis

Registration and Guidelines

The present study followed the Preferred Reporting Items for Systematic Reviews and Meta-Analyses (PRISMA) guidelines (Moher et al., 2009). The review protocol was registered in the International Prospective Register of Systematic Reviews (PROSPERO) under the code CRD420251151451.

Search Strategy

Systematic search was conducted in PubMed,

Scopus, and Web of Science databases in order to identify studies reporting variations of the anterior belly of the digastric muscle. The following search strategy was applied:

("Digastric Muscle" OR "anterior belly of digastric" OR "anterior digastric" OR "anterior belly" OR "digastricus anterior") AND ("anatomic variation" OR "anatomical variation" OR "muscle variation" OR "morphological variation" OR "variant" OR "accessory muscle" OR "duplicated muscle" OR "muscle anomaly" OR "asymmetry").

Eligibility Criteria

Inclusion criteria comprised observational studies with primary human data that investigated the anterior belly of the digastric muscle and reported quantitative data on the prevalence or frequency of variations. Exclusion criteria included animal studies, computational simulations, review articles, and primary studies lacking sufficient quantitative data.

Data Extraction

Records retrieved from databases were imported into Zotero software for organization and screening. Two authors independently performed data extraction, removing duplicates and assessing eligibility based on titles and abstracts. The following information was collected: first author's name, year of publication, sample size, sex distribution, age, geographic origin, and prevalence of variations.

Meta-analytical procedures

Effect sizes were calculated for prevalence estimates. Confidence intervals (95% CI) were computed using the Freeman-Tukey double arcsine transformation. Cochran's Q test and the I^2 statistic were used to assess heterogeneity; values of $p < 0.05$ and $I^2 > 25\%$ were considered indicative of significant heterogeneity. All statistical analyses were performed using OpenMeta[Analyst] software.

RESULTS

Anatomical study

The mean gestational age of the fetuses was

29.4 (± 3.58) weeks. Among the 26 dissected specimens, six fetuses (three male and three female) exhibited variations in the anterior belly of the digastric muscle. All accessory bellies were classified as type II, with one bilateral and five unilateral occurrences (Fig. 1). Morphometric data of the accessory bellies are presented in Table 1.

No association was found between gestational age, sex, or morphometric parameters of the accessory bellies.

Study identification

A total of 441 records were retrieved from the three databases. After the removal of 202 duplicates, the remaining records were screened by title and abstract to determine relevance. Thirty-one studies were selected for full-text assessment, of which 16 met the inclusion criteria and were included in the present review (Fig. 2).

Characteristics of the included studies

The review comprised 787 individuals, with 14 cadaveric dissection studies and two imaging-based studies. Of these, five were conducted in Brazil, four in Turkey, three in the United States, one in Kenya, one in Taiwan, one in Thailand, one in China, and one in India (Table 2).

Prevalence of variation in the anterior belly of the digastric muscle

The variations in the anterior belly of the digastric muscle, across the sample of studies, presented an overall prevalence of 25.1% (95% CI:

15.5 – 35.9; $I^2 = 90.6\%$; $p < 0.001$; Fig. 3). In subgroup analysis by geographical regions, Turkey showed a prevalence of 22.9% (95% CI: 1.4 – 57.3; $I^2 = 96.56\%$; $p < 0.001$; Fig. 4A), followed by Brazil with 25.2% (95% CI: 13 – 39.4; $I^2 =$

77.14%; $p < 0.001$; Fig. 4B) and the United States with 16.9% (95% CI: 1.6 – 41.7; $I^2 = 89.33\%$; $p < 0.001$; Fig. 4C).

The analysis of laterality among the digastric muscles of the sample revealed that the right side presented 6.8% (95% CI: 3.4 – 11.2; $I^2 = 70.51\%$; $p < 0.001$; Fig. 5A) of variations, while the left side presented 8.6% (95% CI: 4.1 – 14.5; $I^2 = 80.7\%$; $p < 0.001$; Fig. 5B).

For sex subgroups, variations were present in 26% (95% CI: 13.1 – 41.3; $I^2 = 79.93\%$; $p < 0.001$; Fig. 6A) of the male sample and 15.4% (95% CI: 5.4 – 27.9; $I^2 = 36.13\%$; $p = 0.201$; Fig. 6B) of the female sample.

DISCUSSION

This study aimed to investigate the characteristics of variations in the anterior belly of the digastric muscle by integrating two distinct investigative approaches: ontogenetic validation in a fetal sample and a global quantitative synthesis through meta-analysis. The relevance of this dual approach lies in its ability not only to quantify the prevalence of these variations across different populations, but also to anchor their origin in early embryonic developmental events. The results revealed the following findings regarding the digastric muscle: (1) no relationship was

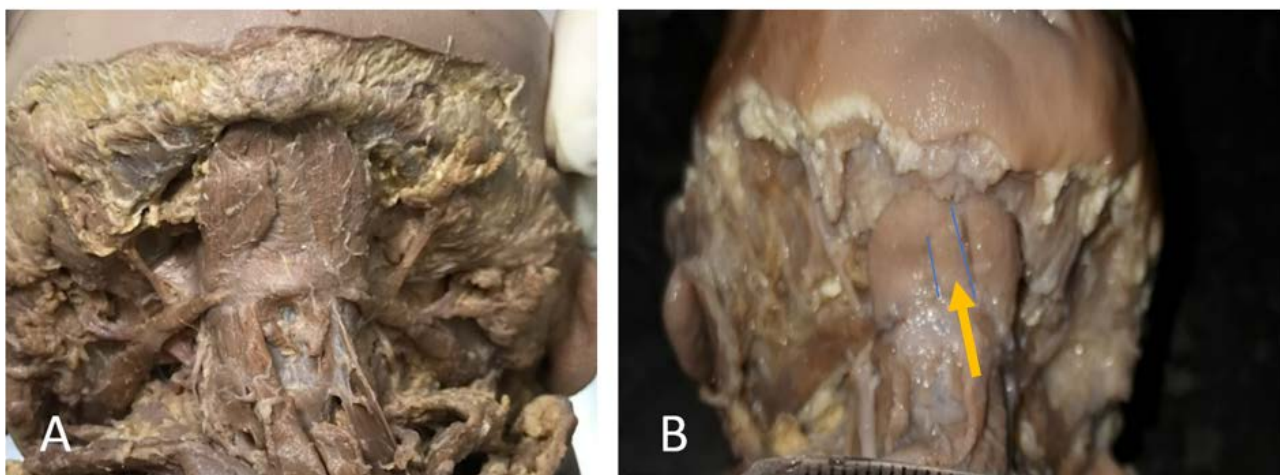


Fig. 1.- Classification of the anterior belly of the digastric muscle in human fetuses. A) Type I anterior bellies. B) Type II right anterior belly; Yellow arrow indicating the accessory belly.

Table 1. Morphological characteristics

	Gestacional Age (weeks)	RAAB (mm)	LAAB (mm)	AT RAAB (mm)	MT RAAB (mm)	PT RAAB (mm)	AT LAAB (mm)	MT LAAB (mm)	PT LAAB (mm)
N	6	4	3	4	4	4	3	3	3
Mean	29.1	12.8	16.3	2.13	2.59	2.95	1.33	1.92	2.54
Median	28.8	13.0	17.0	2.50	2.53	2.71	1.12	1.86	2.56
Standard Deviation	2.83	3.64	1.38	0.977	0.991	1.31	0.703	0.393	0.226
Minimum	25.9	8.22	14.7	0.680	1.44	1.74	0.750	1.56	2.30
Maximum	33.9	17.0	17.1	2.83	3.86	4.62	2.11	2.34	2.75
Shapiro-Wilk W test	0.942	0.988	0.790	0.781	0.951	0.930	0.935	0.983	0.992
Shapiro-Wilk P-value	0.676	0.947	0.090	0.072	0.721	0.594	0.508	0.747	0.829
25th percentile	27.3	11.3	15.8	2.00	2.23	2.00	0.935	1.71	2.43
50th percentile	28.8	13.0	17.0	2.50	2.53	2.71	1.12	1.86	2.56
75th percentile	30.1	14.5	17.1	2.62	2.88	3.66	1.61	2.10	2.66

RAAB – Right accessory anterior belly; LAAB – Left accessory anterior belly; AT RAAB- Anterior third of Right accessory anterior belly; MT RAAB- Middle third of Right accessory anterior belly; PT RAAB- Posterior third of Right accessory anterior belly; AT LAAB- Anterior third of Left accessory anterior belly; MT LAAB- Middle third of Left accessory anterior belly; PT LAAB- Posterior third of Left accessory anterior belly.

found between fetal age or sex and the characteristics of the accessory anterior belly; (2) the overall prevalence was 25.1% (95% CI: 15.5–35.9); (3) prevalence varied among different geographic subgroups; and (4) a higher occurrence was observed on the left side and in the male population. In the present study, conducted with human fetuses of mean gestational age 29.4 (3.58) weeks, most specimens presented a type I morphology of the anterior belly, while six fetuses exhibited a type II accessory belly, with similar mean lengths to the main bellies but smaller mean widths (Prado et al., 2025). This morphometric pattern is consistent with findings in adult populations describing accessory bellies as thinner bundles than the main belly. The smaller width of the accessory belly suggests that it does not represent a complete duplication of the main belly, but rather a secondary or partial muscular condensation (Gross et al., 2023). De-Ary-Pires et al. (2003) reported a similar mean length between type I and type II anterior bellies in both sexes, but smaller mean widths for type II in males.

In the present fetal sample, no relationship was found between gestational age or sex and the occurrence of variations, but age was shown to influence the morphometry of the main bellies.

The anterior and posterior bellies of the digastric muscle derive embryologically from the first and second pharyngeal arches, respectively (Kim and Loukas, 2019; Tranchito and Bordoni, 2025). Consequently, variations in this muscle arise from the complex development of these arches, and since other muscles originate from the same embryonic structures, their anomalies are often found together (Sargon and Çelik, 1994).

The identification of anterior belly variations in fetuses demonstrates that these anatomical patterns arise during early stages of muscle differentiation, rather than representing postnatal adaptations. The consistent presence of type II configurations before the third trimester suggests that such variations are the result of deterministic embryological processes involving the first pharyngeal arch. From an anatomical perspective, recognizing that these variants are congenital and stable contributes to a more accurate understanding of normal muscular diversity in the suprahyoid region. This knowledge may indirectly support anatomical interpretation in clinical settings; however, the present findings should primarily be interpreted within the context of developmental and descriptive anatomy.

In the literature, several reports describe varia-

Table 2. Characteristics of the included studies

Study (Year)	Country	Study Design	Sample Size (n)	Population	Age Range (Years)	Sex (M/F)
Larsson & Lufkin (1987)	USA	Imaging (CT/MR) observational	75 (40 CT, 35 MR)	Mixed clinical cohort	NR	37M / 38F
Unur et al. (1999)	Turkey	Cadaveric cross-sectional	50 cadavers	Turkish adults	NR	NR
De-Ary-Pires et al. (2003)	Brazil	Cadaveric cross-sectional	74 cadavers (146 sides)	Brazilian adults	20–86	37M / 37F
Liquidato et al. (2007)	Brazil	Cadaveric cross-sectional	10 cadavers	Brazilian male adults	NR	10M / 0F
Ozgun et al. (2007)	Turkey	Cadaveric observational	30 cadavers (60 sides)	Anatolian adult males	43–75	30M / 0F
Mangalgi et al. (2009)	India/Saudi Arabia	Cadaveric cross-sectional	15 cadavers	Indian/Saudi adults	63–81	15M /
Zdilla et al. (2018)	USA	Cadaveric cross-sectional	19 cadavers	White Americans	F: 76.1 ±17.2, M: 81.6 ±11.2*	11M / 8F
Ortug et al. (2020)	Turkey	Cadaveric cross-sectional	40 cadavers	Turkish adults	65.27 ± 6.82*	22M / 18F
Hsiao & Chang (2019)	Taiwan	Cadaveric observational	15 cadavers	Taiwanese adults	45–56	11M / 4F
Anderson & Tucker (2021)	USA	Cadaveric observational	48 cadavers	Ethnically diverse (California)	75*	23M / 25F
Arayapisti et al. (2022)	Thailand	Cadaveric cross-sectional	91 cadavers	Thai adults	47–96	55M / 36F
Sarna et al. (2023)	Kenya	Cadaveric cross-sectional	41 cadavers (82 sides)	Kenyan adults	20–35	33M / 8F
Alves et al. (2023)	Brazil	Cadaveric cross-sectional	50 digastric muscles	Brazilian adults	NR	NR
Gross et al. (2022)	Brazil	Cadaveric observational	31 cadavers	Brazilian adults	18–80	29M / 2F
Ünsal et al. (2024)	Cyprus/Turkey	Ultrasonographic cross-sectional	151 patients	Mixed population	19–60	81M / 70F
Shen et al. (2025)	China	Cadaveric observational	72 cadavers (144 sides)	Chinese adults	38–97	48M / 24F

NR - not reported; M – male; F- female; *These papers did not reported age range, but mean age.

tions in the anterior belly of the digastric muscle, including accessory bellies with ipsilateral origin and insertion relative to the main belly, contralateral insertion into the intermediate tendon, origin or insertion into the mylohyoid raphe, crossing between accessory bellies, and the presence of multiple accessory bellies (Kim and Loukas, 2019). In the present dissections, the accessory bellies were found ipsilateral to the main bellies, and thus the De-Ary-Pires et al. (2003) classification was applied, with type II bellies predominating.

The meta-analysis, which included 16 observational studies totaling 787 individuals, revealed

an overall combined prevalence of 25.1% (95% CI: 15.5–35.9) for variations in the anterior belly of the digastric muscle. This finding robustly establishes that approximately one in every four individuals may present some form of variation. Tranchito and Bordoni (2025) reported a prevalence of 65.8%, while Kim and Loukas (2019) observed digastric muscle variations in 33.4% of cadaveric populations.

The subgroup analysis by geographic region showed prevalence rates of 22.9% in Turkey, 25.2% in Brazil, and 16.9% in the United States. Although these subgroups exhibited high heterogeneity, the prevalence range (16.9–25.2%) re-

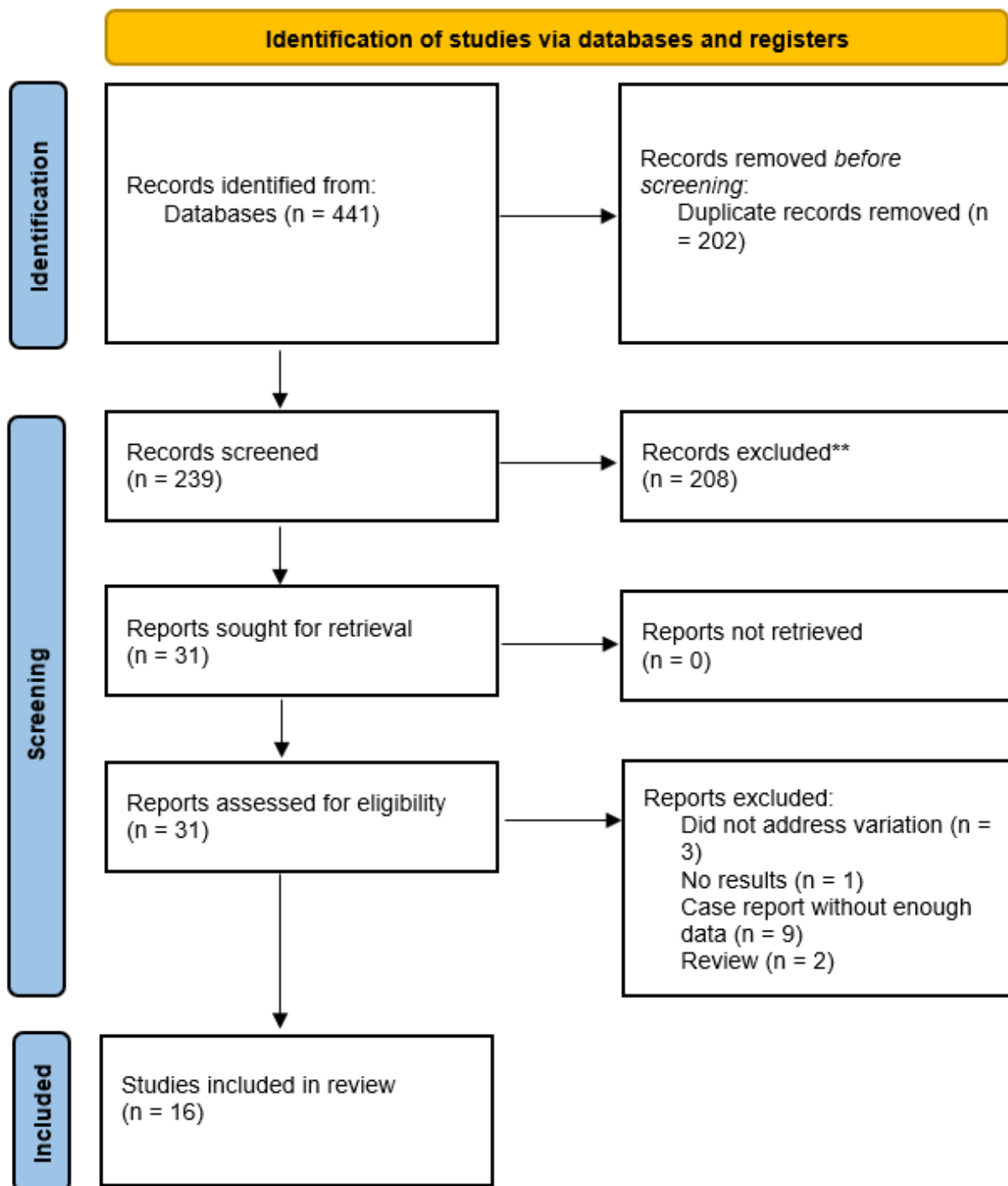


Fig. 2.- Study selection process.

mained relatively homogeneous, reflecting populations that are mostly of European or mixed ancestry. Similarly, Kim and Loukas (2019) reported that digastric variations were present in 51.7% of Asian populations, and when excluding Asian samples from their overall analysis, they found lower prevalence rates, suggesting that these variations may be more frequent among Asians. This observation implies that the occurrence of digastric muscle variations may be influenced by genetic or ethnic factors, emphasizing

the importance of further studies to identify such underlying determinants.

The combined data revealed no major discrepancies in variation incidence between sides, but a higher prevalence in males. Kim and Loukas (2019) reached similar conclusions. The male predominance may be interpreted from two perspectives: (a) it could reflect a sampling bias inherent in anatomical literature, as many cadaveric studies included predominantly male specimens; or (b) it could indicate a biological difference, pos-

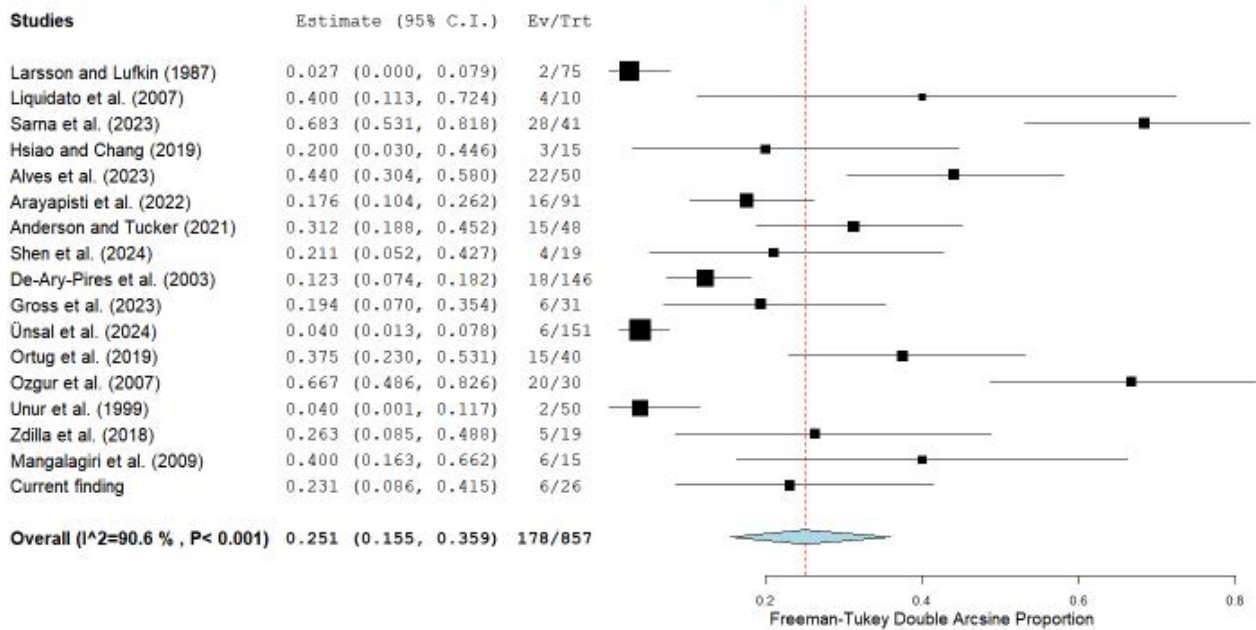


Fig 3.- Overall prevalence.

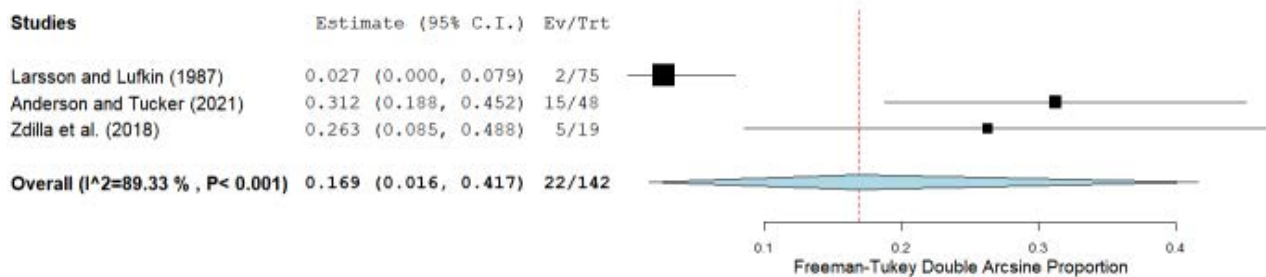
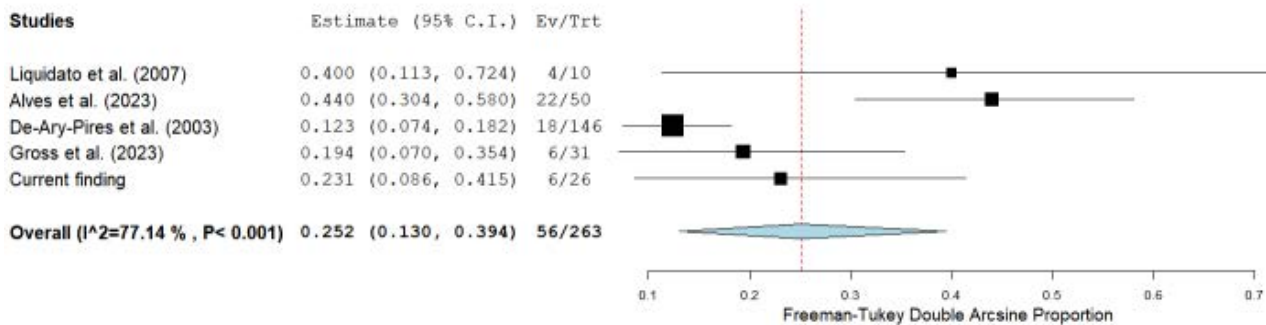
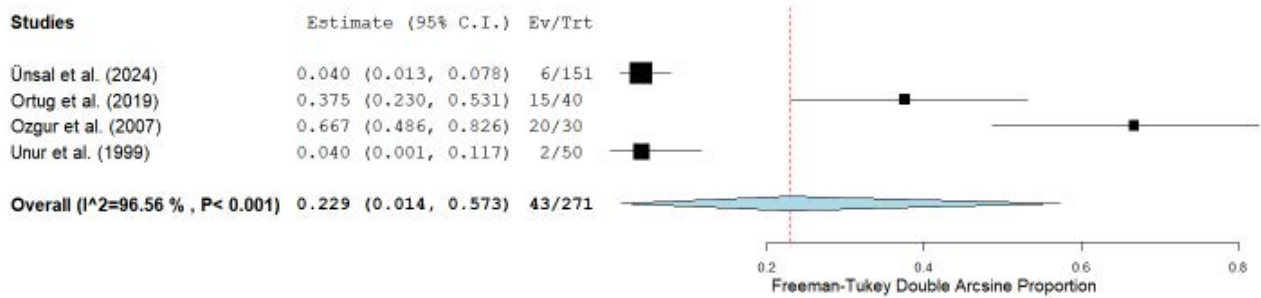
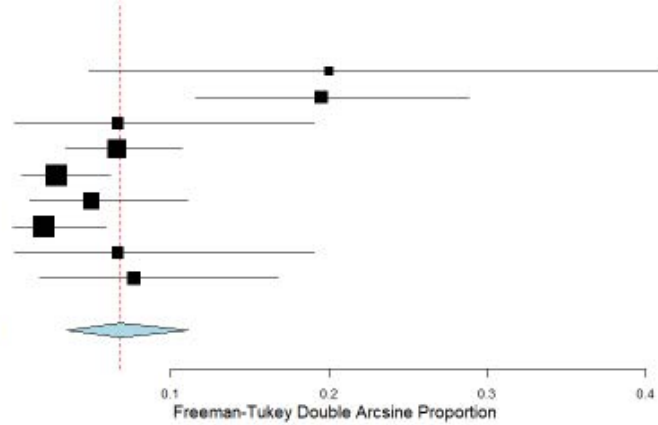


Fig. 4A.- Prevalence in the population of Turkiye. 4B.- Prevalence in the population of Brazil. 4C.- Prevalence in the population of USA.

sibly linked to subtle genetic factors or hormonal

influences affecting extracellular matrix organi-

Studies	Estimate (95% C.I.)	Ev/Trt
Liquidato et al. (2007)	0.200 (0.049, 0.408)	4/20
Sarna et al. (2023)	0.195 (0.116, 0.289)	16/82
Hsiao and Chang (2019)	0.067 (0.001, 0.191)	2/30
Arayapisti et al. (2022)	0.066 (0.034, 0.107)	12/182
Shen et al. (2024)	0.028 (0.006, 0.062)	4/144
Ortug et al. (2019)	0.050 (0.011, 0.111)	4/80
Unur et al. (1999)	0.020 (0.000, 0.059)	2/100
Mangalagiri et al. (2009)	0.067 (0.001, 0.191)	2/30
Current finding	0.077 (0.017, 0.168)	4/52
Overall ($I^2=70.51\%$, $P<0.001$)	0.068 (0.034, 0.112)	50/720



Studies	Estimate (95% C.I.)	Ev/Trt
Liquidato et al. (2007)	0.100 (0.002, 0.278)	2/20
Sarna et al. (2023)	0.268 (0.177, 0.370)	22/82
Hsiao and Chang (2019)	0.100 (0.013, 0.238)	3/30
Arayapisti et al. (2022)	0.077 (0.042, 0.121)	14/182
Shen et al. (2024)	0.028 (0.006, 0.062)	4/144
Ortug et al. (2019)	0.075 (0.026, 0.145)	6/80
Unur et al. (1999)	0.020 (0.000, 0.059)	2/100
Mangalagiri et al. (2009)	0.200 (0.073, 0.365)	6/30
Current finding	0.058 (0.007, 0.141)	3/52
Overall ($I^2=80.7\%$, $P<0.001$)	0.086 (0.041, 0.145)	62/720

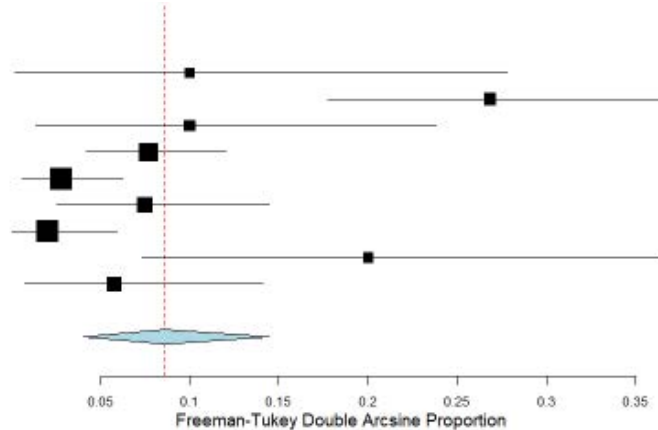
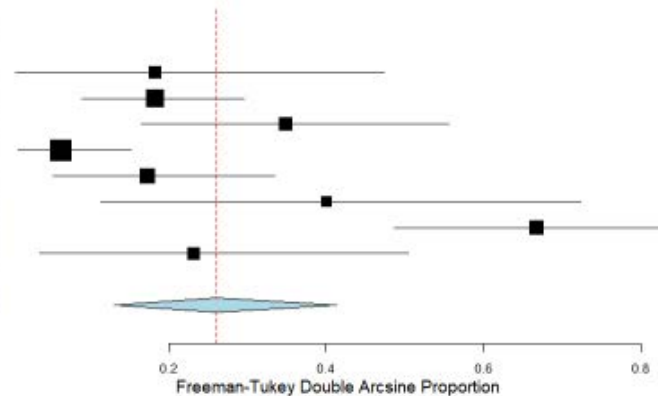


Fig. 5A.- Prevalence on the right side. 5B.- Prevalence on the left side.

Studies	Estimate (95% C.I.)	Ev/Trt
Hsiao & Chang (2019)	0.182 (0.005, 0.474)	2/11
Arayapisti et al. (2022)	0.182 (0.090, 0.296)	10/55
Anderson & Tucker (2021)	0.348 (0.164, 0.556)	8/23
Shen et al. (2024)	0.062 (0.008, 0.152)	3/48
Gross et al. (2023)	0.172 (0.053, 0.335)	5/29
Liquidato et al. (2007)	0.400 (0.113, 0.724)	4/10
Ozgur et al. (2007)	0.667 (0.486, 0.826)	20/30
Current finding	0.231 (0.036, 0.504)	3/13
Overall ($I^2=79.93\%$, $P<0.001$)	0.260 (0.131, 0.413)	55/219



Studies	Estimate (95% C.I.)	Ev/Trt
Hsiao & Chang (2019)	0.250 (0.000, 0.793)	1/4
Arayapisti et al. (2022)	0.167 (0.060, 0.309)	6/36
Anderson & Tucker (2021)	0.280 (0.119, 0.474)	7/25
Shen et al. (2024)	0.042 (0.000, 0.170)	1/24
Gross et al. (2023)	0.500 (0.000, 1.000)	1/2
Current finding	0.231 (0.036, 0.504)	3/13
Overall ($I^2=36.13\%$, $P=0.201$)	0.154 (0.054, 0.279)	19/104

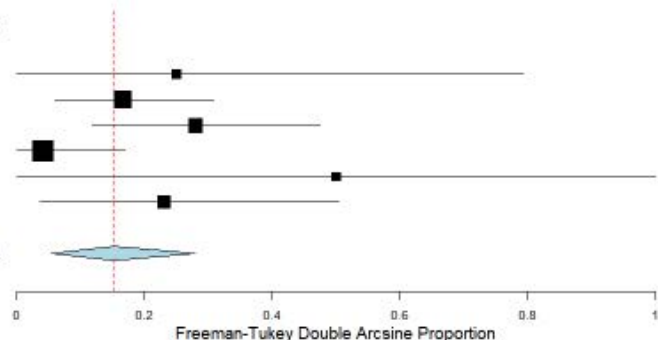


Fig. 6A.- Prevalence in the male population. 6B.- Prevalence in the female population.

zation or differential muscle growth during development. The absence of laterality differences reinforces the symmetrical embryonic development of the pharyngeal arches.

Evaluating the characteristics of the digastric muscle and its variations can be helpful, because this muscle is involved in various clinical and surgical procedures. The presence of an accessory belly alters the expected anatomical map. In procedures such as neck dissection (used in head and neck cancer staging) or floor-of-mouth approaches, surgeons rely on correct identification of muscular boundaries to ensure safety and preserve adjacent neurovascular structures (Alagöz et al., 2004; Buffoli et al., 2016). An unexpected variation may lead to disorientation and, consequently, increase the risk of iatrogenic injury (Kikuta et al., 2019). Therefore, recognizing digastric variations is essential for accurate differential diagnosis in imaging examinations and for surgical interventions involving the cervical region (Larsson and Lufkin, 1987).

The meta-analysis was not intended to redefine prevalence estimates, but rather to determine whether the frequency of variations observed in fetuses aligns with the range reported across postnatal populations, thereby supporting the hypothesis of developmental continuity. Among the limitations of this study were the high number of case reports found during the search and the heterogeneity of data, since the included studies differed in origin, age, and ethnicity of their samples, requiring subgroup analyses for more precise estimates. Additionally, some studies lacked sufficient data for analysis, necessitating the exclusion of certain comparisons or isolated interpretation. Future multicenter investigations, incorporating genetic analyses and standardized imaging methodologies, may help clarify the influence of ethnic factors and contribute to the development of a universal morphological classification.

CONCLUSION

The present study demonstrates that variations of the anterior belly of the digastric muscle are established during fetal development and occur at frequencies comparable to those reported in post-

natal populations. These findings support a congenital and developmentally stable origin of this anatomical variability. By integrating fetal morphological data with a comprehensive synthesis of existing literature, this study contributes to the understanding of normal developmental diversity of the suprahyoid musculature. The meta-analysis revealed different prevalence rates according to geographic and sex subgroups, although without disproportionate differences between sexes.

AUTHORS' CONTRIBUTION

MLL Prado– Protocol/project development; Data collection or management; Data analysis; Manuscript writing/editing. JCOMM Neto– Manuscript writing/editing. CVR Basto– Manuscript writing/editing. ICS Aragão– Manuscript writing/editing. FMS Aragão– Manuscript writing/editing. JA Aragão– Protocol/project development; Manuscript writing/editing. FP Reis– Manuscript writing/editing.

ACKNOWLEDGEMENTS

The authors wish to sincerely thank those who donated their bodies to science so that anatomical research could be performed. Results from such research can potentially improve patient care and increase mankind's overall knowledge. Therefore, these donors and their families deserve our highest gratitude.

REFERENCES

- ALAGÖZ MŞ, UYSAL AÇ, TÜCCAR E, SENSÖZ O (2004) The vascular anatomy of the digastric muscle. *J Craniofac Surg*, 15(1): 114-117.
- ALVES N, TORRES-VILLAR C, DE SOUSA-RODRIGUES CF, DEANA F (2023) Study of digastric muscle in Brazilian individuals. *Int J Morphol*, 41(6): 1620-1624.
- ANDERSON H, TUCKER RP (2021) A cadaveric analysis of anatomical variations of the anterior belly of the digastric muscle. *Folia Morphol (Warsz)*, 80(3): 691-698.
- ARAGÃO JJA, SANTOS RS, BEATRIZ M, LACERDA RL, FERREIRA GS, REIS FP (2022) Ventre acessório do músculo digástrico em feto humano: relato de caso. Editora Científica Digital eBooks, pp 195-203.
- ARAYAPISIT T, VORAKULPIPAT C, SRIMANEKARN N, SONGSAAD A, CHANTADUL V (2022) Anatomical variations of the anterior belly of the digastric muscle in Thai cadavers: a cross-sectional study. *J Int Soc Prev Community Dent*, 12(2): 171-177.
- BUFFOLI B, LANCINI D, FERRARI M, BELOTTI F, NICOLAI P, TSCHABITSCHER M, REZZANI R, RODELLA LF (2016) Symmetrical anatomical variant of the anterior belly of the digastric muscle: clinical implications. *Folia Morphol (Warsz)*, 75(1): 112-116.
- DE-ARY-PIRES B, ARY-PIRES R, PIRES-NETO MA (2003) The human digastric muscle: patterns and variations with clinical and surgical correlations. *Ann Anat*, 185(5): 471-479.
- GOLDSTEIN I, REECE EA, HOBBS JC (1988) Sonographic appearance of the fetal heel ossification centers and foot length measurements provide independent markers for gestational age estimation. *Am J Obstet Gynecol*, 159(4): 923-926.

GROSS DJ, ROSSI AC, FERREIRA-PILEGGI BC, WATANABE LNO, BOTACIN PR, PRADO FB, FREIRE AR (2023) Morphological study of the anatomical variations of anterior belly of digastric muscle in Brazilian cadavers. *Folia Morphol (Warsz)*, 82(3): 677-682.

HSIAO TH, CHANG HP (2019) Anatomical variations in the digastric muscle. *Kaohsiung J Med Sci*, 35(2): 83-86.

KIKUTA S, IWANAGA J, KUSUKAWA J, TUBBS RS (2019) Triangles of the neck: a review with clinical/surgical applications. *Anat Cell Biol*, 52(2): 120-127.

KIM SD, LOUKAS M (2019) Anatomy and variations of digastric muscle. *Anat Cell Biol*, 52(1): 1-11.

LARSSON SG, LUFKIN RB (1987) Anomalies of digastric muscles. *J Comput Assist Tomogr*, 11(3): 422-425.

LIQUIDATO B, BARROS M, ALVES A, PEREIRA C (2007) Estudio anatómico del músculo digástrico: variación en el vientre anterior. *Int J Morphol*, 25(4): 797-800.

MANGALGIRIA, RAZVI M (2009) Variations in the anterior belly of digastric. *Int J Health Sci (Qassim)*, 3(2): 257-262.

MOHER D, LIBERATI A, TETZLAFF J, ALTMAN DG; PRISMA Group (2009) Preferred reporting items for systematic reviews and meta-analyses: the PRISMA statement. *PLoS Med*, 6(7): e1000097.

ORTUG G, SIPAHI B, ORTUG A, IPSALALI HO (2020) Variations of the digastric muscle and accessory bellies – a study of gross anatomic dissections. *Morphologie*, 104(345): 125-132.

OZGUR Z, GOVSA F, OZGUR T (2007) The cause of the difference in the submental region: aberrant muscle bundles of the anterior belly of the digastric muscle. *J Craniofac Surg*, 18(4): 875-881.

PRADO MLDL, FILHO ALB, TRINDADE JGS, ARAGÃO I, ARAGÃO F, FEITOSA V, FURTADO DE MENDONÇA D, PRADO REIS F, ARAGÃO JA (2025) Morphological and morphometric study of the digastric muscle in human fetuses. *Braz J Implantol Health Sci*, 7(8): 560-577.

ROSNER B, GLYNN RJ, LEE ML (2006) The Wilcoxon signed rank test for paired comparisons of clustered data. *Biometrics*, 62(1): 185-192.

ROYSTON P (1992) Approximating the Shapiro–Wilk W-test for non-normality. *Stat Comput*, 2(3): 117-119.

SARGON MF, ÇELIK HH (1994) An abnormal digastric muscle with three bellies. *Surg Radiol Anat*, 16(2): 215-216.

SARNA K, NGEOW WC, KANDIMALLA A, ESTREED MA, SONIGRA KJ, KAMAU M (2023) More than two – a cadaveric study on the morphometry and classification of the digastric muscle in a selected Kenyan population. *Morphologie*, 107(357): 182-192.

SHEN BZ, TANG MF, ZHUANG XJ, CHAN PR, ZHANG YJ (2025) Variation and arrangement of the digastric muscle in a Chinese population. *J Craniofac Surg*, 36(4): 1368-1371.

STANDRING S (2008) Gray's anatomy: the anatomical basis of clinical practice. 40th ed. Churchill Livingstone Elsevier, London.

TRANCHITO EN, BORDONI B (2025) Anatomy, head and neck, digastric muscle. *StatPearls*. Treasure Island (FL): StatPearls Publishing.

UNUR E, EKINCI N, ÜLGER H, AYCAN K (1999) Variations of the anterior belly of the digastric muscle. *Erciyes Med J*, 21(4): 192-194.

ÜNSAL G, GÖKSEL S, KARABAŞ HÇ, ERTÜRK AF, ÖZCAN İ, EVLİ C, ÖNDER M, ORHAN K (2024) Variations and thicknesses of anterior belly of the digastric muscle: an ultrasonographic study. *Eur Arch Otorhinolaryngol*, 281(1): 411-418.

ZDILLA MJ, MANGUS KR, SWEARINGEN JV, MILLER KD, LAMBERT HW (2018) The submental arrowhead variation of the mylohyoid and anterior belly of the digastric muscles. *Surg Radiol Anat*, 40(12): 1429-1436.

Innovative museum techniques in enhancing Medical Education: a study on interactive and experiential learning for medical students

Priya G, Mahima Sophia M

Panimalar Medical College Hospital and Research Center, Varadharajapuram, Poonamallee, Chennai -600123, Tamil Nadu, India

SUMMARY

The anatomy museums that provide students with access to cadaveric specimens and bones for their learning purpose are essential in the field of medical education. It is now mandatory for every medical college to have an anatomy museum. Therefore, for every medical student it will be useful to know about the museum techniques. The purpose of this study was to acquaint medical students with museum technique. To achieve this objective, third-year medical students of Panimalar medical college hospital and research institute Chennai who came to department of Anatomy for their elective courses were selected for the study. All aspects of museum techniques, starting from specimen preparation using dissected cadavers, and later preservation techniques, preparing jars using acrylic sheet, labelling, mounting of both dry and wet specimens, were taught to the elective students. The students were divided into four groups with five students in each group. The stipulated time used for the study was 15 days. The museum work was divided and given to each group accordingly, and asked the groups to show innovation in mounting specimens. The students learnt

all the museum techniques within the stipulated time. They mounted the museum specimens and showed their innovative skills and knowledge. All the steps followed in making museum specimens and jars were photographed, and the procedures were recorded in the log book. The enthusiastic work of the students creates innovation with respect to traditional method of education. The medical students visiting anatomy museums during their first year of the course gives them an idea about human body. Museums are important educational resources, and are considered a supplemental approach in providing medical education. This study has facilitated their independent training in museum techniques, which will help in better comprehension and knowledge enrichment about museum preparation among medical students.

Key words: Anatomy museum – Acrylic sheets – Formalin – Chloroform – Table saw and scale

INTRODUCTION

A museum by definition is “An institution that houses and cares for a collection of artefacts and

Corresponding author:

Priya G. Department of Anatomy, Panimalar medical college hospital and research center, Varadharajapuram, poonamallee, Chennai - 600123, Tamil Nadu, India. Phone: 9443644219. E-mail address: priyagunalan2006@yahoo.co.in - Orcid: 0000-0002-3767-3378

Submitted: November 29, 2025 **Accepted:** December 13, 2025

<https://doi.org/10.52083/EDIN1101>

other objects of scientific, artistic or historical importance and makes them available for public viewing through exhibits that may be permanent or temporary". The early museums predominantly comprised paintings and models. This was because the preservative formalin was not discovered until 1859. In 1859, Alexander Mikhailovich Butlerov discovered formaldehyde, which was then isolated in 1868 by August Wilhelm Von Hoffmann as formalin. These have been used as preservatives for the specimens (Kamath et al., 2016).

The museums in a medical institution are the primary resource for teaching Anatomy. The students, by viewing the mounted anatomical specimens, both wet (gross specimens) and dry (bones) models, are provided with a visualized image regarding the human body's structure and organization, which may be difficult to understand from textbooks and lectures. Apart from that, nowadays the museums are important learning tools in medical education, as they help students in self-directed learning; they also develop better communication skills.

The medical students have visited museum but they have not been trained in museum techniques. This study involved the students in preparing jars, mounting specimens, preparing mounting solution and labelling by themselves in order to create an interest in museum-making among the student community. It aimed to promote the innovation skills or talents of the medical students in museum techniques.

MATERIALS AND METHODS

The study was conducted in Panimalar medical college hospital and research institute for the third-year medical students who came to the department of anatomy for elective course. A total number of 20 medical students opted to study museum techniques. The students were divided into 4 groups (five students in each group).

Group I – Specimen preparation. The specimens were dissected from the embalmed cadavers.

Group II – Preservation technique and preparing mounting solution.

Group III – Mounting technique and labelling.

Group IV – Preparing Museum jars with acrylic sheet.

Specimen preparation

The first step done in the preparation of specimens was selection of the cadavers. The cadavers were collected from the Anatomy dissection hall. Already dissected cadavers by the first-year undergraduate medical students were preferred for the study. The specimens were dissected accordingly for preparation of dry and wet specimens. For making dry specimens, the hyoid bone was dissected out using a scalpel and the bone was removed from the midline of the neck. The dissection steps were followed in accordance with Cunningham's dissection manual, vol. 3, Head & Neck (Romanes, 2001). The procured bone was put in a tray, filled with water and kept for about two days. After two days, the bone was taken and the soft tissue attached to the bone was scraped out using a blunt scalpel, forceps and scissors. The bone was washed well in running water, and with a brush it was cleaned clearly and placed in 5% hydrogen peroxide. Then the bone was kept under the sunlight for two days to get dried. This method was a little time-consuming, but the advantage is that all the features of the bones will be preserved. For making wet specimens, the dissected-out specimens were placed in a bucket filled with 10% formalin.

Preservation technique and preparing mounting solution

The following steps were followed:

1. Fixation: for preserving the specimens, 10% formalin was used as fixative.

2. Restoration of specimen: it is a method that required restoring the natural color of the specimens, as they lose it on fixation. The Kaiserling II method was followed (Pulvertaft, 1950). The neatly dissected specimens were washed in running water and transferred to 95% alcohol for a time from 10 minutes to 1 hour, depending on the size of the specimen. A change of color of the specimen was observed after leaving the specimen in the solution for 1-2 hrs.

3. Preservation of specimen:

Kaiserling III solution: Glycerin – 4 liters, Distilled water – 10 liters, Potassium acetate – 14 grams. The prepared solution was left to stand for 2-3 days to ensure proper mixing of the chemicals (Proger, 1958; Culling et al., 1985).

Mounting technique and labelling

The specimens were mounted on to a center plate made of acrylic sheet measuring about 3mm in thickness. The specimen was stitched on the center plate using nylon threads. Points for stitches were marked using a marker pen on the center plate, and holes of 1/16 inch diameter were made using a drill (Fig. 1 A, B).

In case of dry specimens, labelling was done inside the jar. A coat of amyl acetate and quick fix was applied to the labels. Labelling was also done using acrylic sheets of 1/16 inch in thickness. The labelling was written on these sheets. The sheets were then cemented to the bottom of the center plate or to the bottom of the outer aspect of the jar (Natarajan et al., 2012).

Preparing museum jars with acrylic sheet

Step 1: Measurement of each specimen was taken.

Step 2: Sheets were cut according to the measurement.

Acrylic sheets were cut with a table-saw. A 48-tooth carbide-tipped blade 10 inches in diameter was used for cutting the sheets. The cut edge of the acrylic sheet should be smooth, straight, square to the faces and sharp on the edges, because along this area the glue is applied in order to stick the sheets (Latha V. Prabhu et al., 2015). The edges were trimmed with a router (Fig. 1C).

Step 3: Pasting of sheets using chloroform.

The Chloroform was used as a solvent to bind the cut pieces of acrylic sheets. Methods for using chloroform to bind acrylic sheets:

a) Firstly, the students were asked to follow safety precautions while using chloroform, due to its toxicity. They worked in a well-ventilated area, wearing gloves and eye protection to prevent skin and eye contact.

b) The measured and trimmed acrylic sheets which had to be joined were taken. Its surfaces were cleaned for dust.

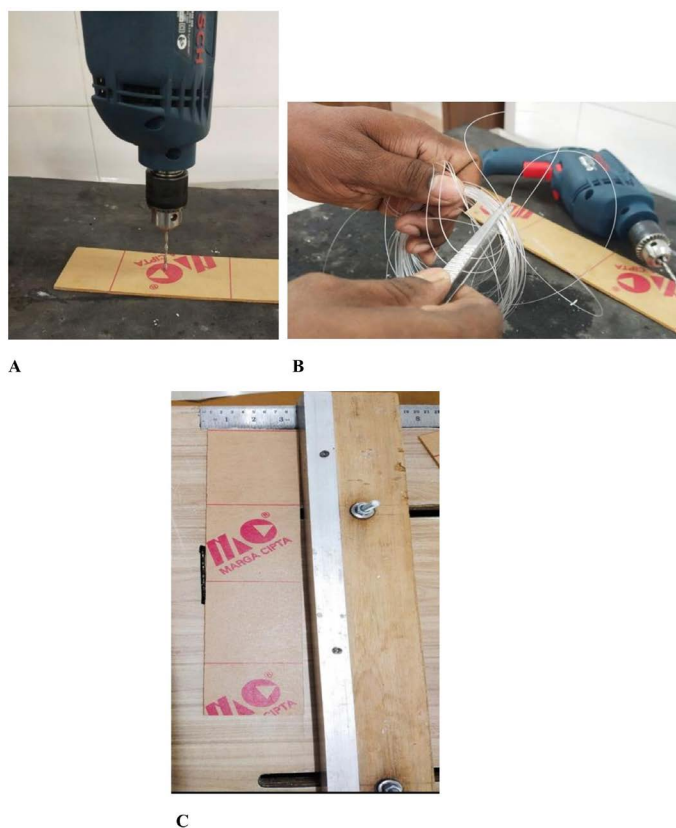


Fig.1.- A. Making hole in the center sheet with a driller. B. Nylon thread for tying the specimens. C. Table saw.

c) The chloroform-acrylic solution was prepared: the scraps of acrylic (small pieces of acrylic sheets) which were obtained during the cutting of the sheets with a saw were dissolved in chloroform. They were mixed well until a syrupy consistency is achieved. The ratio of acrylic to chloroform was used in a 1:10 ratio (scraps of acrylic to chloroform).

d) The prepared solution was applied to one of the surfaces to be joined, ensured even coverage of the solvent (Harris et al., 1977; Brune, 1987). The edges of the acrylic pieces were aligned correctly and joined together (Fig. 2).

Step 4: Drying the jars for sticking of sheets with each other:

After pasting, the jars were allowed to dry. The weights (stone) were kept on the pasted jars to secure the pieces in place. The jars were kept in this position for at least two days to allow the adhesive to dry completely (Fig. 3).

Step 5: Checking for leakage of jars.

Before mounting, the jars were checked for leakage. The leakage was checked using adhesive application method. The chloroform was used

as an adhesive to seal the gaps at the joints. To achieve this, the students were asked to hold the jar slantly; a little chloroform was poured along the edges of the jars, and the jars were rotated as the fluid touched the joints of the jar (Azubuike and Onwusi, 2018; Jain et al., 2013; Nim, 2012; Winkelmann, 2007; Domanski et al., 2023).

RESULTS

It was observed that each of the four groups mounted the specimens accordingly as described below:

Group I mounted the spinal cord (wet specimen) and ear ossicles (dry specimen) (Fig. 4).

Group II mounted the hyoid bone and the cartilages of the larynx (dry specimen) (Fig. 5).

Group III mounted the malleus bone (dry specimen with a model depicts the bone) (Fig. 6A, B).

Group IV mounted the incus bone (dry specimen with a model drawing of other bones) (Fig. 6C).

Models form the most important part in the anatomy museum and bring reality to the stu-



Fig. 2.- A. Acrylic scraps. B. Mixing chloroform with acrylic scraps using glass needle. C. Pouring the solvent (adhesive) along the trimmed edges of acrylic sheets. D. Joining/pasting the sheets.



A

B

Fig. 3.- A. Weight (stone) kept on the pasted jars. B. After 2-3 days the adhesive got dried and the jar is ready (sticked properly).

dents' imagination of human organs. With the help of the models, the three-dimensional and two-dimensional views of the organs can be demonstrated to the medical students in the museum itself. In the present study, the models are made with the help of Plaster of Paris, wood and thermacol. The students presented the models in an innovative method (Fig.6).

DISCUSSION

The anatomy museum is considered a science museum, because it is not only used by medical students but also by the science students as they display various anatomical structures of the human body. Indirectly or directly, the museum plays an important role in understanding the structure of an organ by visualizing the specimens mount-



A

B

Fig. 4.- A. Spinal cord. B. Ear ossicles.



Fig. 5.- A, B. Innovation in mounting cartilages of larynx. C. Hyoid bone.

ed. Nowadays, the students’ learning skills have been changed: they are fascinated towards what they see and learn. When they perform all the techniques by themselves, this creates an interest to the medical students and while studying, they get an opportunity to show their innovative ideas. Thereby, the present study may be the first study to incorporate the undergraduate medical students in performing the museum techniques and exploring their innovative technique in mounting the specimens.

Recent CBME curriculum has emphasized the role of anatomy museums, as they contribute to the field of research and education from time immemorial, by understanding the various aspects of human Anatomy (Maraldi et al., 2000). Therefore, the anatomy museum plays a crucial role in the life of the first-year medical students. They get totally exposed to a different world, where their

imagination of the human organs is seen really in the museums (Sachin and Darshana, 2020).

Kagan HJ et al. designed a study to explore how an integrative art-museum-based program might benefit 3rd and 4th year medical students. Their results suggest that participants perceive visual arts-based methods as useful for teaching many core competencies in medicine in a novel way compared to traditional scientific-based medical pedagogy (Kagan et al., 2022).

There has been an increasing effort to incorporate fine art education into medical training, primarily to enhance visual perception skills and empathy. Fine art curricula incorporating pattern recognition skills could help enhance diagnostic acumen and efficiency. Deep seeing involves the ability to perceive textures and colors that may not be immediately distinguishable. This can



Fig. 6.- A, B. Anterior and posterior view of Malleus bone (dry specimen). Model made of Plaster of Paris shows the markings of the bone. The real bone was pointed in the upper part of the jar by a bug. C. Students' innovation in mounting ear ossicles. The incus bone was focused by a lens.

translate clinically to observing details beyond the most prominent colors and textures. Moreover, with the increasing use of telemedicine, it is important for residents to be able to “see” the textures in the absence of a full physical examination. Interpretation of facial expressions of a painting’s subject(s) often helps identify the artist’s intention or message. In medicine, similarly, accurate interpretation of facial expressions is likely to enhance empathy and quality of care. The framework of VTS (visual thinking strategies) seems to be effective, and the evidence suggests that instructors comprise both clinicians and art curators. Future efforts would benefit from a standardized curriculum and assessment guidelines (Dalia et al., 2020).

A study was conducted to evaluate whether students’ exposure to VTS (visual thinking strat-

egies) would improve their physical observation skills, increase tolerance for ambiguity, and increase interest in learning communication skills. There are about 32 students that attended three 90-minute sessions, at which they observed and commented on three pieces of art in small groups led by museum educators.

Pre- and post-test evaluations included Geller and colleagues’ version of Budner’s Tolerance of Ambiguity Scale, the Communication Skills Attitudes Scale, and free responses to art and patient images. Students significantly increased their tolerance for ambiguity ($P = .033$), as well as positive views toward health care professional communication skills ($P = .001$) (Klugman et al., 2011).

Similarly, another study which conducted a student survey at Leiden University has indicated that all students (100%) found audio-guided

museum tours to be useful for learning, and the majority of them found guided tours to be clinically relevant (87%). However, 69% of students felt that museum visits should be optional rather than compulsory within the medical training curriculum (Marreez et al., 2010).

By heeding the importance of VTS and skill-based study introduced by the NMC (national medical commission) in the CBME curriculum in India, the present study was conducted to the medical students in order to initiate their innovative talents, learning skill and communication skill. The students were very much interested, interactive and intellectual during the study. They showed their innovative talents, which will be useful during their further course of the study.

CONCLUSION

The Competency-based Medical Curriculum adopted by the National Medical Commission in India emphasizes on Self Directed Learning (SDL). Thereby the author believes that creating innovative museums will encourage the students in the learning process in this regard.

ACKNOWLEDGEMENTS

The authors sincerely thank those who donated their bodies to science so that anatomical research could be performed. Results from such research can potentially increase mankind's overall knowledge that can then improve patient care. Therefore, these donors and their families deserve our highest gratitude.

REFERENCES

- AZUBUIKE NC, ONWUSI KU (2018) Evaluation of a new technique for supporting anatomical museum specimens: a comparative study. *Int J Anat Res*, 6(4.2): 5929-5935.
- BRUNE EO (1987) Labelling structures and eliminating air bubbles in fluid-mounted museum specimens. *J Audiov Media Med*, 10(2): 72-74.
- CULLING CFA, ALLISON RT, BARR WT (1985) Cellular Pathology Techniques, 4th ed. Butterworth and Co., London, pp 523-524.
- DALIA Y, MILAM EC, RIEDER EA (2020) Art in Medical Education: A review. *J Grad Med Educ*, 12(6): 686-695.
- DOMAŃSKI J, JANCZURA A, WANAT M, WIGLUSZ K, GRAJZER M, SIMMONS JE, DOMAGAŁA Z, SZEPIETOWSKI JC (2023) Preservation fluids of heritage anatomical specimens - a challenge for modern science. Studies of the origin, composition and microbiological contamination of old museum collections. *J Anat*, 243(1): 148-166.
- HARRIS PF, PRITCHARD CA, SILVO F (1977) Adaptation of museum specimens for use in anatomical teaching aids. *Med Educ*, 11(3): 171-174.
- JAIN LT, BABEL H, VIJAY N (2013) New technique to mount specimen in the formalin filled jar for anatomy with almost invisible support. *Int J Curr Res Rev*,

5(12): 45-50.

KAGAN HJ, KELLY-HEDRICK M, BENSKIN E, WOLFFE S, SUCHANEK M, CHISOLM MS (2022) Understanding the role of the art museum in teaching clinical-level medical students. *Med Educ Online*, 27(1): 2010513.

KAMATH VG, BHAT S, ASIF M, AVADHANI R (2016) Anatomy museums of southern India and medical education: Original research. *Ind J Clin Anat Physiol*, 3(1): 45-49.

KLUGMAN CM, PEEL J, BECKMANN-MENDEZ D (2011) Art Rounds: teaching interprofessional students visual thinking strategies at one school. *Acad Med*, 86(10): 1266-1271.

LATHA V. PRABHU, MANGALA M. PAI, DIVYA PREMCHANDRAN, RAJANIGANDHA VADGAONKAR, MURLIMANJU BV (2015) A novel method for coloring and labeling specimens in the anatomy museum. *Int J Anat Res*, 3(2):1165-1167.

MARALDINI M, MAZZOTTI G, COCCO L, MANZOLI FA (2000) Anatomical wax work modeling: The history of the Bologna Anatomy Museum. *Anat Rec*, 261(1): 5-10.

MARREEZ YM, WILLEMS LN, WELLS MR (2010) The role of medical museums in contemporary medical education. *Anat Sci Educ*, 3(5): 249-253.

NATARAJAN S, RANJAN J, BOAZ K (2012) Museum mounting techniques: Revisited econo-mode. *Ind J Pathol Microbiol*, 55(2): 260-261.

NIM VK (2012) Wax mounting of specimen in anatomy museum. *J Anat Soc India*, 61: 41-43.

PROGER LW (1958) Perspex jars for pathological museums. *J Clin Pathol*, 11(1): 92-95.

PULVERTAFT RJ (1950) Museum techniques: a review. *J Clin Pathol*, 3(1): 1-23.

ROMANES GJ (2001) Cunningham's manual of practical anatomy. 15th edition. Oxford medical publications. Vol. 3, Head and Neck, pp 70-75.

SACHIN T, DARSHANA T (2020) Anatomy Museum: influence on first year MBBS students. *Int J Anat Radiol Surg*, 9(3): 04-05.

WINKELMANN A (2007) Anatomical dissection as a teaching method in medical school: a review of the evidence. *Med Educ*, 41(1): 15-22.

Anatomy Museums in Medical Education: utilization patterns and perceived learning benefits among Indian medical graduates

Manikanta Reddy V¹, Rajesh S², Maruti R. Annamraju³, Teresa Rani S⁴, Krishna Manasa A¹

¹ Department of Anatomy, Sri Venkateswara Medical College, Andhra Pradesh, India

² Department of Anatomy, Dhanalakshmi Srinivasan Institute of Medical Sciences, Tamil Nadu, India

³ Department of Anatomy, Government Medical College, Kadapa, Andhra Pradesh, India

⁴ Department of Anatomy, Apollo Institute of Medical Sciences and Research, Andhra Pradesh, India

SUMMARY

The anatomy Museum is an important educational resource for medical students, offering preserved specimens, models, and charts. However, its utilization varies, and its educational value remains unclear. This study examined utilization patterns of anatomy museums among Indian medical graduates (IMGs) and explored whether frequent academic visits enhance anatomy comprehension and exam preparation. A cross-sectional, questionnaire-based survey was conducted from July 2024 to February 2025 among IMGs who had completed Phase 1 of MBBS. Participants were categorized as non-visitors or museum attendees. Attendees were further classified by purpose (academic, non-academic, or both) and frequency (regular: ≥ 10 visits/year; infrequent < 10 visits/year). Data were analyzed using descriptive statistics and chi-square tests. Of 1270 respondents, 81.3% (n = 1032) visited the museum during Phase 1, while 18.7% (n = 238) had never visited. Among attendees, 72.6% (n = 749) engaged in structured learning, and 26.6% (n = 274) visited casually. Within structured learning,

50.3% (n = 377) were regular visitors and 49.7% (n = 372) infrequent visitors. Regular visitors reported greater benefits than infrequent visitors in exam preparation (93.9% vs. 76.6%, $\chi^2 = 44.656$, $p < 0.001$) and anatomy understanding (98.7% vs. 94.6%, $\chi^2 = 9.520$, $p = 0.002$). Barriers included academic workload and restricted access. Participants recommended unrestricted entry, structured faculty-led sessions, and upgraded infrastructure. Frequent academic visits were perceived to significantly enhance anatomy comprehension and exam preparedness, highlighting the need to integrate structured museum learning into the curriculum.

Key words: Anatomy museums – Medical education – Structured learning – Museum utilization – Perceived educational value

INTRODUCTION

Anatomy is fundamental to medical education and surgical practice, but remains challenging due to its vast content and structural complexity (Drake, 2009; Turney, 2007). Cadaveric dissection,

Corresponding author:

Dr. Manikanta Reddy V. Department of Anatomy, S.V Medical College, Tirupati, Andhra Pradesh, India 517 501. Phone: +91 76740 35146. E-mail: manikantareddy.v@gmail.com

Submitted: September 12, 2025 Accepted: February 18, 2026

<https://doi.org/10.52083/GKHQ8208>

though considered the gold standard (Sugand, 2010; Aziz et al., 2002), is primarily useful for learning gross anatomy. It offers limited scope for embryology, radiological anatomy, and osteology; and even within gross anatomy exposure is often restricted and unequal, particularly in large classes. Since repeated learning opportunities are essential, supplementary resources are required. Anatomy museums help bridge this gap by providing preserved specimens, bones, embryology models, skeletons, charts, and radiological images that reinforce understanding and clinical relevance (Cornwall and Stringer, 2009).

Historically, anatomy museums evolved from Renaissance collections of drawings, wax models, and preserved specimens into organized centers for medical education. Developed primarily in Europe during the 17th to 19th centuries, these museums enabled the study of human morphology when cadaveric dissection was limited. Over time, they expanded to include plastinated specimens, skeletal models, and interactive displays, fostering both professional learning and public engagement (Kamath et al., 2013). In modern medical education, particularly in India, anatomy museums continue to complement dissection-based teaching by providing repeated, visual, and integrative learning experiences.

Globally, medical museums are increasingly adopting digital tools such as photogrammetry, three-dimensional modeling, and virtual collections to enhance accessibility and preservation. By contrast, Indian anatomy museums remain largely traditional, with digitalization still rare and limited to a few institutions. Their use in teaching is not mandatory, and student engagement often depends on faculty initiative or individual interest. Access policies, resources, and teaching methods vary widely across institutions, reflecting a lack of standardization.

Given this context, it becomes essential to assess how medical students utilize anatomy museums and perceive their educational value. Understanding usage patterns, barriers, and learning outcomes can help clarify the museum's continuing role in anatomy education and inform strategies for its better integration into modern curricula.

MATERIALS AND METHODS

Study design and setting

This cross-sectional, questionnaire-based survey was conducted between July 2024 and February 2025 among medical students and professionals across India. A convenience sampling approach was employed, supplemented by a snowball sampling strategy, wherein participants were encouraged to share the survey within their professional networks.

Questionnaire development and data collection

The survey questionnaire was developed specifically for the purpose of this study. It was initially developed on the basis of personal interviews with medical students and doctors from various government and private medical colleges. External validation was conducted through an expert panel review comprising eight anatomists, whereas internal reliability was assessed via Cronbach's alpha, which was 0.7, indicating acceptable reliability. The final version of the questionnaire used in the study is provided in Annex 1.

Sample size calculation

The required sample size was determined via the single population proportion formula:

$$n = (Z_{\alpha/2})^2 p(1-p)/d^2$$

where p was set at 68.3% on the basis of the pilot study, with a margin of error of 4% and a confidence interval of 98% (z score = 2.33). On the basis of this calculation, the required sample size was 738.3, which was rounded to 800 participants.

The study included Indian medical graduates (IMGs) who had completed Phase 1 of the MBBS program (i.e., currently in Phase 2 or beyond), and medical professionals who had completed the MBBS from any medical college in India.

Foreign medical graduates (FMGs), IMGs who did not provide consent and participants with incomplete survey responses were excluded from the study.

Survey instrument and data collection

The questionnaire was distributed via Google

Forms, with the survey link circulated through WhatsApp groups (state-level and national-level anatomy community groups, student groups, and medical professional groups) and official institutional emails.

The questionnaire consisted of three sections to facilitate comprehensive data collection. Section 1 included an online-informed consent form, and only participants who successfully submitted their consent were directed to the next section. Section 2 collected information on the country where participants completed or were currently pursuing their MBBS. Only the IMGs were directed to section 3. Section 3 presents demographic details, such as the year of MBBS study and the type of medical college (government or private). This was followed by a structured questionnaire assessing the perceived educational value of museum visits and the factors influencing museum utilization. The questionnaire explored aspects such as the frequency and purpose of visits, reasons for non-visitation or infrequent visitation, the impact of museum visits on anatomy learning and examinations, and recommendations for improving museum utilization.

Statistical analysis

The data were analyzed via SPSS version 20.0. Descriptive statistics were used to summarize categorical variables, while the chi-square test was applied to assess associations between visit frequency and perceived educational benefits. A “p” value <0.05 was considered to indicate statistical significance, and a 95% confidence interval was used to interpret the results.

Ethical approval

This study was conducted in accordance with the ethical principles outlined in the Declaration of Helsinki. Ethical approval was obtained from the Institutional Ethical Committee of Sri Venkateswara Medical College (SVMC), Tirupati, Andhra Pradesh, India (Approval No: 309/SRC/2024). Participation was voluntary, and only those who provided online consent were allowed to proceed with the survey.

RESULTS

A total of 1319 participants responded to the survey. After applying the exclusion criteria (foreign medical graduates: $n = 28$, incomplete data: $n = 21$), 1270 responses were included in the final analysis. Of these, 65.5% ($n = 832$) were from government medical colleges, whereas 34.5% ($n = 438$) were from private medical colleges in India.

Museum utilization patterns

The participants were categorized into non-visitors ($n = 238$, 18.7%) and museum attendees ($n = 1032$, 81.3%). Among non-visitors, 73.1% ($n = 174$) reported various reasons for not visiting the anatomy museum during their first year of MBBS. Similarly, among museum attendees, 52.6% ($n = 543$) provided reasons for their infrequent visits. The most commonly reported barrier across both groups was a busy academic schedule due to theory and practical classes in Anatomy, Physiology and Biochemistry and the need for permission from the head of the department/faculty to access the museum. Additional reasons are detailed in Table 1.

Perceived benefits of museum visits

Among the 1032 museum attendees, 54.9% ($n = 567$) were academic users utilizing the museum for structured learning activities such as group discussions, faculty-led sessions and exam preparation. A total of 26.6% ($n = 274$) were non-academic users, visiting primarily for casual viewing or engaging with the museum during faculty-related events, including university exams, Continuing Medical Education programs, or departmental conferences. A total of 17.6% ($n = 182$) were mixed-purpose visitors who participated in both academic and nonacademic visits.

Overall, 72.6% ($n = 749$) of museum attendees participated in structured learning (academic users + mixed-purpose visitors). Within this group, 50.3% ($n = 377$) were classified as regular visitors (≥ 10 visits per academic year), and 49.7% ($n = 372$) were infrequent visitors (< 10 visits per academic year). A total of 93.9% of regular visitors and 76.6% of infrequent visitors felt that museum visits were beneficial for final examinations

(both theoretical and practical). A statistically significant association was observed between the frequency of museum visits and their perceived usefulness for examination preparation ($\chi^2(1) = 44.656$, $p < 0.001$). Similarly, 98.7% of regular visitors and 94.6% of infrequent visitors reported that museum visits enhanced their understanding of anatomy. This association between visit frequency and improved anatomy comprehension was also statistically significant ($\chi^2(1) = 9.520$, $p = 0.002$).

Recommendations by non-visitors and museum attendees

Both non-visitors and museum attendees provided recommendations to improve museum utilization, which were categorized into three key areas:

1. Accessibility: i.e. granting students unrestricted access to the museum without requiring mandatory permission from the head of the department/faculty.

2. Curriculum Integration: i.e. incorporating structured museum visits into the regular teaching schedule (e.g., weekly guided sessions led by faculty).

3. Museum upgrading: enhancing museum resources through the introduction of 3D models, well-prepared region-specific specimens, self-explanatory catalogs, and digitalization.

Recommendations for enhancing museum utilization were provided by 32 non-visitors and 95 museum attendees, the details of which are presented in the bar diagram (Fig. 1).

DISCUSSION

The primary objective of this study was to assess the perceived educational benefits of academic visits to the anatomy museum during Phase 1 of the MBBS, particularly in relation to final exam preparation and comprehension of anatomy. Our findings suggest that regular museum visitors reported greater perceived benefits than infrequent visitors did. A significantly greater proportion of regular visitors (93.9%) perceived that museum visits improved their exam readiness in high-

er degrees than did infrequent visitors (76.6%). Similarly, 98.7% of the regular visitors felt that museum exposure enhanced their understanding of anatomy, whereas 94.6% of the infrequent visitors did. These results highlight the potential of museums as effective supplements to traditional anatomy teaching by providing a three-dimensional view that reinforces theoretical knowledge and spatial understanding.

Anatomy museums have historically been integral to medical education, evolving from passive displays to interactive spaces that blend art, science, and medicine (Kamath et al., 2013). Digital technologies like 3D scanning, Virtual Reality, and Augmented Reality have enhanced accessibility and engagement with anatomical content (Teplá et al., 2022; Rajaram et al., 2023). In India, however, most museums remain traditional, with limited digital integration, except for a few, such as the Manipal Museum of Anatomy and Pathology.

Since museum visits are neither mandatory nor formally integrated into the medical curriculum in India, establishing a direct correlation between museum usage and academic performance, such as examination scores, is not feasible. Unlike structured lectures or practical sessions, the frequency and purpose of museum visits vary across students and institutions, with no standardized learning hours or guidelines. Additionally, medical students utilize multiple resources, including textbooks, online materials and peer discussions, all of which contribute to academic performance. Given these confounding factors, attributing examination scores solely to museum visits would be misleading. Therefore, this study focused on the students' perceived educational value of museum visits rather than objective academic outcomes. However, future explorations are warranted to assess the potential impact of museum-based preparation on objective measures such as exam performance. Given the number of confounding factors, this assessment would require controlled exposure to the museum to ensure standardized conditions for comparison.

The finding that 81.3% of the participants visited the anatomy museum during Phase 1 of the MBBS underscores its relevance as a learning resource, which is consistent with global trends

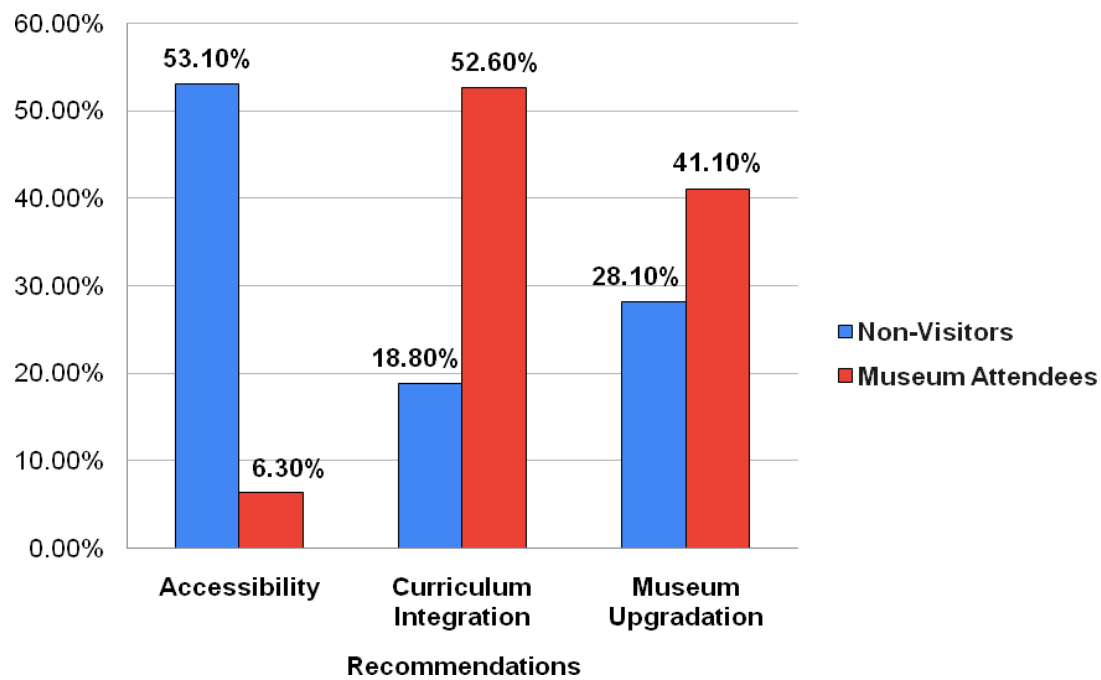


Fig. 1.- Bar diagram showing recommendations for enhancing museum.

where anatomy museums supplement traditional teaching methods such as dissection and lectures (Sugand et al., 2010). However, 18.7% of non-visitations and 49.7% of infrequent visits among attendees highlighted barriers to optimal utilization.

The predominant reasons for non-visitation as well as infrequent visitations were busy academic schedules (35.6% non-visitors, 49.4% attendees) and the requirement of permission to access museums (30.5% non-visitors, 20.8% attendees). These findings align with those of a study by Pradeepkumar et al. (2010), who noted that time constraints and free accessibility to museums are barriers to supplementary learning in medical education. The influence of the COVID-19 pandemic further highlights these results, as online classes likely reduced physical access to museums, which is in accordance with the reports of Singal et al. (2021) and Ali (2020).

Recommendations from both non-visitors and museum attendees highlight key areas for improving museum utilization. Non-visitors prioritized ease in accessibility (53.1%), whereas attendees emphasized curriculum integration (52.6%) and museum upgrading (41.1%), indicating a desire for structured and modernized learning experiences. Suggestions such as 3D models, digitali-

zation and faculty-led museum sessions into the curriculum align with global shifts toward technology-enhanced anatomy education (Trelease, 2016; Kamath et al., 2016; Karim et al., 2022), whereas curriculum integration echoes call for active learning in India's medical reforms. These findings suggest that addressing accessibility and incorporating museum visits into teaching schedules could increase museum utilization.

The strengths of this study include its large, diverse sample size and statistical rigor, as well as its ability to draw reliable conclusions. However, limitations exist. Retrospective data from Phase 2 students and professionals may introduce recall bias, potentially inflating perceived benefits. Additionally, the low response rate for recommendations (13.4% non-visitors, 9.2% attendees) limits their generalizability, possibly owing to the optional nature of this question.

CONCLUSION

This study highlights the perceived educational benefits of anatomy museums, with frequent academic visits linked to improved self-reported exam preparedness and anatomical understanding. However, restricted access, faculty supervision requirements, and time constraints limit optimal utilization. Enhancing accessibility, inte-

grating structured museum visits into the curriculum, and upgrading infrastructure with interactive models and digital exhibits could maximize their impact. While this study focused on perceived benefits, future research should explore controlled comparisons and longitudinal assessments to evaluate the direct influence of museum utilization on academic performance.

REFERENCES

- ALI W (2020) Online and remote learning in higher education institutes: a necessity in light of COVID-19 pandemic. *Higher Educ Studies*, 10(3): 16-25.
- AZIZ MA, MCKENZIE JC, WILSON JS, COWIE RJ, AYENI SA, DUNN BK (2002) The human cadaver in the age of biomedical informatics. *Anat Rec*, 269(1): 20-32.
- CORNWALL J, STRINGER MD (2009) The wider importance of cadavers: Educational and research diversity from a body bequest program. *Anat Sci Educ*, 2(5): 234-237.
- DRAKE RL, MCBRIDE JM, LACHMAN N, PAWLINA W (2009) Medical education in the anatomical sciences: The winds of change continue to blow. *Anat Sci Educ*, 2(6): 253-259.
- KAMATH V, BHAT S, ASIF M, RAMAKRISHNA AVADHANI (2016) Anatomy museums of Southern India and medical education: an original research. *Indian J Clin Anat Physiol*, 3(1): 45-49.
- KAMATH VG, RAY B, PAI SR, AVADHANI R (2013) The origin of anatomy museums. *Eur J Anat*, 17(5): 345-351.
- KARIM N, RAZIF JAMIL M, AIZUDDIN M, LATIP M, AZMAN A, IQBAL M, MUHAMAD AH, ABDUL MUTALIB MAF, ROSWATI MN (2022) The perception on pathology museum in learning pathology: a survey of undergraduate medical students at the Universiti Kuala Lumpur Royal College of Medicine Perak. *Asian J Med Health Sci*, 5(2): 206-215.
- PRADEEPKUMAR NS, JOSEPH NM, KOTASTANE D, KANADE V (2010) Students' perspective of a pathology museum. *National Med J India*, 23(6): 377.
- RAJARAM A, Fiset PO, FRASER R (2023) Photogrammetry of "Wet" pathology museum specimens: a pilot project. *Collections: Journal for Museum and Archives Professionals*, 19(4): 536-552.
- SINGAL A, BANSAL A, CHAUDHARY P, SINGH H, PATRA A (2021) Anatomy education of medical and dental students during COVID-19 pandemic: a reality check. *Surg Radiol Anat*, 43(4): 515-521.
- SUGAND K, ABRAHAMS P, KHURANA A (2010) The anatomy of anatomy: A review for its modernization. *Anat Sci Educ*, 3(2): 83-93.
- TEPLÁ M, TEPLÝ P, ŠMEJKAL P (2022) Influence of 3D models and animations on students in natural subjects. *Int J STEM Educ*, 9: 65.
- TRELEASE RB (2016) From chalkboard, slides, and paper to e-learning: How computing technologies have transformed anatomical sciences education. *Anat Sci Educ*, 9(6): 583-602.
- TURNEY B (2007) Anatomy in a Modern Medical Curriculum. *Annals Royal College Surg England*, 89(2): 104-107.

Role of spatial cognition ability in teaching and learning human embryology: traditional versus 3D atlas

Rakhshinda Iram, Zilli Huma, Najma Baseer, Shah Khalid

Institute of Basic Medical Sciences, Khyber Medical University, Peshawar, Pakistan

SUMMARY

This study aimed to evaluate and compare the cognitive and spatial learning outcomes of two instructional modalities, traditional 2D atlas-based learning and 3D atlas-based visualization, in the teaching of human embryology. Conducted as a cross-over experimental study at Khyber Medical University, the research involved thirty-four post-graduate students equally divided into Group A and Group B. In Phase 1, Group A received 2D instruction while Group B received 3D instruction. Each participant completed a pretest, a two-hour instructional session on heart development, a post-test immediately after, and a delayed post-test two weeks later. Cognitive understanding was assessed using a structured questionnaire, while spatial ability was evaluated using the Visualization of Rotation (ROT) test. After Phase 1, the instructional methods were flipped between the groups, and the assessments were repeated.

Before flipping, a significant difference was observed in pretest cognitive scores between the groups ($F = 5.405$, $p = 0.026$), with the Group B (3D in Phase 1) scoring higher; however, this difference did not persist in post-test or delayed post-test results. Spatial scores also showed a clear advantage for the Group B before the flip, with significantly higher post-test ($F = 27.781$, $p < 0.05$)

and delayed post-test scores ($F = 55.07$, $p < 0.05$). After flipping, the group receiving 3D instruction achieved higher spatial scores at both the post-test and delayed post-test stages confirming the consistent advantage of 3D visualization across both phases. Within-group analysis revealed modest improvements after instruction for both groups, followed by a normal decline at delayed testing.

Overall, the findings suggest that 3D atlas-based learning enhances spatial reasoning and visualization skills, while traditional 2D learning remains effective for factual content mastery. The cross-over design minimized the influence of baseline differences and allowed direct comparison of both modalities within the same participants. These results support an integrated pedagogical approach where 3D visualization tools are introduced early to build spatial frameworks, followed by 2D resources to reinforce conceptual understanding and retention.

Key words: Spatial ability – ROT (visualization of Rotation) – Cognition – Embryology – 3D learning

INTRODUCTION

Embryology is a fundamental component of

Corresponding author:

Prof. Zilli Huma. Anatomy, Institute of Basic Medical Sciences, Khyber Medical University, Peshawar, Pakistan. Phone: +923209894379. E-mail: zillihuma.ibms@kmu.edu.pk

Submitted: September 19, 2025 **Accepted:** January 22, 2026

<https://doi.org/10.52083/QPTY1069>

medical education, providing essential knowledge for the understanding of the complex-organ spatial connectivity and identifying the roots of congenital birth defects (Chekrouni et al., 2020). Traditional education systems deliver embryological information to students through textbooks alongside didactic lectures as they serve as baseline learning materials in medical programs. Understanding embryonic development demands more than simple textual information, because the process remains complicated in nature. The understanding of spatial relationships needs visualization to strengthen anatomical connections, and this proves difficult when using standard teaching methods independently (Alharbi et al., 2020).

Anatomical instruction has developed through time by leaving behind traditional paper methods to adopt modern interactive technological methodologies (McBride and Drake, 2018). The COVID-19 pandemic highlighted a permanent transition by using digital platforms to replace traditional classrooms so that anatomical education progressed through virtual platforms. These technological advances have shown successful achievements in anatomy teaching, but researchers need to study how they affect long-term educational outcomes (Losco et al., 2017).

Medical students require memorization with comprehension and visualization techniques to build a thorough grasp of anatomy according to recent studies. The ability of students to remember and recall how anatomical parts relate spatially helps them create mental photographs and spatial awareness, which proves critical for medical practice (Pradhan et al., 2024). Research poses the pivotal question whether spatial cognitive competency by nature increases anatomy learning skills or medical education courses enhance spatial capabilities (Langlois et al., 2017).

Research established that three-dimensional (3D) visualization tools lead students to obtain better factual as well as spatial knowledge about anatomical representations than traditional two-dimensional (2D) approaches (Vorstenbosch et al., 2013; Triepels et al., 2020). The enhancement of spatial abilities occurs following repeated exposure and training, according to multiple re-

search papers which show that visualization and anatomy learning work in tandem (Langlois et al., 2020; Gonzales et al., 2020). Two studies focused on the comparative analysis between two-dimensional and three-dimensional learning methods showed that virtual and augmented-reality technology offers better spatial anatomical comprehension and presents itself as a suitable choice for teaching replacement (Birbara et al., 2020; Dharamsi et al., 2022).

Arguments that produce better educational results increase, since students increasingly use online education while having restricted access to physical cadaver dissection spaces and anatomical model collections. The research investigates cognitive and spatial performance scores in developmental embryology education between two student groups to evaluate spatial cognition impact on anatomy learning through emerging digital educational tools in medical curricula.

MATERIALS AND METHODS

The experimental pre-test and post-test study were performed at the Institute of Basic Medical Sciences within Khyber Medical University in Peshawar. The study was conducted in accordance with the Institutional Review Board through NO: KMU/IBMS/IRBE/meeting/2022/8071. All participants involved in this study had approved to join the research through informed consent. Moreover, the participants in this study were postgraduate medical students currently pursuing M.Phil. degrees in Anatomy at the Institute of Basic Medical Sciences, Khyber Medical University. All of them had already completed their bachelors in allied health sciences, so they entered the program with a similar baseline understanding of embryology. Because of this shared academic background, it was anticipated that the group was uniform in their foundation knowledge before the educational intervention. To avoid confusion between instructional modalities before and after the crossover, the two groups were referred to Group A and Group B throughout the study. At the start of the study, participants were randomly assigned to these two groups. In Phase 1, Group A received traditional 2D atlas instruction and Group B received 3D digital atlas instruction. In Phase 2 (af-

ter flipping), the modalities were flipped: Group A received 3D instruction, and Group B received 2D instruction. This consistent naming style prevents ambiguity in interpreting results before and after the instructional flip.

The pre-test consisted of two main components:

1. The structured questionnaire determined the results of cognitive assessment.
2. The Visualization of Rotation (ROT) test was used to assess spatial ability during the study (Yoon, 2011).

Both groups participated in a two-hour instructional session on heart development. The instructional duration, learning objectives, and assessment timelines were kept the same for both modalities to avoid procedural bias. Netter's Atlas of Human Embryology and Langman's Human Embryology were used as reference materials for traditional learning group (Group A in Phase 1) used Netter's Atlas of Human Embryology and Langman's Human Embryology as reference materials, while the 3D learning group (Group B in Phase 1) viewed the interactive digital platform available at <http://www.3datlasofhumanembryology.com>.

The post-test assessment occurred promptly following instructions and then the delayed post-test took place two weeks after using an identically structured pre-test questionnaire. In the two weeks before the delayed post-test, students were asked not to review or search for any extra material on the topic. When they came in for the delayed test, this reminder was given again. The assessment was held in a supervised classroom environment to make sure that instructions were followed. This approach was used so that the delayed test would reflect what students had retained from the original lesson.

Following completion of phase 1, the study employed a cross-over arrangement. Group A shifted from 2D instruction to 3D instruction, while Group B shifted from 3D to 2D. The duration of instruction and the sequence of assessments were kept consistent across both phases. Although the anatomical topic remained the same, parallel (rather than identical) test items were used to

limit direct recall of previous responses. This approach allowed both groups to engage with both instructional modalities while minimizing learning carryover effects. The cognitive questionnaire and the ROT spatial test were administered in the same order during each phase.

Descriptive and inferential statistical analyses were performed to examine cognitive and spatial learning outcomes. All information was processed by Microsoft Excel and Statistical Package for the Social Sciences (SPSS), version 24. The test included descriptive statistics, which presented the mean (M) and standard deviation (SD). A Shapiro-Wilk test was conducted to check the distributional normality of measured variables. The analysis of score differences between groups included a one-way ANOVA test for the three tests' scores. The evaluation of differences among participants used a repeated measures ANOVA design. The relationship between cognitive scores and spatial ability was evaluated through Pearson's correlation coefficient test. To avoid misinterpretation of group effects, all between-group comparisons were interpreted in relation to the instructional modality delivered in each phase rather than group identity. Although Group A and Group B labels remained constant throughout the study, the instructional modality (2D or 3D) varied by phase. Accordingly, any observed between-group differences at post-test or delayed post-test were attributed to the modality of instruction rather than inherent differences between groups.

RESULTS

A total of 34 participants were included in the study with 50% allocated to each group. Most of the participants were females (76%), and their ages ranged from 27 to 35 years.

Phase 1 (Before Flipping)

Cognition Scores: Table 1 presents the cognition scores for Group A (2D instruction) and Group B (3D instruction) before the cross-over. A statistically significant difference was observed at the pre-test stage ($F = 5.405$, $p = 0.026$), with Group B scoring higher than Group A. However, no significant differences were observed at the post-test

($F = 0.956, p = 0.335$) or delayed post-test stages ($F = 0.814, p = 0.373$). Within-group comparisons showed statistically non-significant changes over time for both Group A ($F = 2.901, p = 0.080$) and Group B ($F = 2.540, p = 0.106$). These results indicate that although Group B began with a higher baseline cognitive score, Group A improved sufficiently to close the gap after instruction.

Spatial Scores: As shown in Table 2, there was no significant difference in spatial scores at the pre-test stage ($F = 1.704, p = 0.201$). However, Group B scored significantly higher at both the post-test ($F = 27.781, p < 0.001$) and delayed post-test stages ($F = 55.078, p < 0.001$). Within-group analysis also demonstrated significant improvement across time in both groups (Group A: $F = 7.019, p = 0.007$; Group B: $F = 11.200, p = 0.001$). This confirms that 3D visualization produced greater spatial skill enhancement compared to 2D instruction.

Phase 2 (After Flipping)

Cognition Score: Table 3 summarizes the cognition results after the instructional cross-over. At the Phase 2 pre-test, Group B scored significantly higher than Group A ($F = 6.847, p = 0.013$), reflecting a persistent baseline difference rather than an instructional effect. Following instructions, no significant differences were found at the post-test ($F = 0.672, p = 0.418$) or delayed post-test ($F = 0.087, p = 0.770$). Both groups showed modest improvement after instruction followed by a decline

at the delayed post-test.

Spatial Scores: Table 4 shows the spatial score comparisons after the cross-over. At the Phase 2 pre-test, there was no significant difference between groups ($F = 1.218, p = 0.278$). However, Group B scored significantly higher than Group A at both the post-test ($F = 25.995, p < 0.001$) and delayed post-test ($F = 40.523, p < 0.001$). Within-group changes remained significant for both Group A ($F = 9.138, p = 0.004$) and Group B ($F = 10.174, p = 0.002$). These results again support the consistent advantage of 3D visualization in improving spatial reasoning.

Correlational Analysis: Pearson correlation analysis showed a weak, non-significant relationship between cognition and spatial scores across all assessment points ($r = 0.325, p = 0.061$), indicating that changes in one domain did not strongly predict changes in the other.

DISCUSSION

This study compared cognitive and spatial learning outcomes between two instructional modalities, traditional 2D atlas-based learning and 3D atlas-based visualization, in the context of teaching embryological heart development. The results demonstrated that the two approaches supported learning in different ways, highlighting the importance of matching instructional tools to the learning objectives.

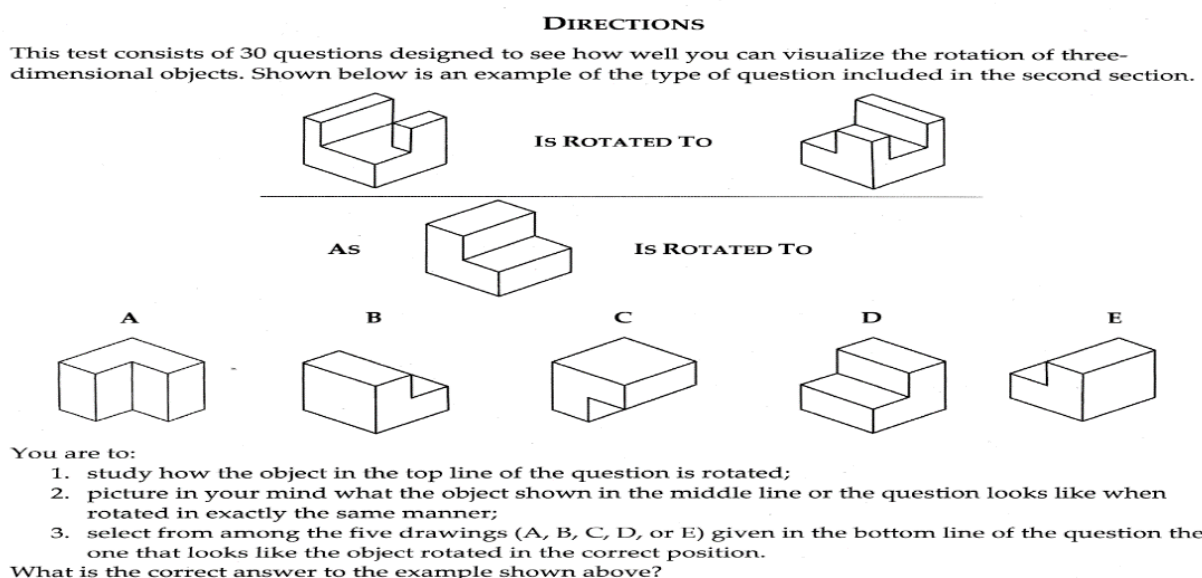


Fig. 1.- Sample question from the ROT Test with instructions (Yoon, 2011).

Table 1. Cognition scores before instructional flipping (Phase 1)

Variable	Assessment stage	Group A (2D instruction) Mean ± SD	Group B (3D instruction) Mean ± SD	F	p
Cognition test (0-10)	Pre-test	3.76 ± 1.3	5.35 ± 2.4	5.405	0.026*
	Post-test	4.94 ± 2.6	5.82 ± 2.6	0.956	0.335
	Delayed post-test	3.82 ± 2.0	4.29 ± 0.77	0.814	0.373

In Phase 1, Group A received traditional 2D atlas instruction and Group B received 3D digital atlas instruction. Statistically significant ($p < 0.05$).

Table 2. Spatial scores before instructional flipping (Phase 1)

Variable	Assessment stage	Group A (2D instruction) Mean ± SD	Group B (3D instruction) Mean ± SD	F	p
Spatial Cognition test (0-10)	Pre-test	3.35 ± 2.1	4.29 ± 2.0	1.704	0.201
	Post-test	4.00 ± 1.6	6.29 ± 0.6	27.781	<0.001*
	Delayed post-test	1.70 ± 1.4	4.82 ± 0.9	55.078	<0.001*

In Phase 1, Group A received traditional 2D atlas instruction and Group B received 3D digital atlas instruction. Statistically significant ($p < 0.05$).

Table 3. Cognition scores after instructional flipping (Phase 2)

Variable	Assessment stage	Group A (2D instruction) Mean ± SD	Group B (3D instruction) Mean ± SD	F	p
Spatial Cognition test (0-10)	Pre-test	4.52 ± 1.5	5.94 ± 1.6	6.847	0.013*
	Post-test	5.64 ± 2.4	6.29 ± 2.0	0.672	0.418
	Delayed post-test	4.23 ± 2.3	4.41 ± 0.8	0.087	0.770

In Phase 2, Group A received 3D digital atlas instruction and Group B received traditional 2D atlas instruction. Statistically significant ($p < 0.05$).

Table 4. Spatial scores after instructional flipping (Phase 2)

Variable	Assessment stage	Group A (2D instruction) Mean ± SD	Group B (3D instruction) Mean ± SD	F	p
Spatial Cognition test (0-10)	Pre-test	3.82 ± 1.9	4.58 ± 2.0	1.218	0.278
	Post-test	4.52 ± 1.4	6.58 ± 0.7	25.995	<0.001*
	Delayed post-test	2.00 ± 1.5	4.88 ± 1.0	40.523	<0.001*

In Phase 2, Group A received 3D digital atlas instruction and Group B received traditional 2D atlas instruction. Statistically significant ($p < 0.05$).

Before the instructional methods were flipped, Group B, which received 3D instruction in Phase 1, achieved significantly higher spatial scores at both the post-test and delayed post-test assessments. This finding supports the established view that dynamic, manipulable 3D visualizations facilitate mental rotation and spatial integration, particularly in anatomy and embryology, where structures evolve in complex three-dimensional planes. This is consistent with earlier reports that 3D models and virtual reality tools promote spatial understanding more effectively than tra-

ditional images alone (Yoon, 2011; Wang et al., 2020). The significant within-group improvement observed in both Group A and Group B also suggests that spatial ability is trainable, aligning with research demonstrating that repeated exposure to visual-spatial challenges enhance mental rotation skills over time (Langlois et al., 2020; Gonzales et al., 2020).

In contrast, the cognitive (factual recall) outcomes showed no consistent advantage for either group across testing points before flipping. While Group B scored higher at baseline in the first

tion is introduced initially to build foundational spatial understanding, followed by targeted reinforcement using traditional 2D resources to consolidate cognitive content.

CONCLUSION

This study demonstrated that 3D atlas-based visualization consistently enhanced students' spatial reasoning across both phases of the cross-over design, regardless of whether learners encountered it first or after traditional 2D instruction. In contrast, cognitive (factual) learning outcomes were comparable between modalities after instruction, indicating that conceptual understanding can be effectively supported by both 2D and 3D resources. The repeated observation that the group receiving 3D instruction, whether in Phase 1 or Phase 2, achieved higher spatial scores highlights the modality-specific advantages of interactive visualization for understanding complex embryological structures.

The cross-over structure further revealed that once spatial understanding is established, its benefits persist even when learners transition to 2D materials, suggesting a durable learning-transfer effect. These results support a sequenced pedagogical approach in which 3D visualization is introduced early to build foundational spatial frameworks, followed by reinforcement and consolidation using traditional 2D atlases for long-term conceptual learning. Future research should employ larger and more diverse samples and explore the integration of virtual or augmented reality technologies to further enhance spatial reasoning and improve long-term retention of embryological concepts.

ACKNOWLEDGEMENTS

The authors express their appreciation and gratitude to Dr Yoona, Assistant Professor, Dept. of Engineering and Computing Education, University of Cincinnati for providing the Revised Purdue Spatial Visualization Test (Revised PSVT:R): Visualization of Rotations.

REFERENCES

ALHARBI Y, AL-MANSOUR M, AL-SAFFAR R, GARMAN A, ALRADDADI A (2020) Three-dimensional virtual reality as an innovative teaching and learning tool for human anatomy courses in medical education: a mixed methods study. *Cureus*, 12(2): e7085.

BIRBARA NS, SAMMUT C, PATHER N (2020) Virtual reality in anatomy: a pilot study evaluating different delivery modalities. *Anat Sci Educ*, 13(4): 445-457.

CHEKROUNI N, KLEIPOOL RP, DE BAKKER BS (2020) The impact of using three-dimensional digital models of human embryos in the biomedical curriculum. *Ann Anat*, 227: 151430.

CODD AM, CHOUDHURY B (2011) Virtual reality anatomy: is it comparable with traditional methods in the teaching of human forearm musculoskeletal anatomy. *Anat Sci Educ*, 4(3): 119-125.

DHARAMSI MS, BASTIAN DA, BALSIGER HA, CRAMER JT, BELMARES R (2022) Efficacy of video-based forearm anatomy model instruction for a virtual education environment. *J Med Educ Curric Dev*, 9: 23821205211063287.

GONZALES RA, FERNS G, VORSTENBOSCH M, SMITH CF (2020) Does spatial awareness training affect anatomy learning in medical students. *Anat Sci Educ*, 13(6): 707-720.

HOYEK N, COLLET C, DI RIENZO F, DE ALMEIDA M, GUILLOT A (2014) Effectiveness of three-dimensional digital animation in teaching human anatomy in an authentic classroom context. *Anat Sci Educ*, 7(6): 430-437.

LANGLOIS J, BELLEMARE C, TOULOUSE J, WELLS GA (2017) Spatial abilities and anatomy knowledge assessment: a systematic review. *Anat Sci Educ*, 10(3): 235-241.

LANGLOIS J, BELLEMARE C, TOULOUSE J, WELLS GA (2020) Spatial abilities training in anatomy education: a systematic review. *Anat Sci Educ*, 13(1): 71-79.

LOSCO CD, GRANT WD, ARMSON A, MEYER AJ, WALKER BF (2017) Effective methods of teaching and learning in anatomy as a basic science: a BEME systematic review: BEME guide no. 44. *Med Teach*, 39(3): 234-243.

MCBRIDE JM, DRAKE RL (2018) National survey on anatomical sciences in medical education. *Anat Sci Educ*, 11(1): 7-14.

PAGELS L, ESCHKE RC, LUEDTKE K (2024) Effectiveness of digital and analog learning methods for learning anatomical structures in physiotherapy education. *BMC Med Educ*, 24(1): 500.

PRADHAN S, DAS C, PANDA DK, MOHANTY BB (2024) Assessing the utilization and effectiveness of YouTube in anatomy education among medical students: a survey-based study. *Cureus*, 16(3): e55644.

TRIEPELS CPR, SMEETS CFA, NOTTEN KJB, KRUITWAGEN R, FUTTERER JJ, VERGELDT TFM, VAN KUIJK SMJ (2020) Does three-dimensional anatomy improve student understanding. *Clin Anat*, 33(1): 25-33.

VORSTENBOSCH MA, KLAASSEN TP, DONDEERS AR, KOOLOOS JG, BOLHUIS SM, LAAN RF (2013) Learning anatomy enhances spatial ability. *Anat Sci Educ*, 6(4): 257-262.

WANG C, DANIEL BK, ASIL M, KHWAOUNJOO P, CAKMAK YO (2020) A randomized control trial and comparative analysis of multi-dimensional learning tools in anatomy. *Sci Rep*, 10(1): 6120.

YOON SY (2011) Revised purdue spatial visualization test: visualization of rotations (Revised PSVT:R). Purdue University Press, USA.



European Journal of Anatomy